

SRF LIMITATIONS

Jean Delayen

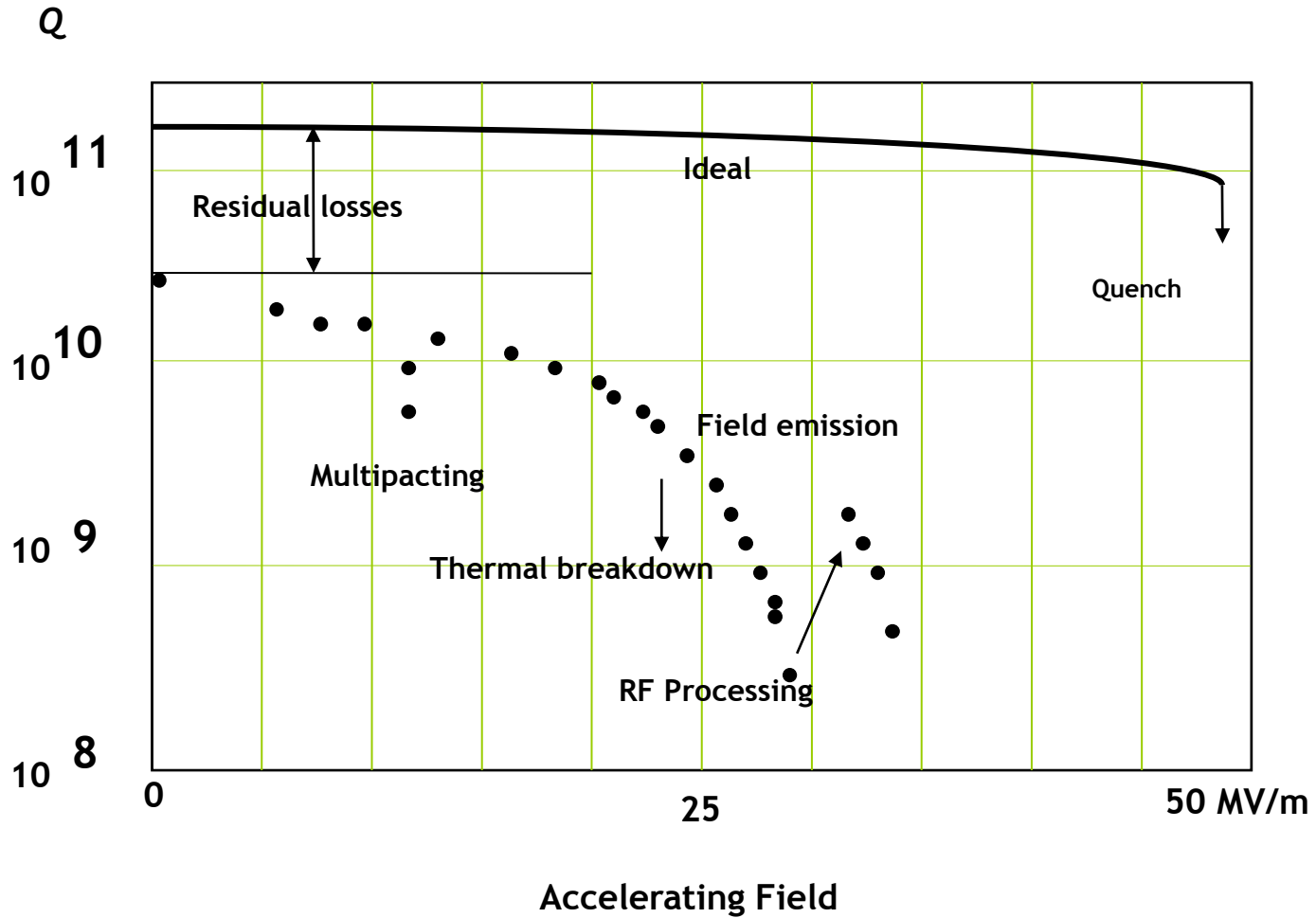
**Center for Accelerator Science
Old Dominion University
and**

Thomas Jefferson National Accelerator Facility

Outline

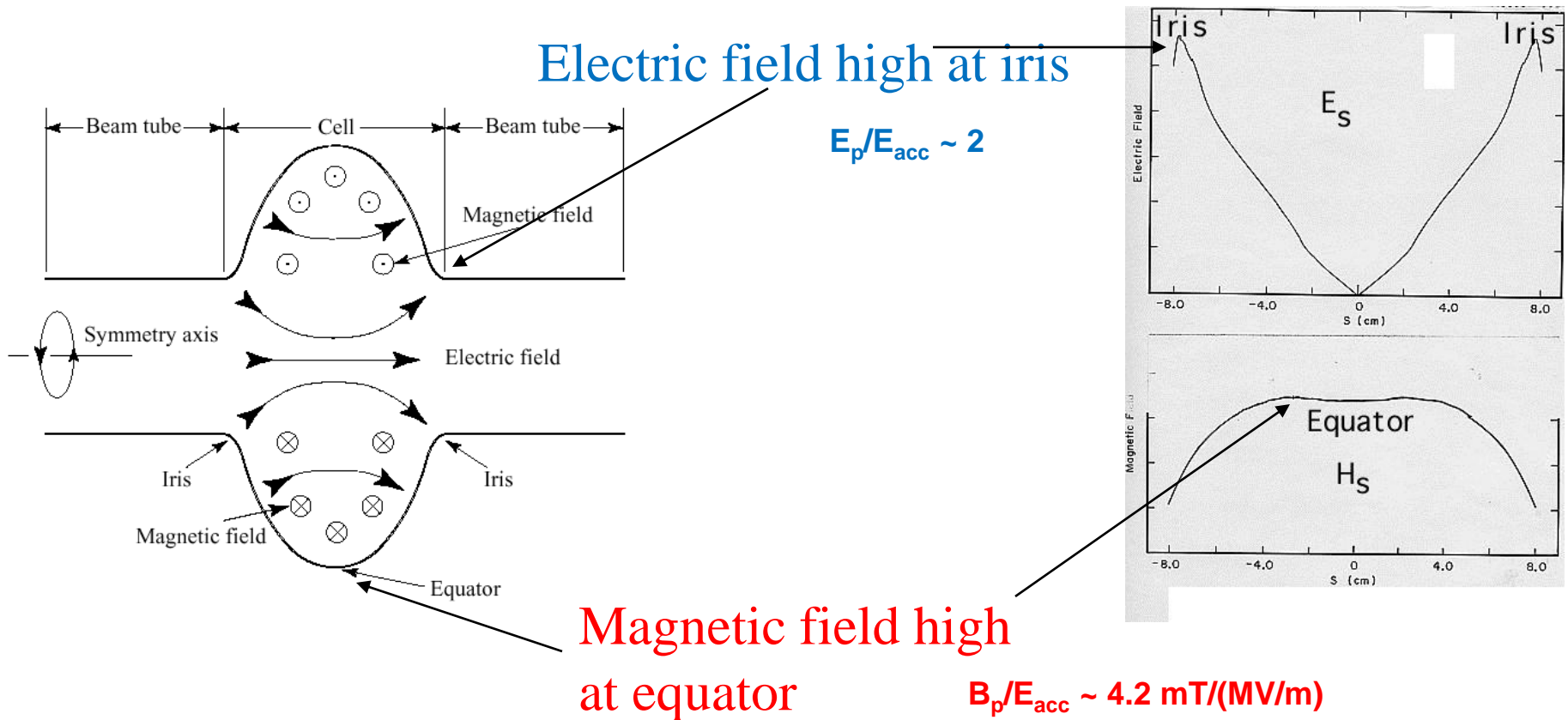
- Residual resistance
- Multipacting
- Field emission
- Quench
- High-field Q-slope

The Real World



Losses in SRF Cavities

- Different loss mechanisms are associated with different regions of the cavity surface



Characteristics of Residual Surface Resistance

- No strong temperature dependence
- No clear frequency dependence
- Not uniformly distributed (can be localized)
- Not reproducible
- Can be as low as 1 n Ω
- Usually between 5 and 30 n Ω
- Often reduced by UHV heat treatment above 800C

Origin of Residual Surface Resistance

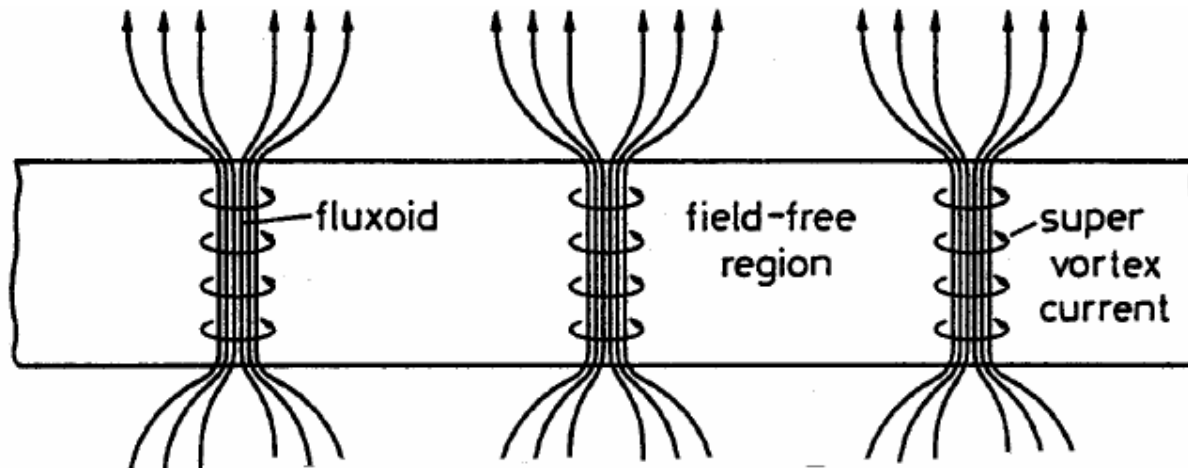
- Dielectric surface contaminants (gases, chemical residues, dust, adsorbates)
- Normal conducting defects, inclusions
- Surface imperfections (cracks, scratches, delaminations)
- Trapped magnetic flux
- Hydride precipitation
- Localized electron states in the oxide (photon absorption)

R_{res} is typically 5-10 n Ω at 1-1.5 GHz

Trapped Magnetic Field

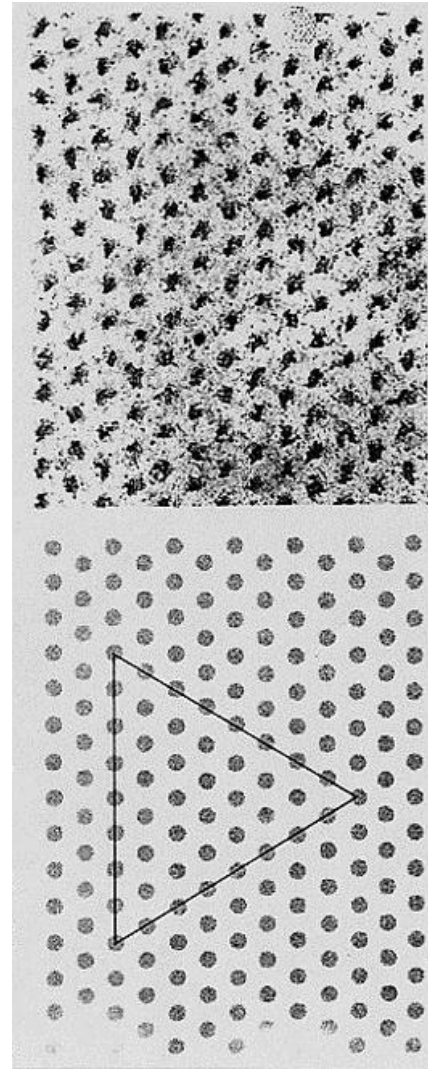
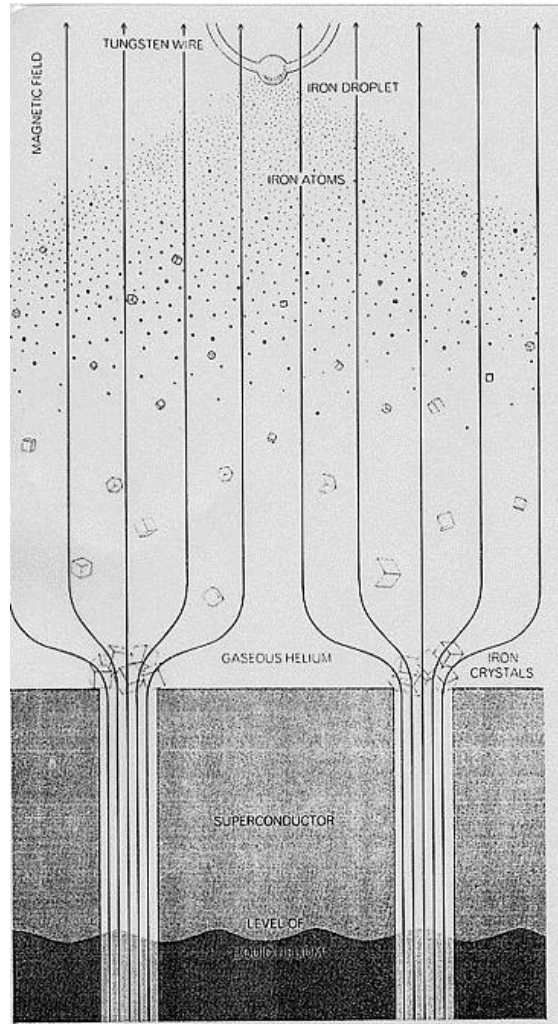
A parallel magnetic field is expelled from a superconductor.

What about a perpendicular magnetic field?

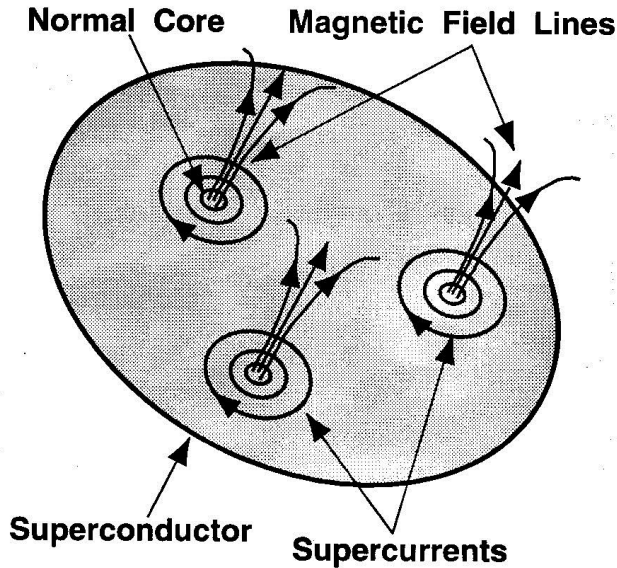


The magnetic field will be concentrated in normal cores where it is equal to the critical field.

Trapped Magnetic Field



Trapped Magnetic Field



- Vortices are normal to the surface
- 100% flux trapping
- RF dissipation is due to the normal conducting core, of resistance R_n

$$R_{res} \cong R_n \frac{H_i}{H_{c2}}$$

H_i = residual DC magnetic field

- For Nb: $R_{res} \approx 0.3 \text{ to } 1 \text{ n}\Omega/\text{mG}$ around 1 GHz

Depends on material treatment

- While a cavity goes through the superconducting transition, the ambient magnetic field cannot be more than a few mG.
- The earth's magnetic field must be effectively shielded.
- Thermoelectric currents can cause trapped magnetic field, especially in cavities made of composite materials.

Trapped Magnetic Field

A fraction H / H_c of the material will be in the normal state.

This will lead to an effective surface resistance $\rho_n (H / H_c)$

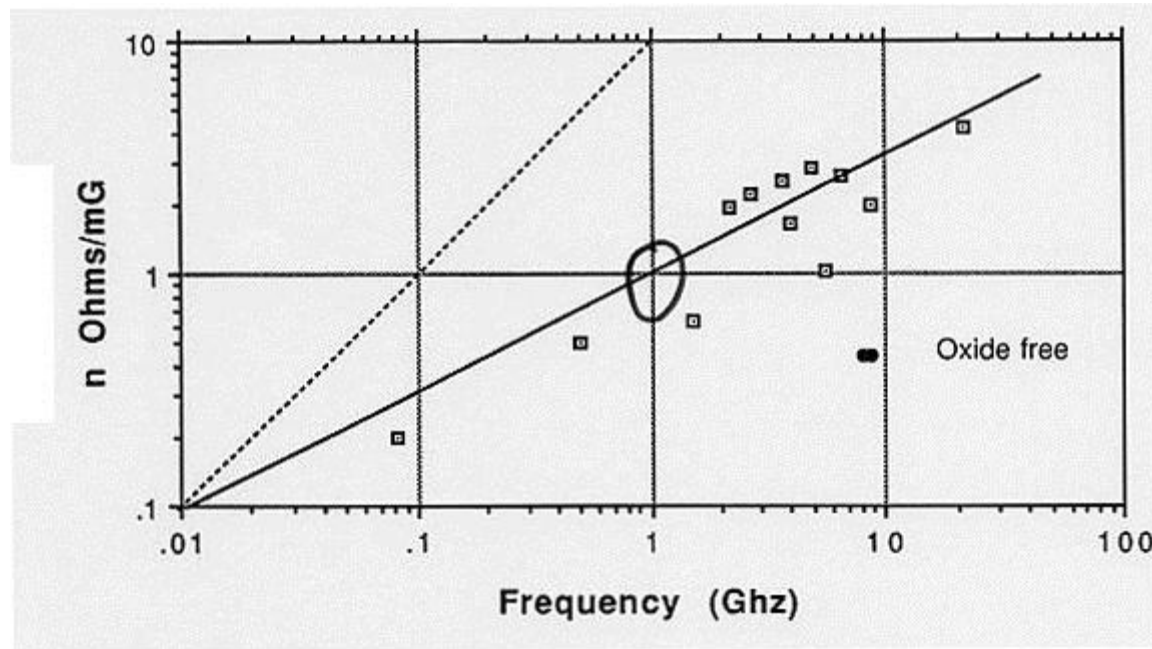
For Nb: $\rho_{eff} \approx 0.5$ to $1 \text{ n}\Omega/\text{mG}$ around 1 GHz

While a cavity goes through the superconducting transition, the ambient magnetic field cannot be more than a few mG.

The earth's magnetic field must be effectively shielded.

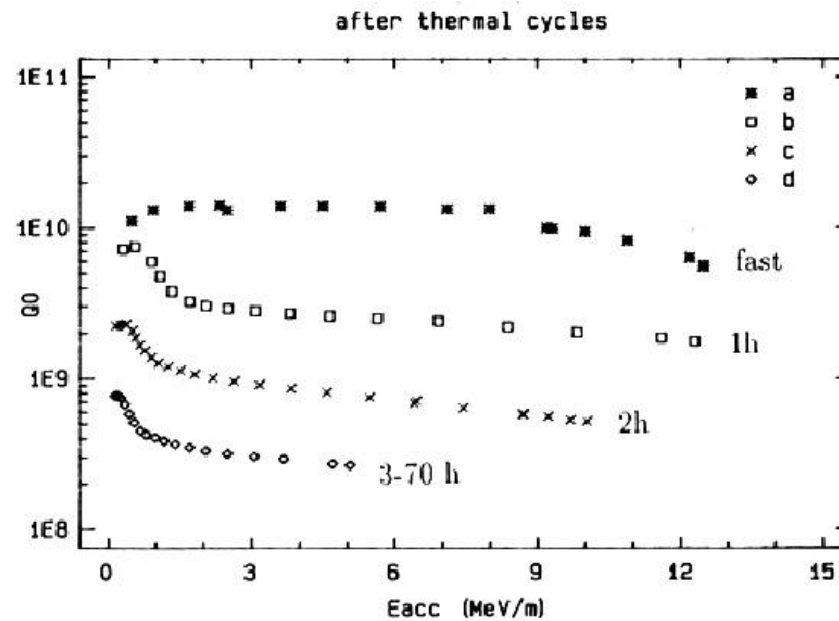
In cavities made of composite materials, thermoelectric currents can cause trapped magnetic field.

Trapped Magnetic Field



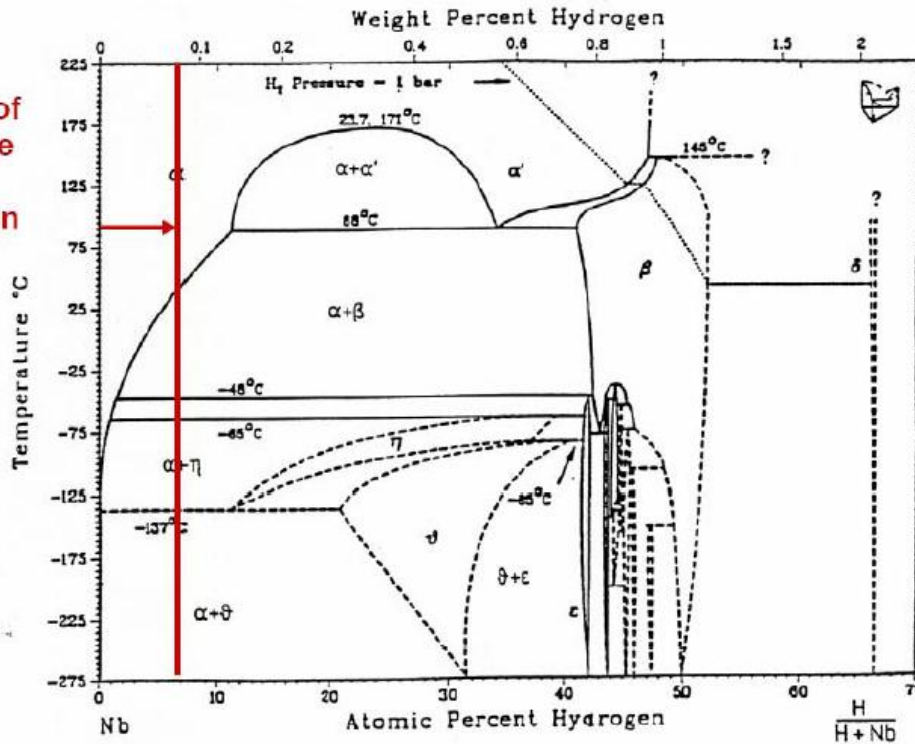
R_{res} Due to Hydrides (Q-Disease)

- Cavities that remain at 70-150 K for several hours (or slow cool-down, < 1 K/min) experience a sharp increase of residual resistance
- More severe in cavities which have been heavily chemically etched



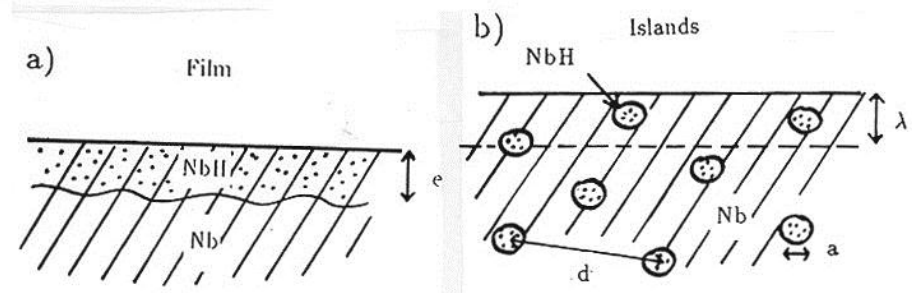
Hydrogen: “Q-disease”

Range of possible H pollution



- H is readily absorbed into Nb where the oxide layer is removed (during chemical etching or mechanical grinding)
- H has high diffusion rate in Nb, even at low temperatures.
- H precipitates to form a hydride phase with poor superconducting properties:

- At room temperature the required concentration to form a hydride is 10^3 - 10^4 wppm
- At 150K it is < 10 wppm



Cures for Q-disease

- Fast cool-down
- Maintain acid temperature below ~ 20 °C during BCP
- “Purge” H_2 with N_2 “blanket” and cover cathode with Teflon cloth during EP
- “Degas” Nb in vacuum furnace at $T > 600$ °C

Q₀ Record

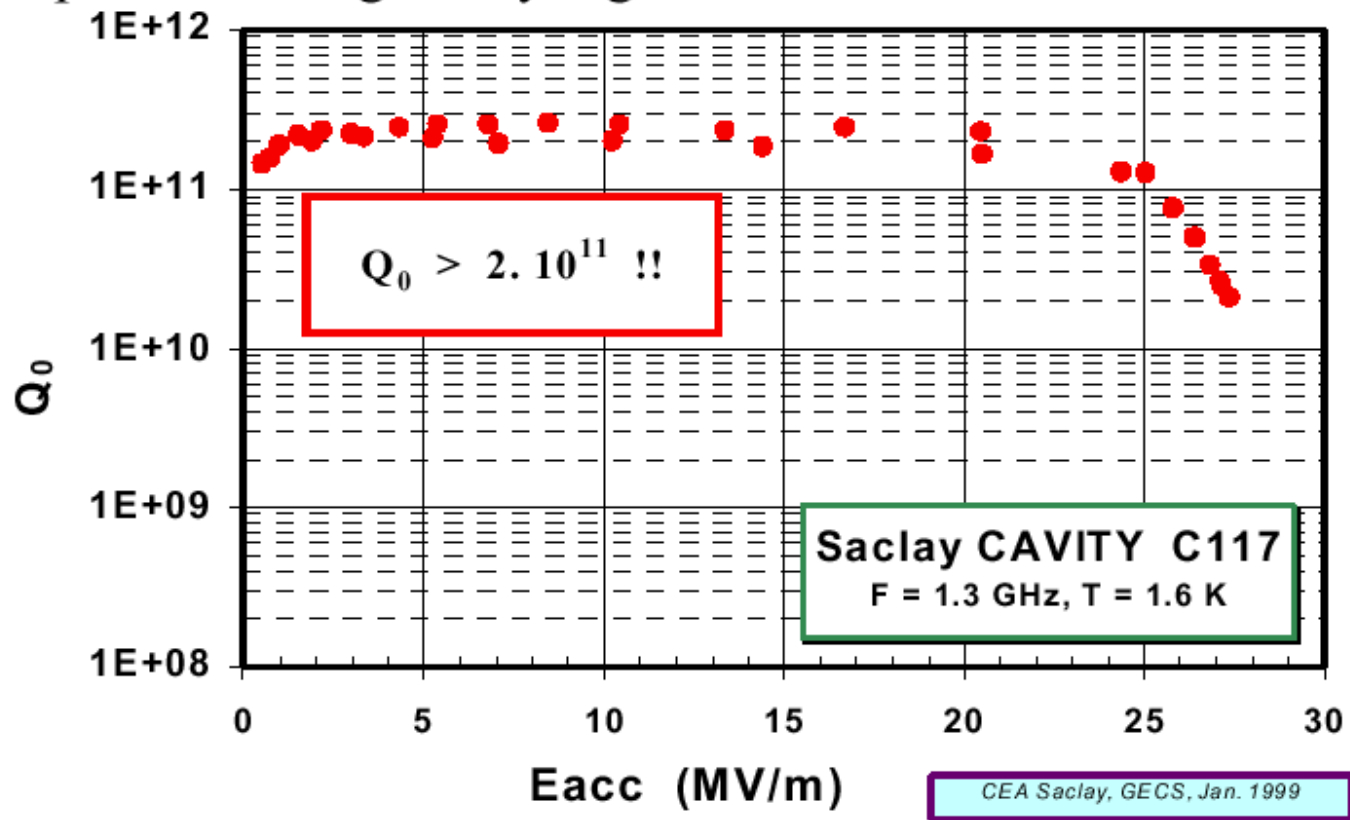
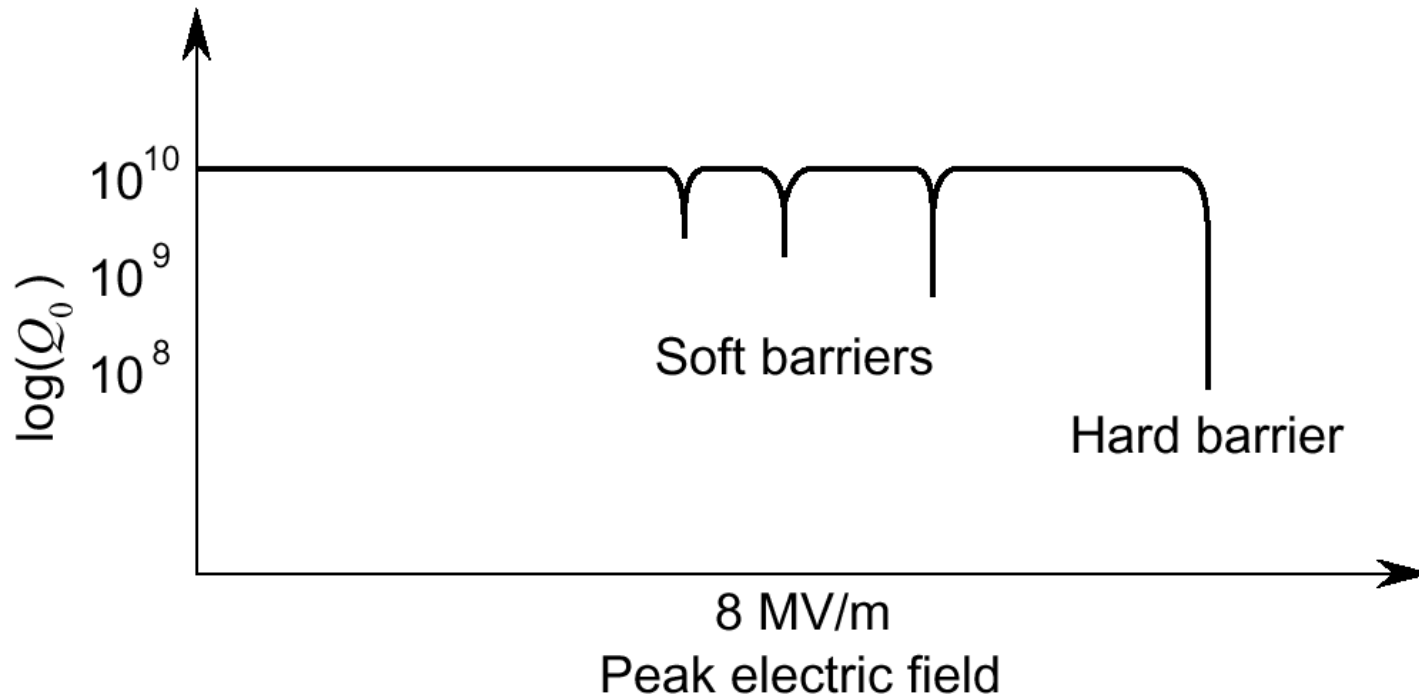
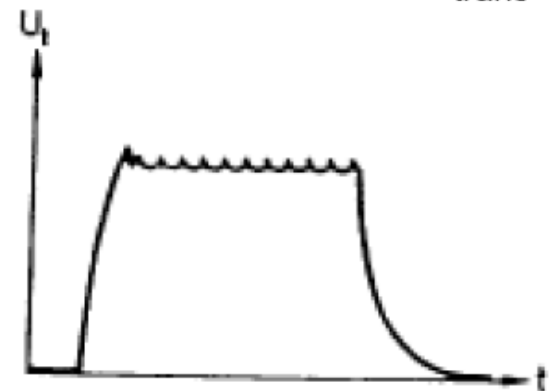


Figure 2 – Residual resistance as low as $0.5 \text{ n}\Omega$ is actually measured on large area cavities, giving an intrinsic quality factor Q_0 exceeding 2.10^{11} .

Multipacting



- No increase of P_t for increased P_i during MP
- Can induce quenches and trigger field emission



Multipacting

Multipacting is characterized by an exponential growth in the number of electrons in a cavity

Common problems of RF structures (Power couplers, NC cavities...)

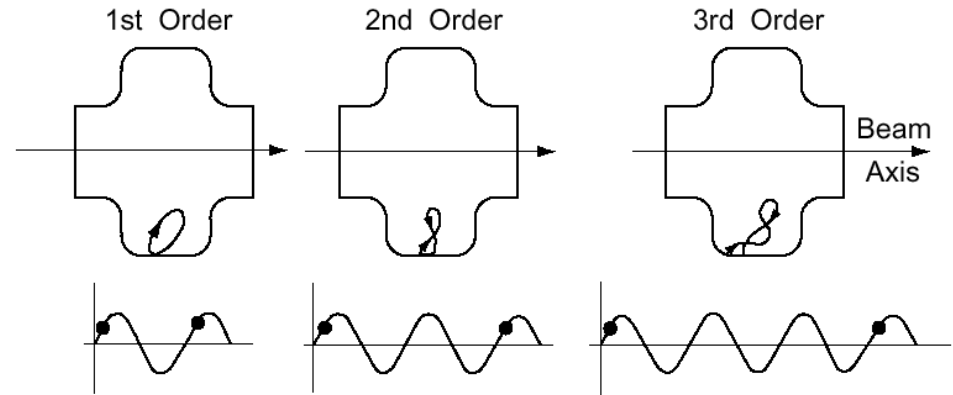
Multipacting requires 2 conditions:

- Electron motion is periodic (resonance condition)
- Impact energy is such that secondary emission coefficient is >1

One-Point Multipacting

One-point MP

Cyclotron frequency: $\omega_c \propto \frac{\mu_0 H e}{m}$



Resonance condition:
Cavity frequency (ω_g) = n x cyclotron frequency

$$\omega_g = n\omega_c$$

n : MP order

→ Possible MP barriers given by $H_n \propto \frac{m\omega_g}{n\mu_0 e}$

+ SEY, $\delta(K)$, > 1 = MP

The impact energy scales as

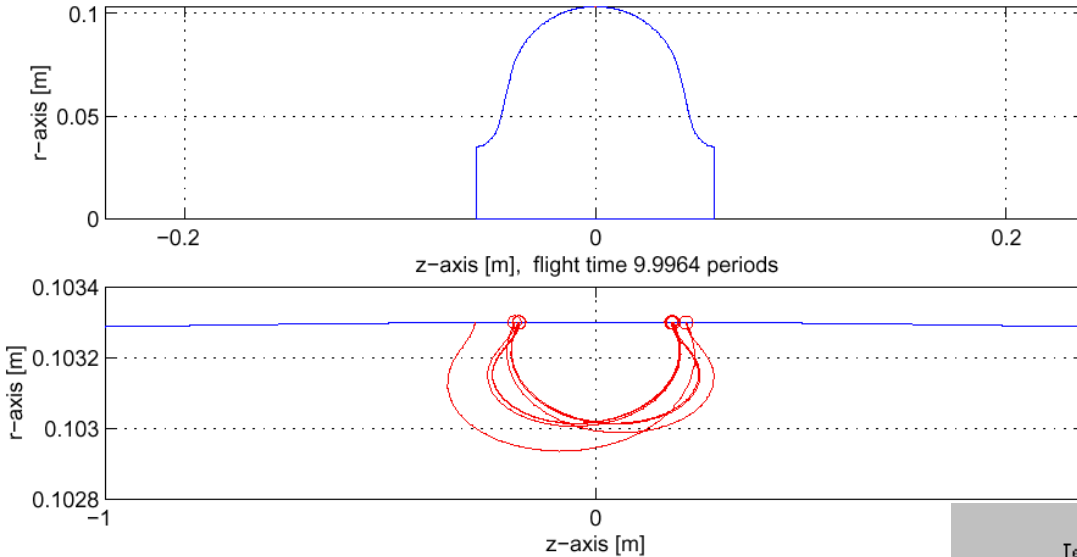
$$K \propto \frac{e^2 E_{\perp}^2}{m\omega_g^2}$$

Empirical formula:

$$H_n [\text{Oe}] = \frac{0.3}{n} f_0 [\text{MHz}]$$

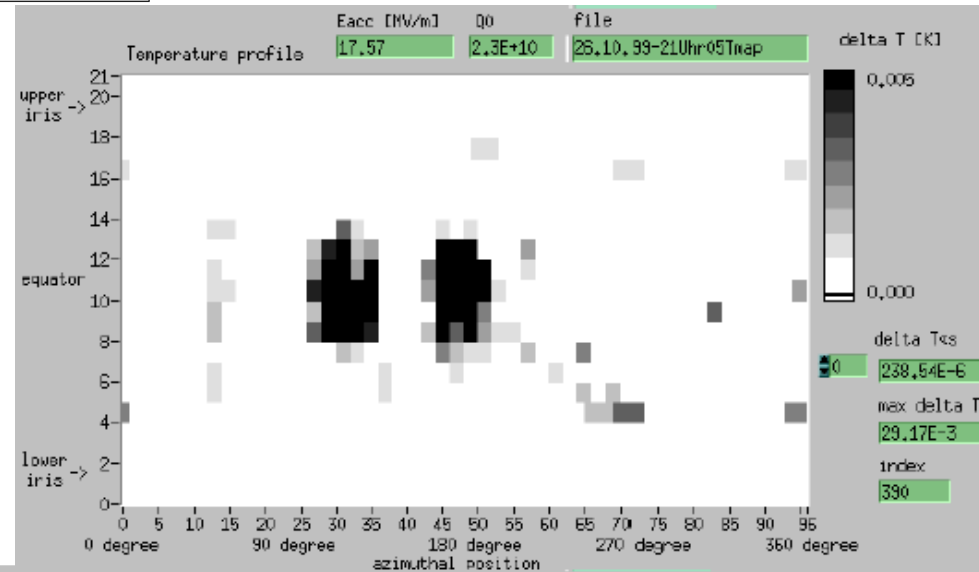
Two-Point Multipacting

MultiPac 2.1 Electron Trajectory, N = 20, 24-Apr-2002



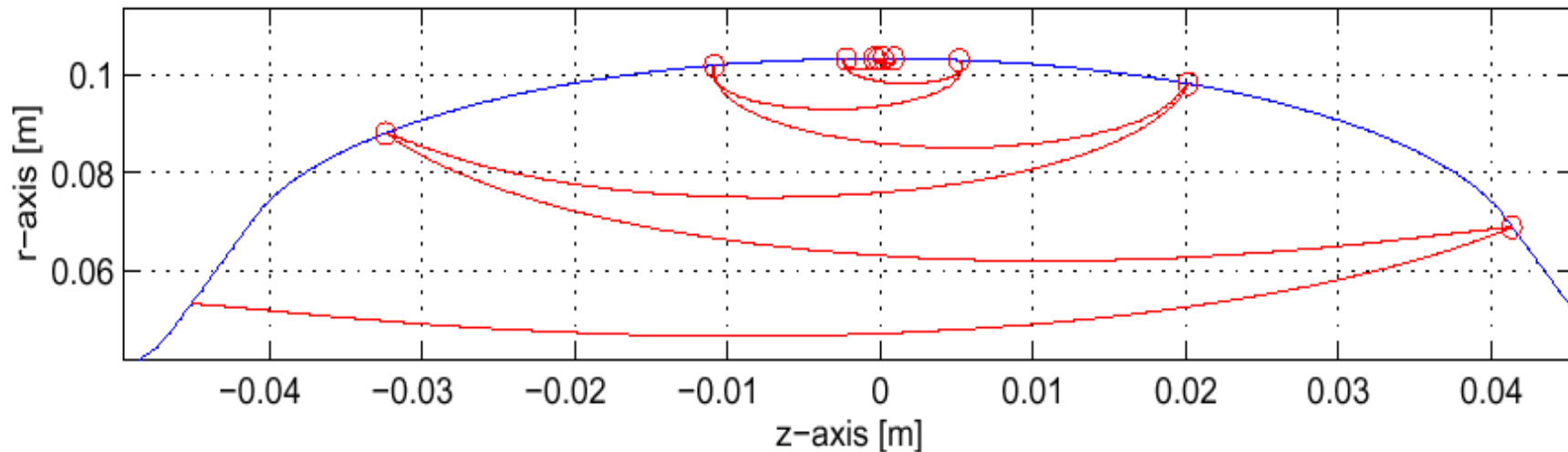
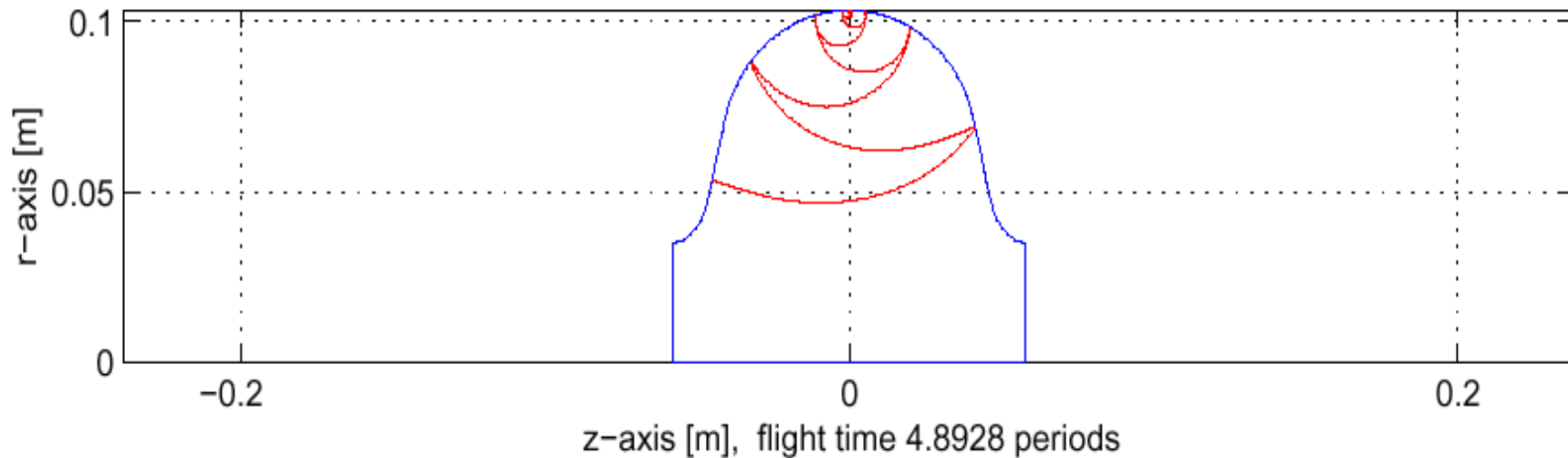
Empirical formula:

$$H_n [\text{Oe}] = \frac{0.6}{2n-1} f_0 [\text{MHz}]$$



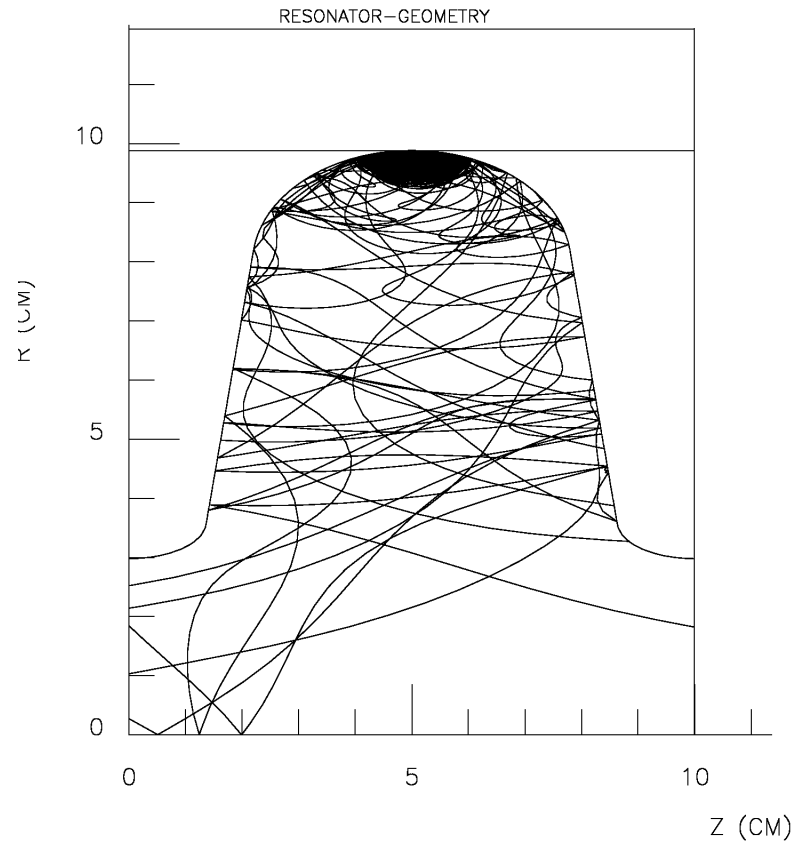
Two-Side Multipacting

MultiPac 2.1 Electron Trajectory, N = 10, 24-Apr-2002

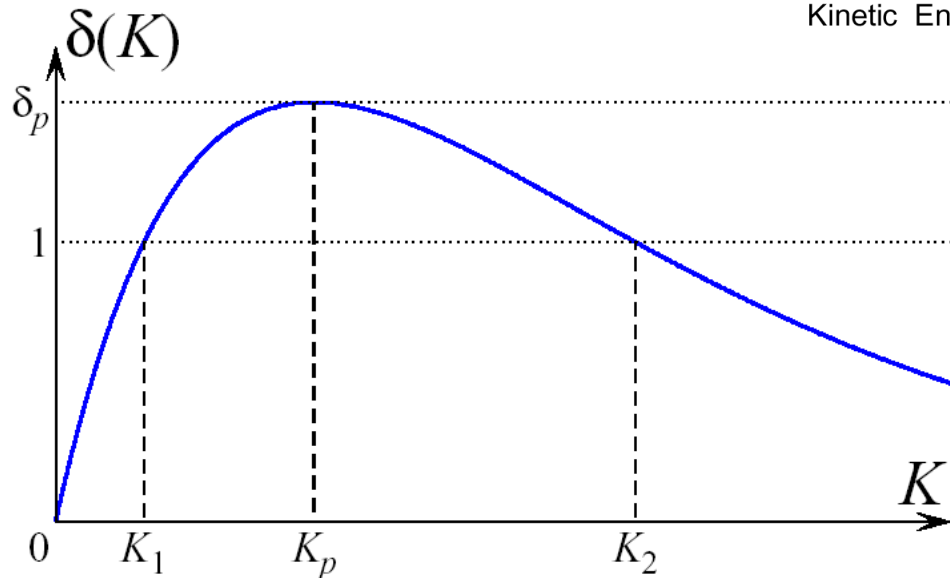
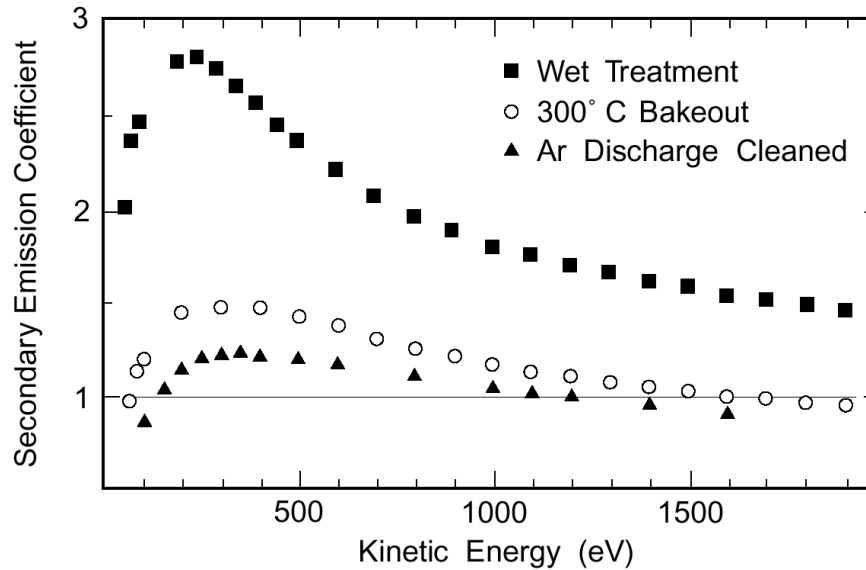


Multipacting Simulation

TRAJECTORIES #
EMAX= -14.260 MV/M BMAX= 224.389 GAUSS



Secondary Emission in Niobium



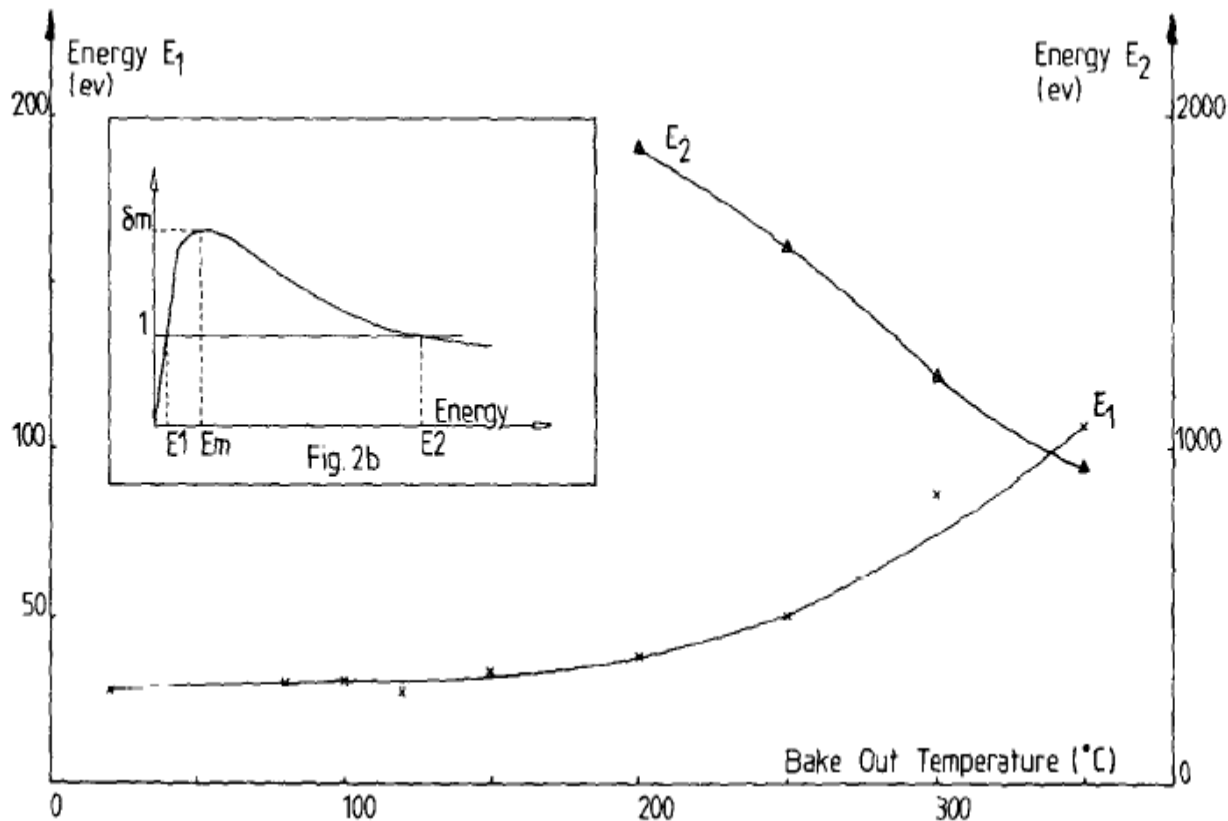
Condition	K_1	K_2
high SEY	~ 27 eV	$\gtrsim 2000$ eV
typical SEY	~ 40 eV	~ 1000 eV
low SEY	~ 150 eV	~ 750 eV

Secondary Emission in Niobium

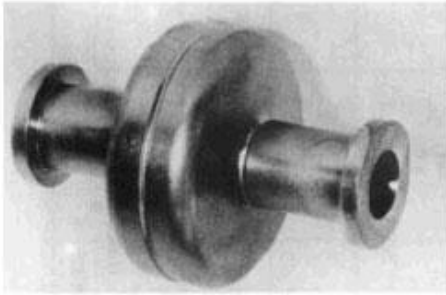
INFLUENCE OF VARIOUS VACUUM SURFACE TREATMENTS ON THE SECONDARY ELECTRON YIELD OF NIOBIUM

Roger CALDER, Georges DOMINICHINI and Noël HILLERET

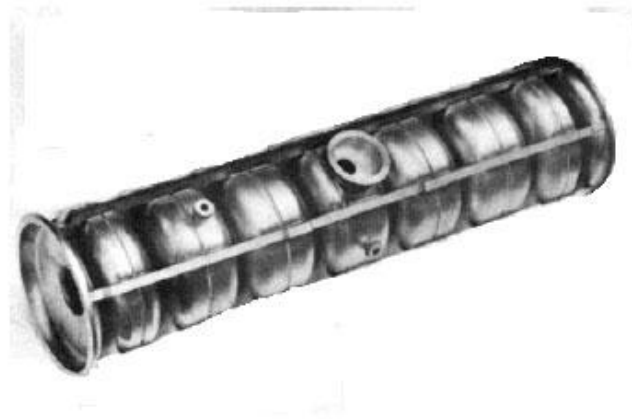
LEP-VA, CERN, 1211 Geneva 23, Switzerland



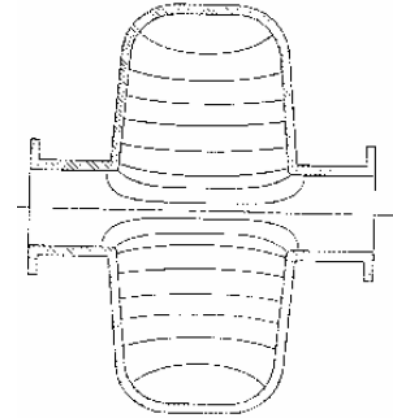
MP in SRF Cavities



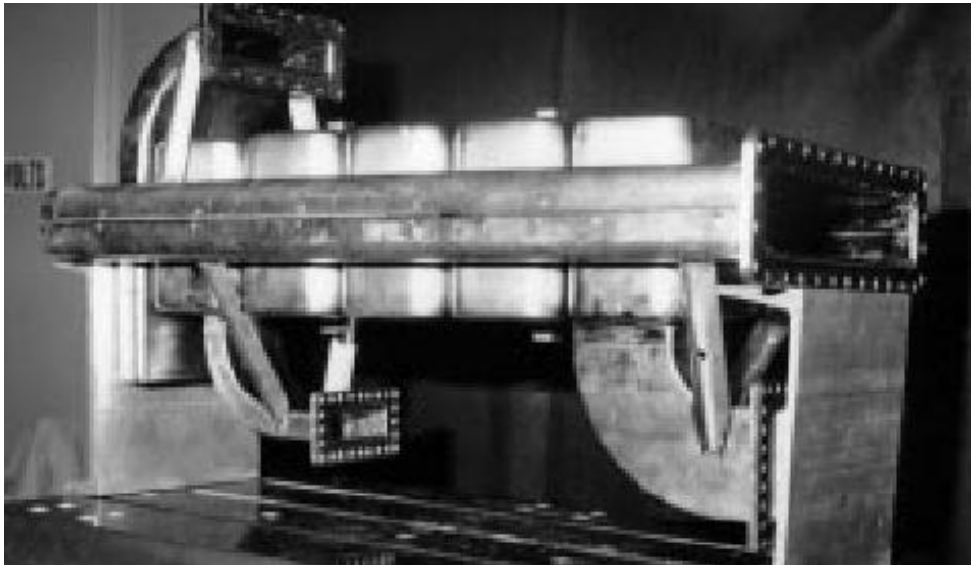
(a)



(b)



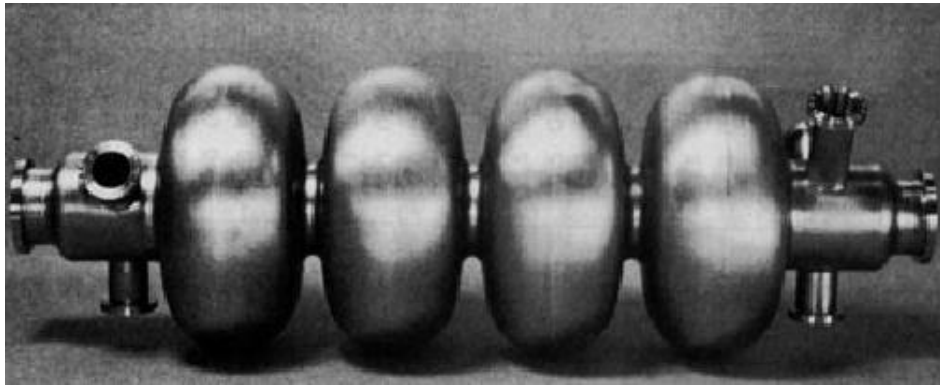
“Near pill-box” shape



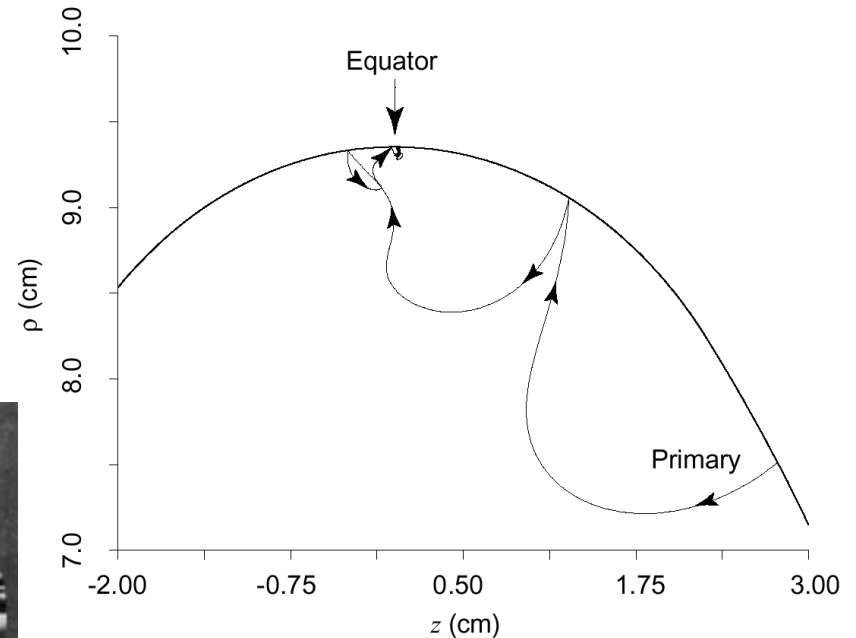
Early SRF cavity geometries (1960s-'70s) frequently limited by multipacting, usually at < 10 MV/m

MP in SRF Cavities

“Elliptical” cavity shape (1980s)



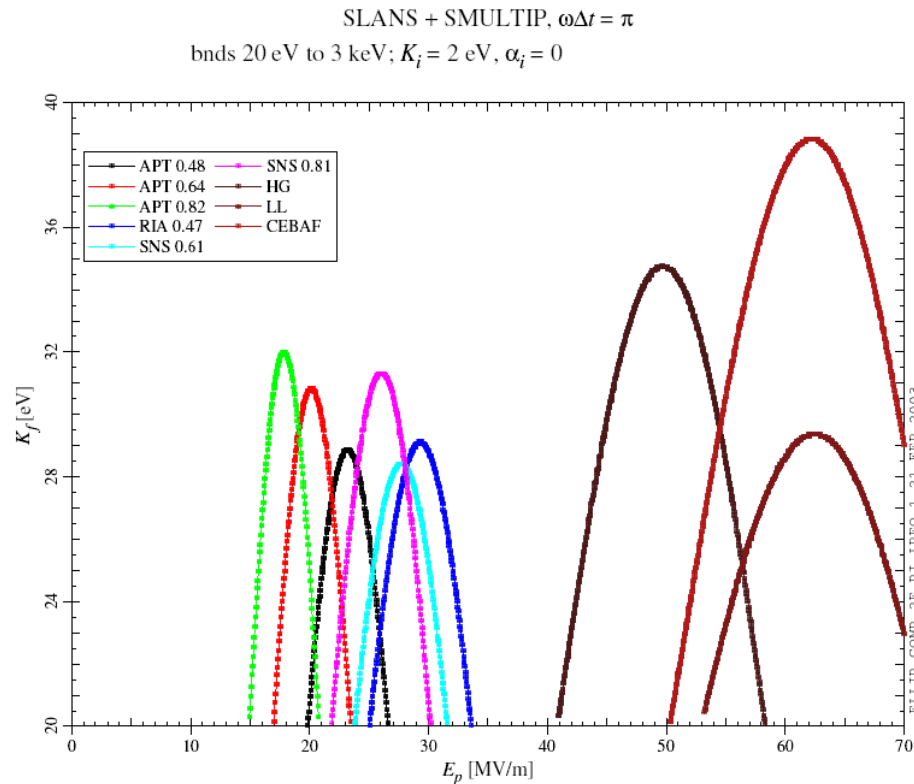
350-MHz LEP-II cavity (CERN)



Electrons drift to equator
Electric field at equator is ≈ 0
→MP electrons don't gain energy
→MP stops

Cures for Multipacting

- Cavity design

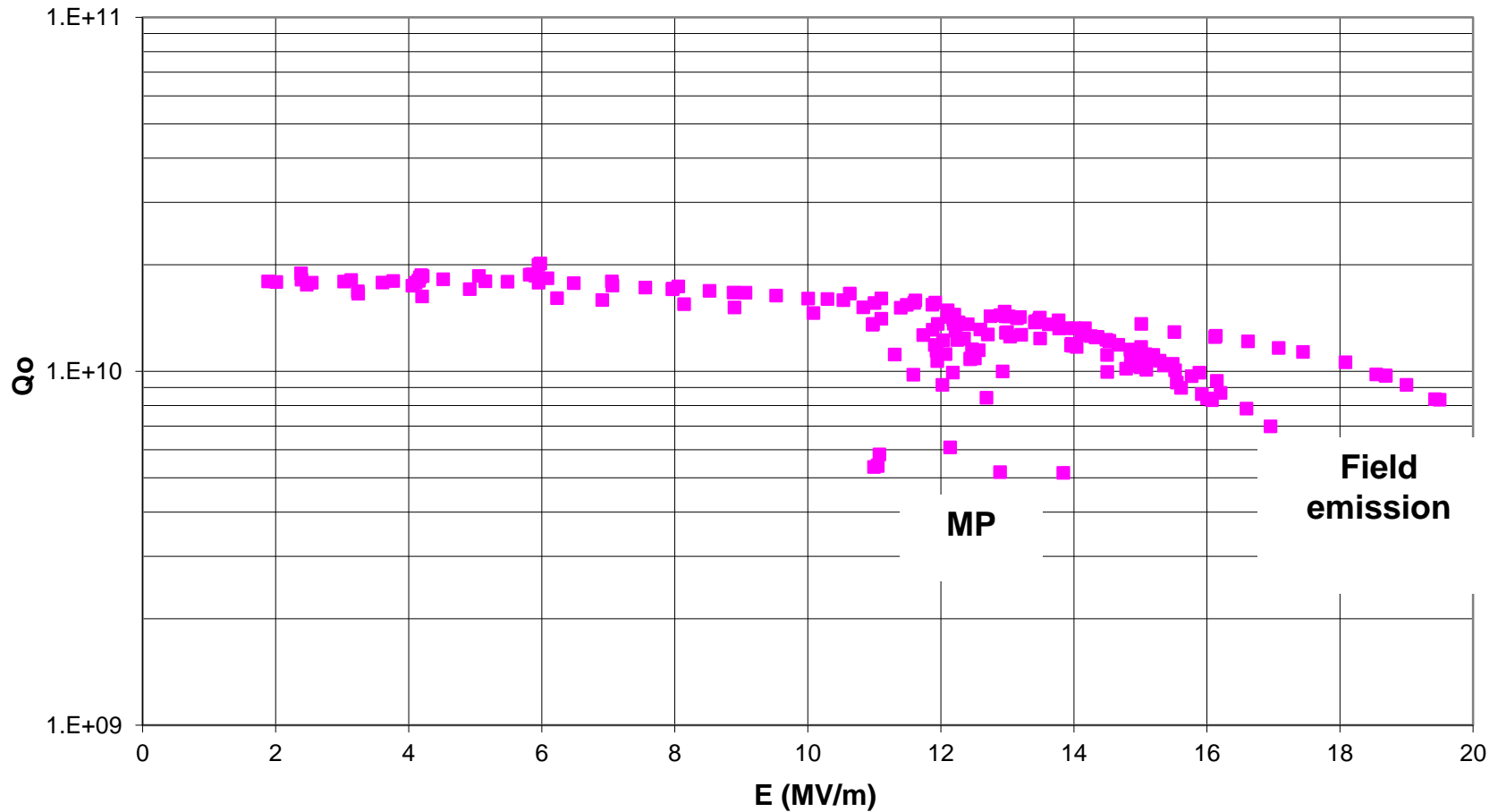


- Lower SEY: clean vacuum systems (low partial pressure of hydrocarbons, hydrogen and water), Ar discharge
- RF Processing: lower SEY by e^- bombardment (minutes to several hours)

Recent Examples of Multipacting

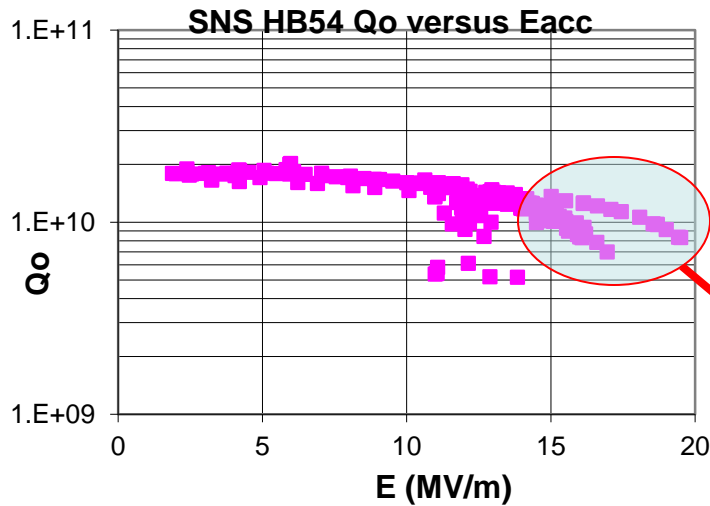
SNS HB54 Qo versus Eacc
Multipacting limited at 16MV/m 5/16/08 cg

2008

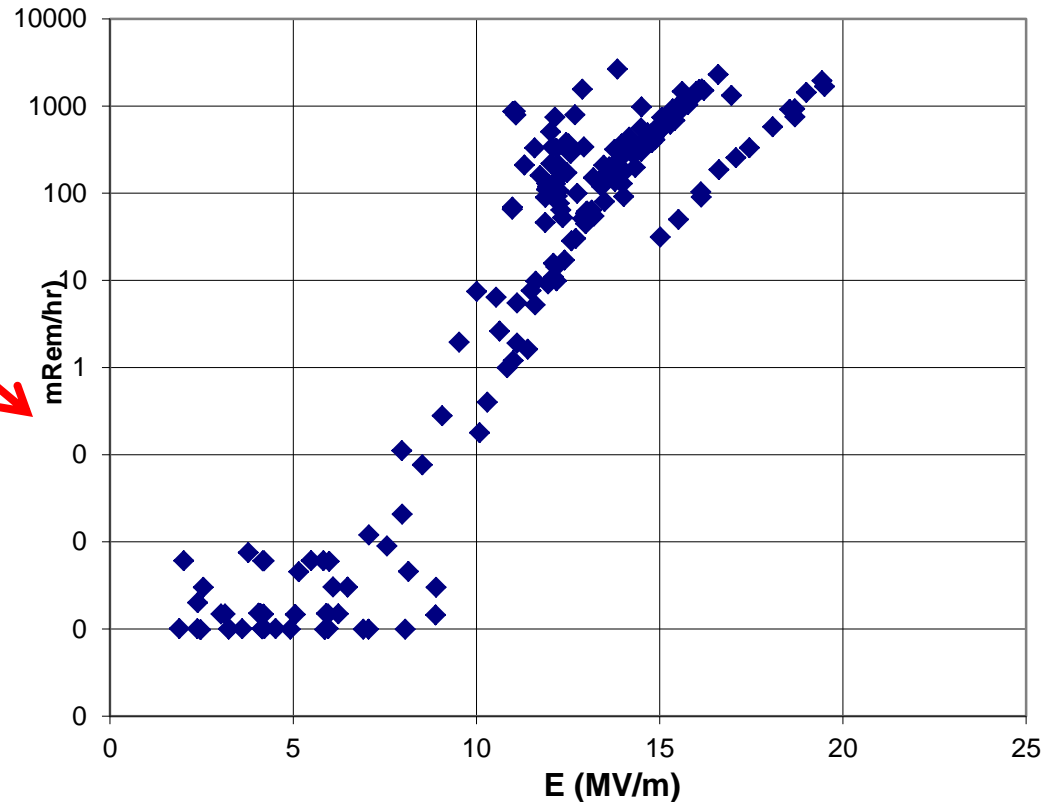


Field Emission

- Characterized by an exponential drop of the Q_0
- Associated with production of x-rays and emission of dark current

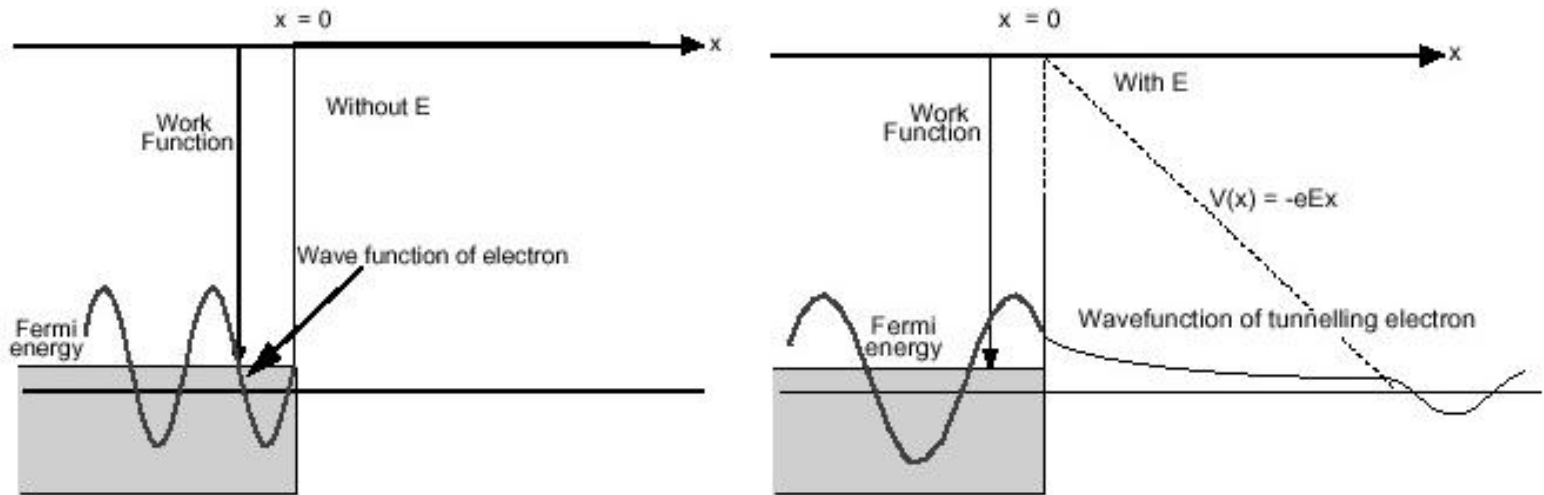


SNS HTB 54 Radiation at top plate versus Eacc 5/16/08 cg



DC Field Emission from Ideal Surface

Fowler-Nordheim model



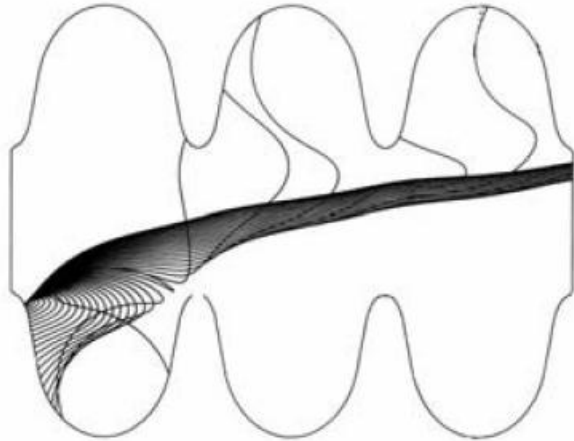
$$J = \frac{1.54 \times 10^{-6} E^2}{\Phi} \exp\left(-\frac{6.83 \times 10^9 \Phi^{3/2}}{E}\right)$$

J : Current density (A/m^2)

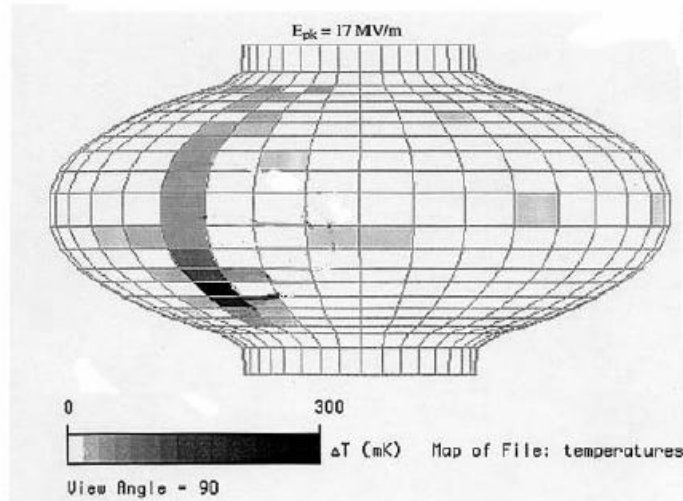
E : Electric field (V/m)

Φ : Work function (eV)

Field Emission in RF Cavities



Acceleration of electrons drains cavity energy



Impacting electrons produce:

- line heating detected by thermometry
- bremsstrahlung X rays



Foreign particulate found at emission site

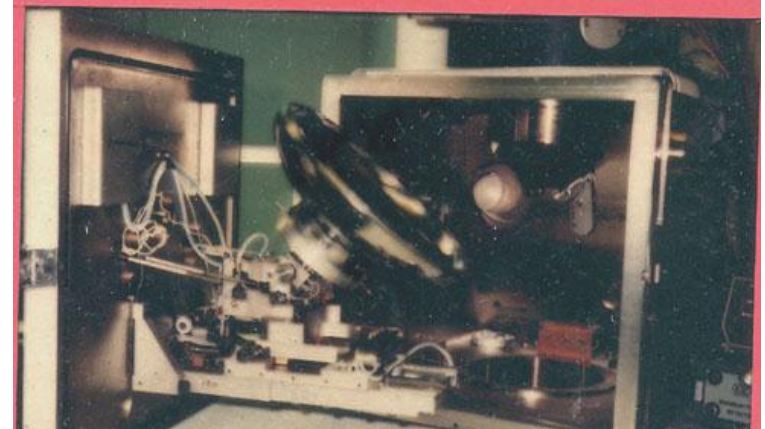
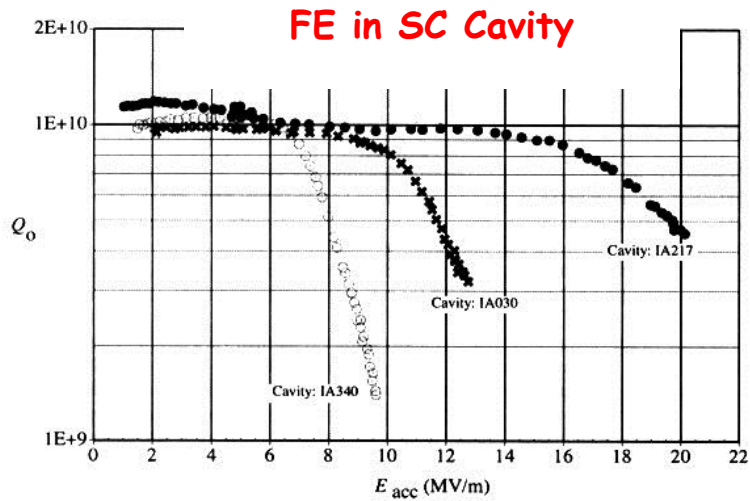
FE in cavities occurs at fields that are up to 1000 times lower than predicted...

$$J = k \frac{1.54 \times 10^{-6} (\beta E)^{5/2}}{\Phi} \exp\left(-\frac{6.83 \times 10^9 \Phi^{3/2}}{\beta E}\right)$$

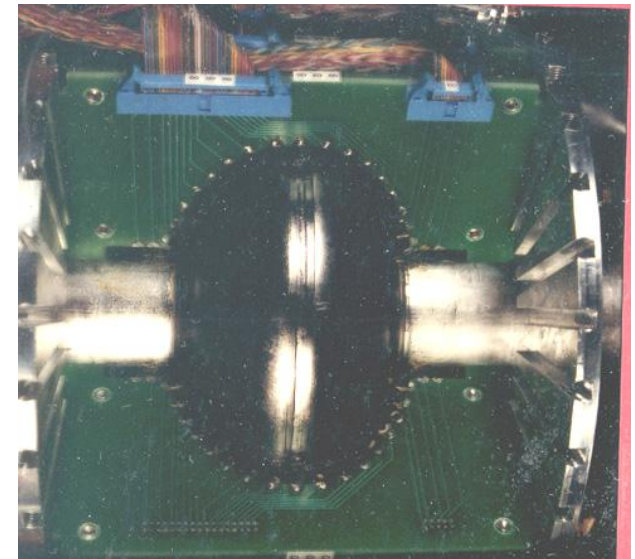
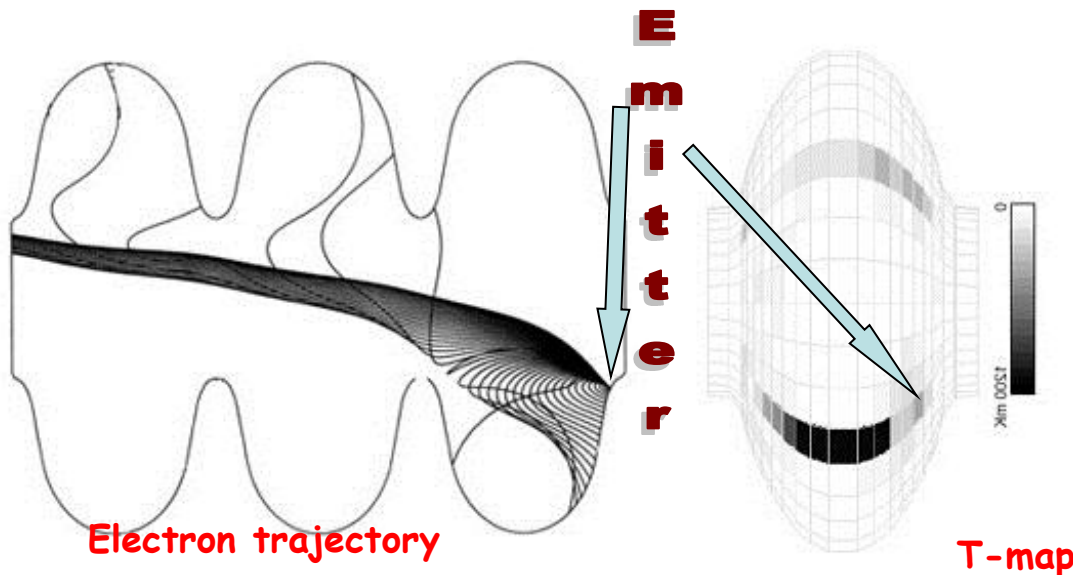
β : Enhancement factor (10s to 100s)

k : Effective emitting surface

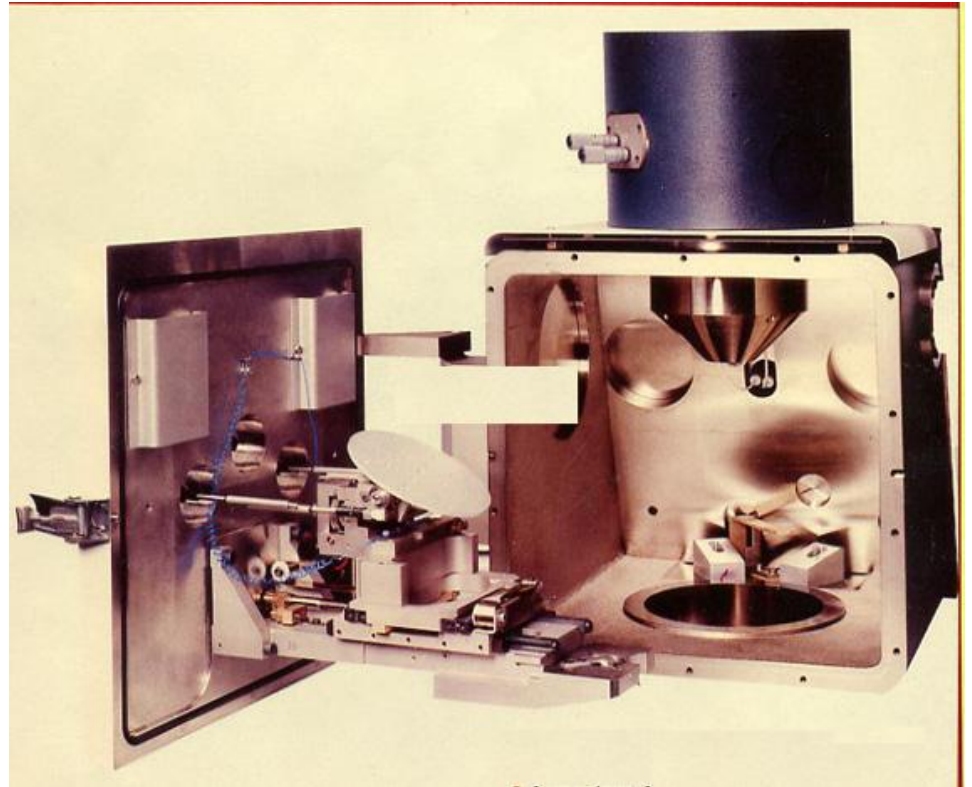
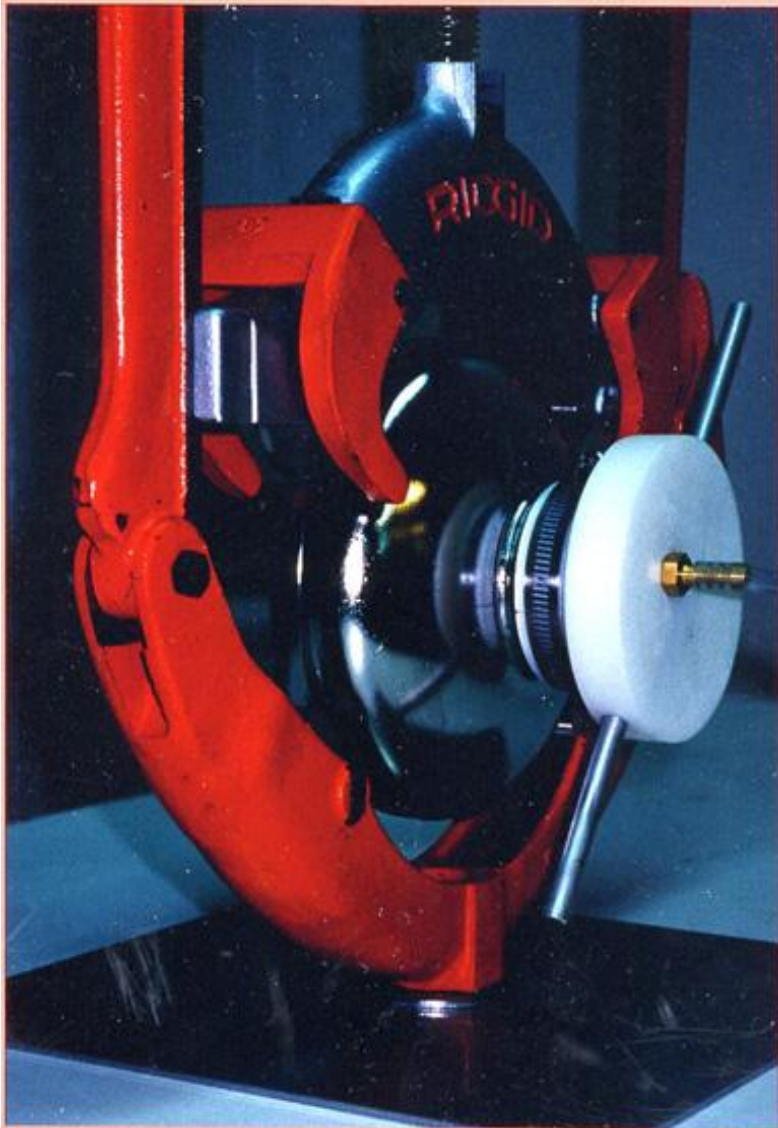
How to Investigate Field Emission



Dissection and analysis

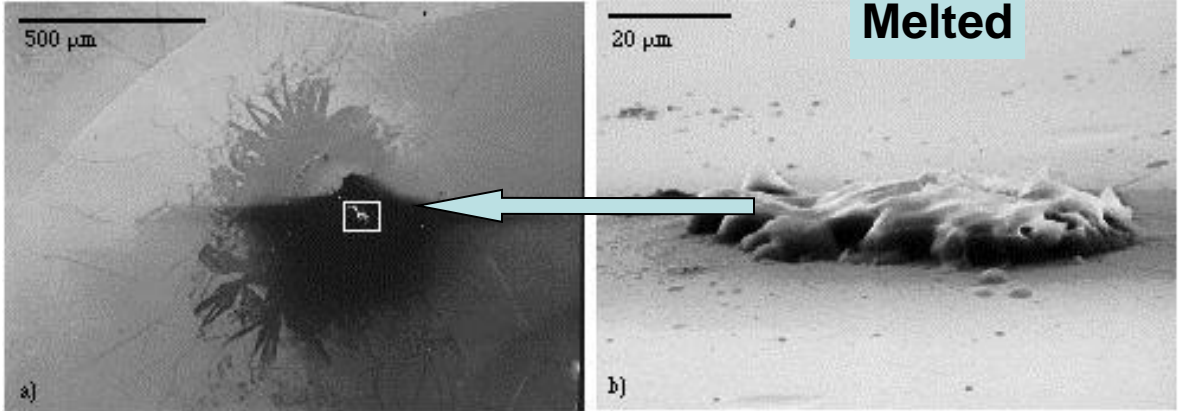
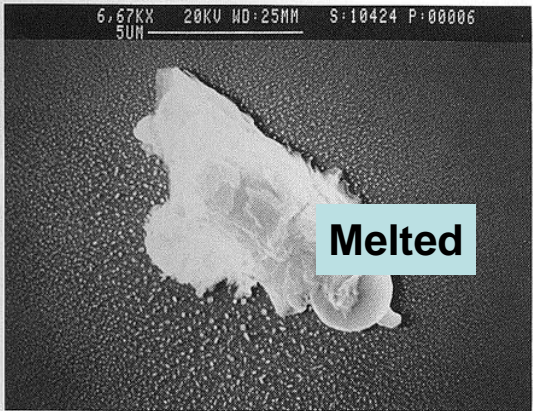
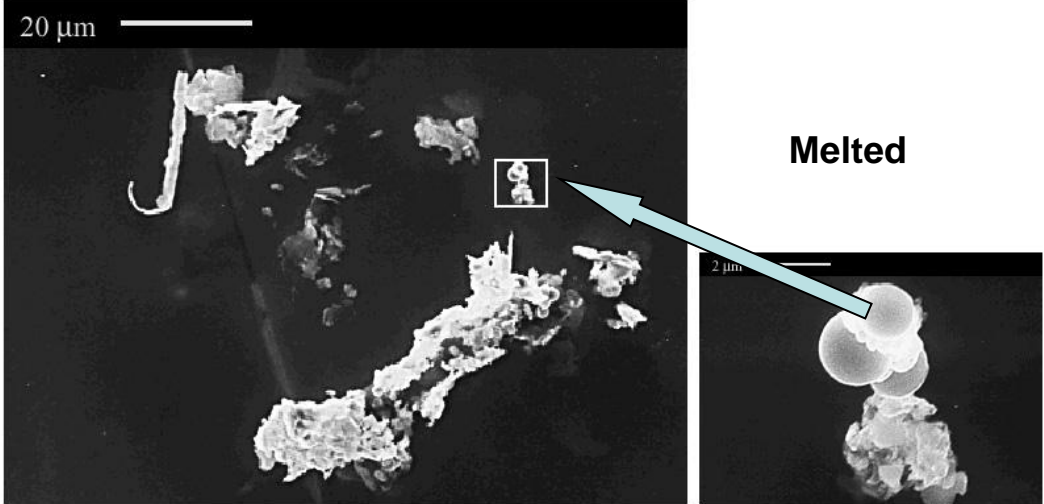
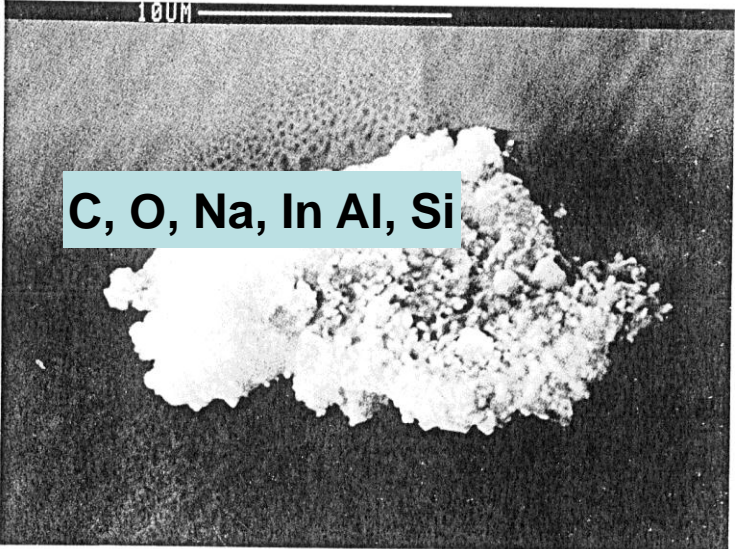


Dissection and SEM

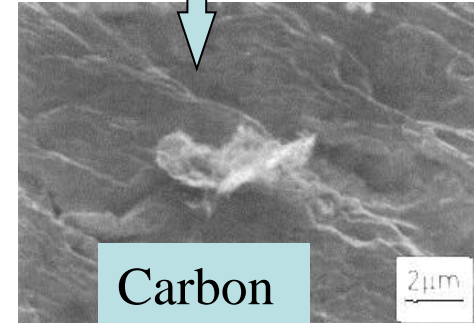
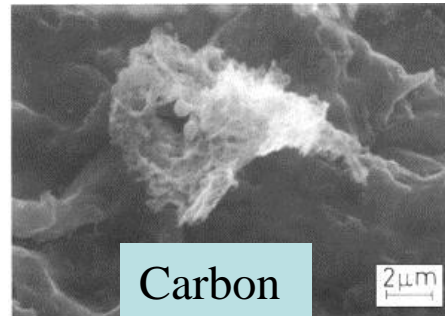
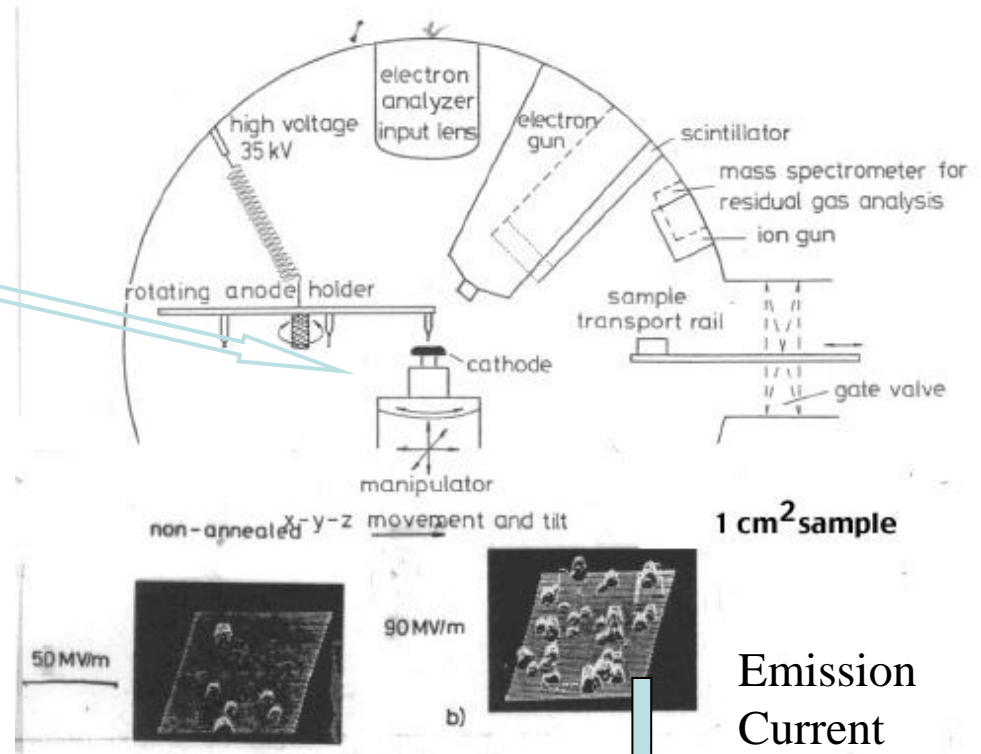
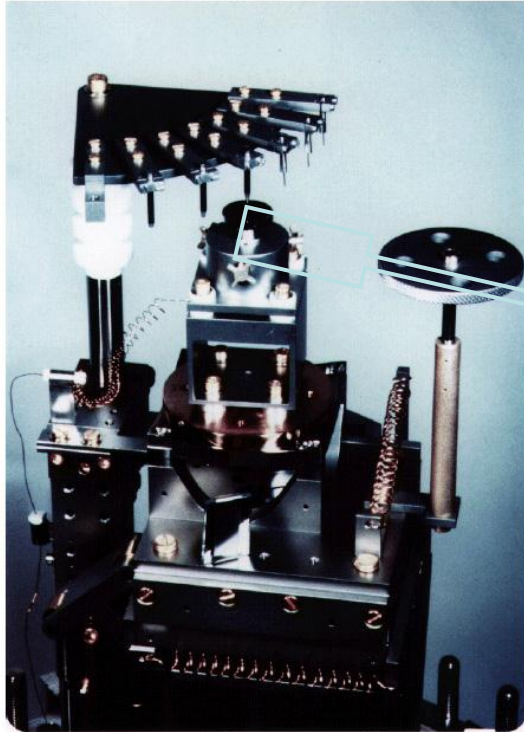


Example of Field Emitters

Stainless steel

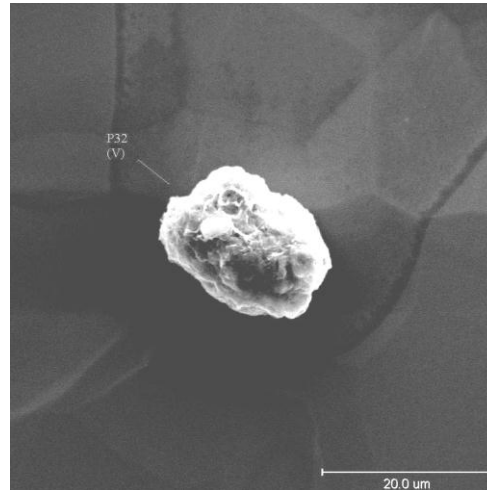
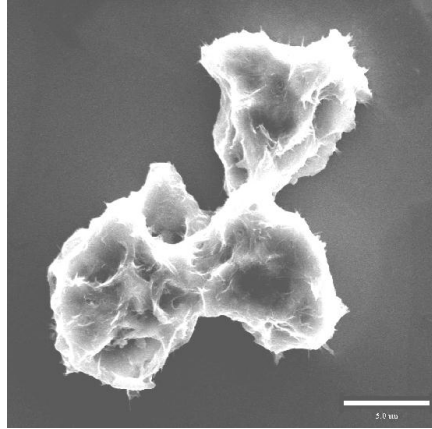


DC Field Emission Microscope



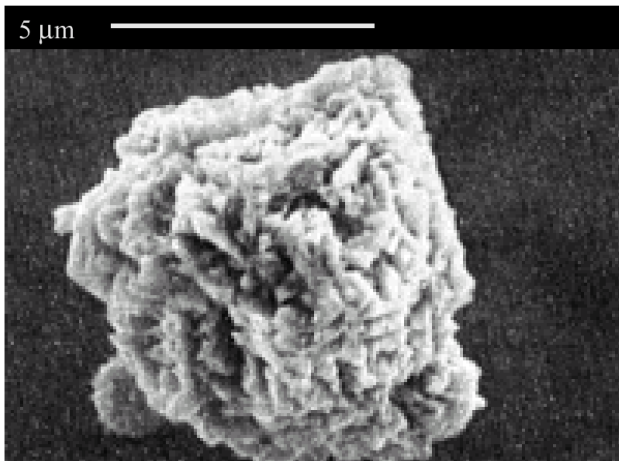
Type of Emitters

V

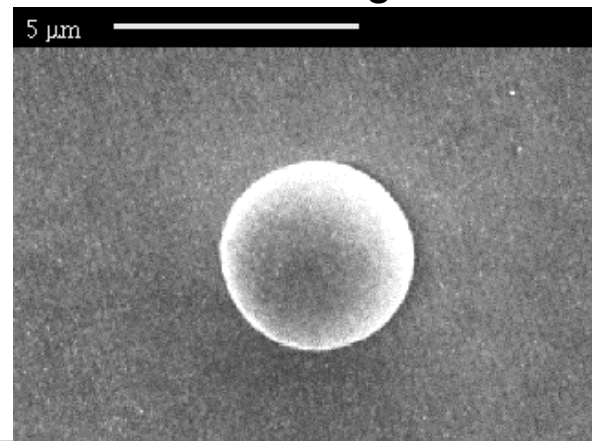


• *Tip-on-tip* model explains why only 10% of particles are emitters for $E_{pk} < 200$ MV/m.

Ni

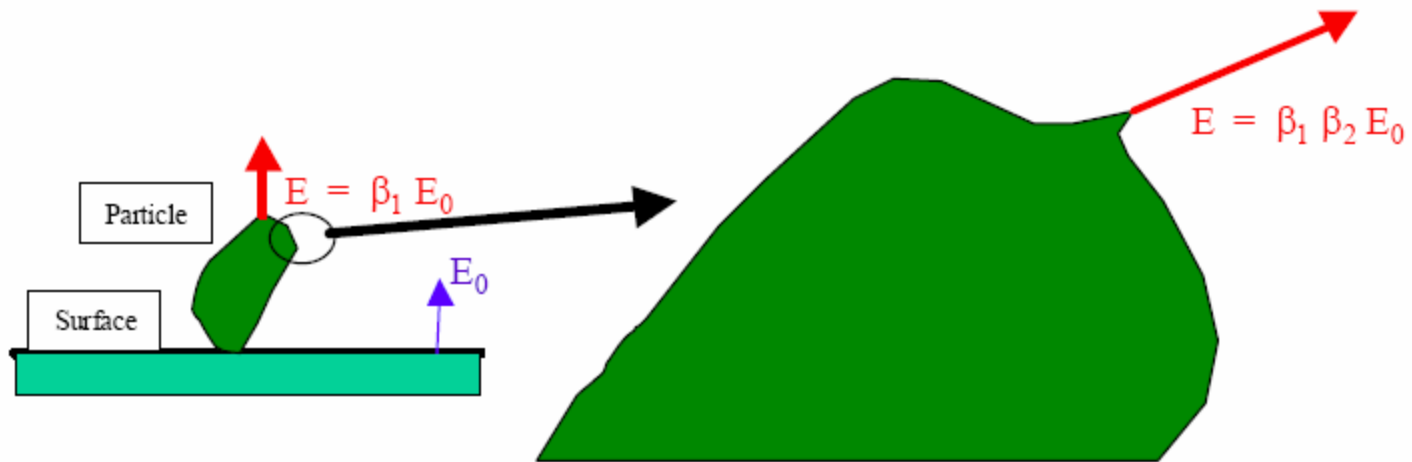


Smooth nickel particles emit less or emit at higher fields.

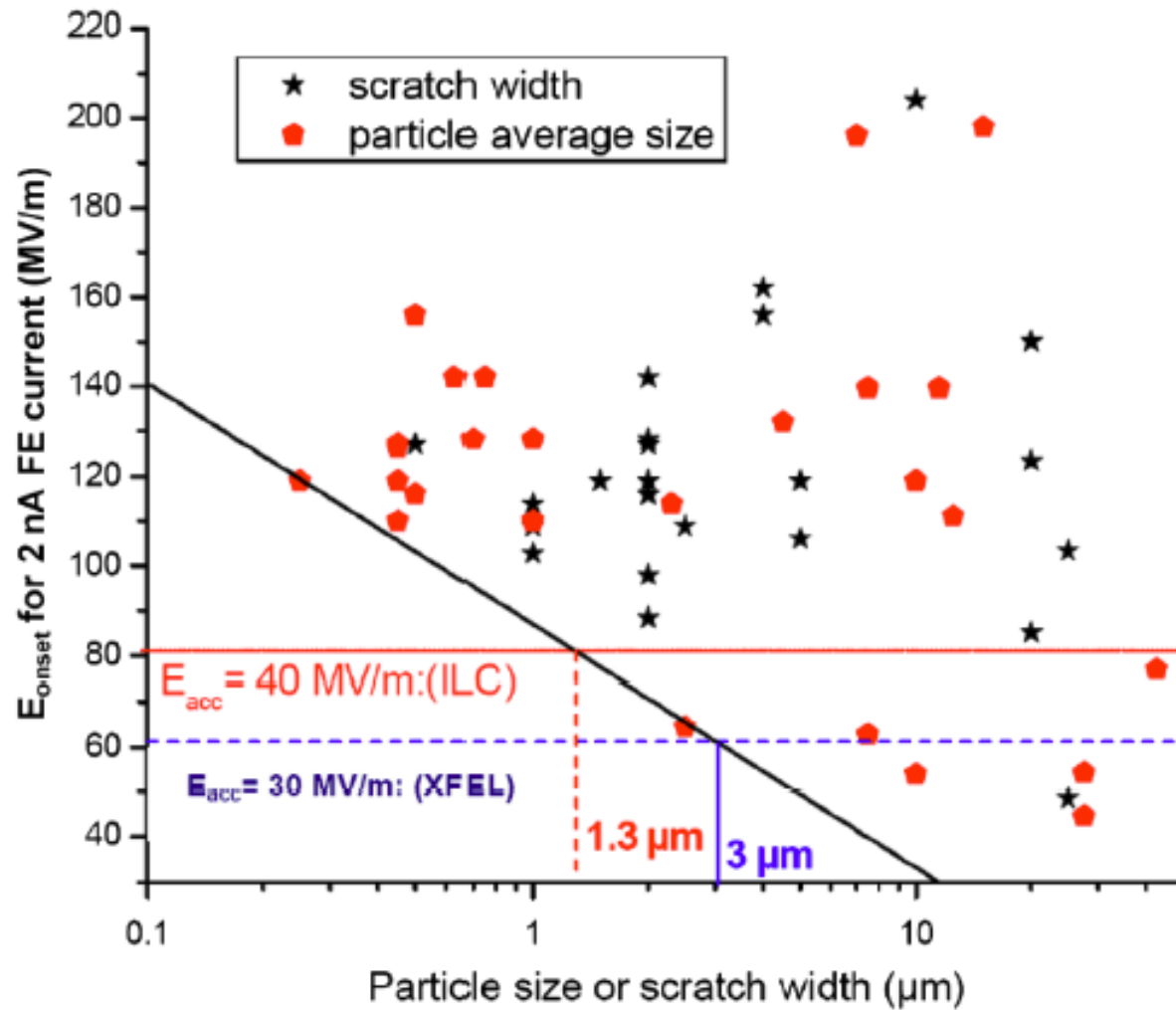


Tip-on-tip Model

- Smooth particles show little field emission
- Simple protrusions are not sufficient to explain the measured enhancement factors
- Possible explanation: tip-on-tip (compounded enhancement)

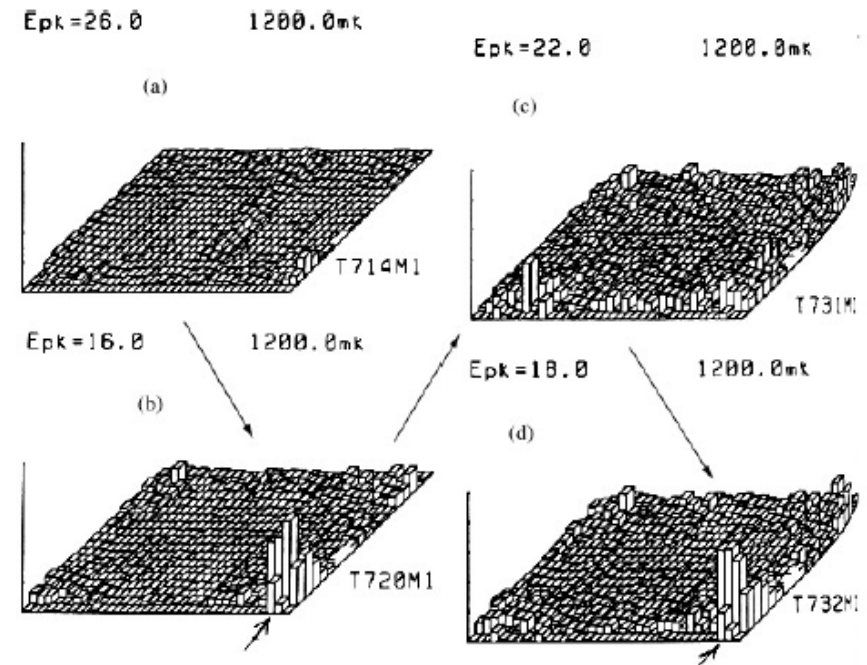
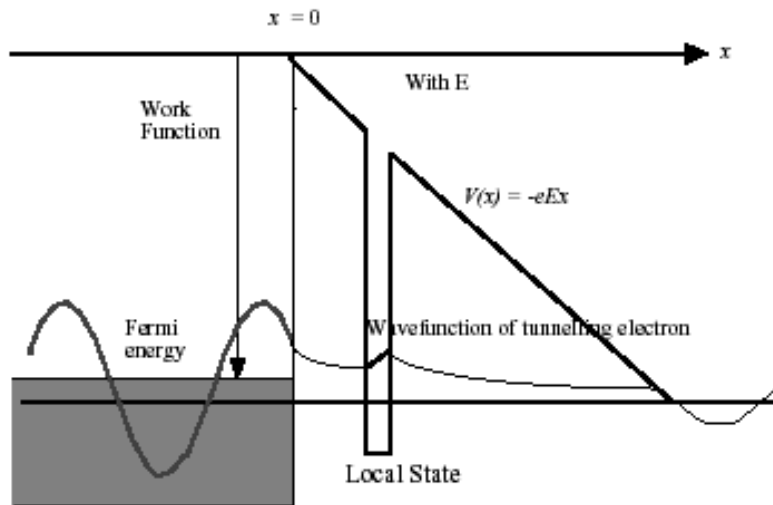


FE onset vs. Particulate Size

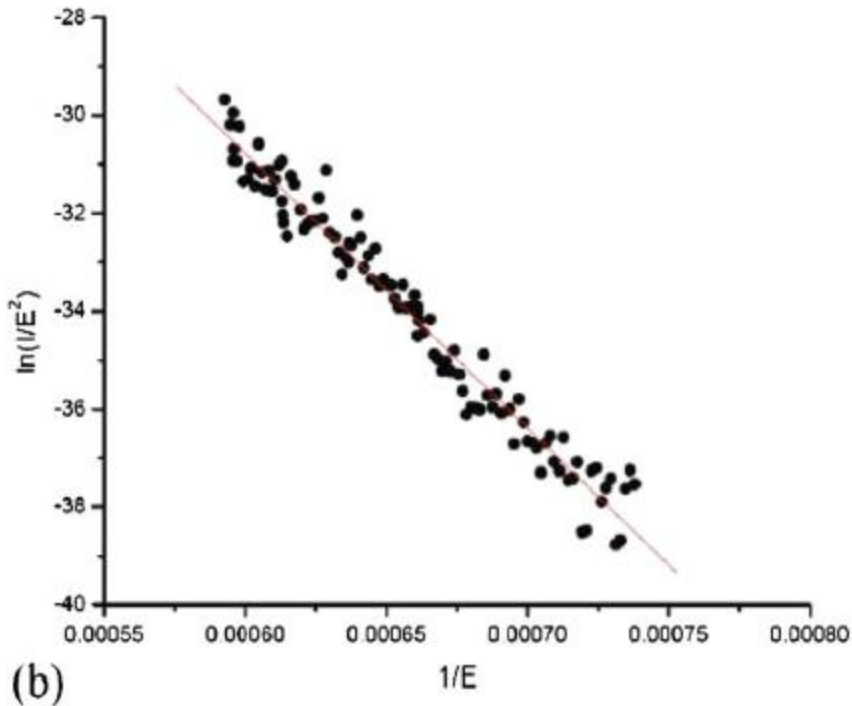


Enhancement by Absorbates

Adsorbed atoms on the surface can enhance the tunneling of electrons from the metal and increase field emission



Intrinsic FE of Nb



Single-crystal Nb samples showed FE onset higher than **1 GV/m**.

The work function was obtained from the I-V curves:

$$\Phi = 4.05 \pm 17\% \text{ eV for Nb (111)}$$

$$\Phi = 3.76 \pm 27\% \text{ eV for Nb (100)}$$

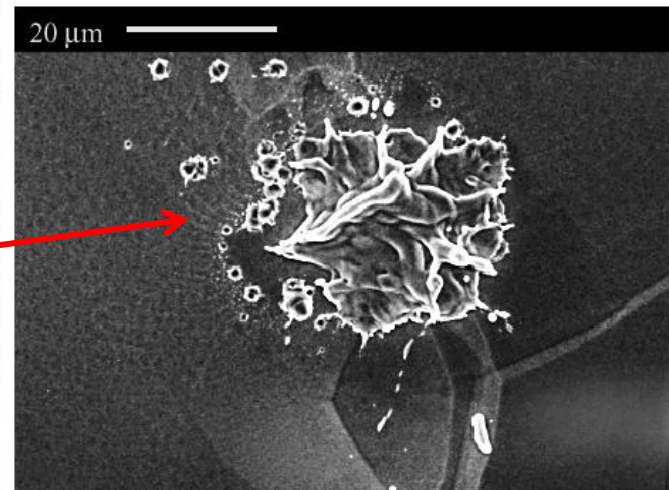
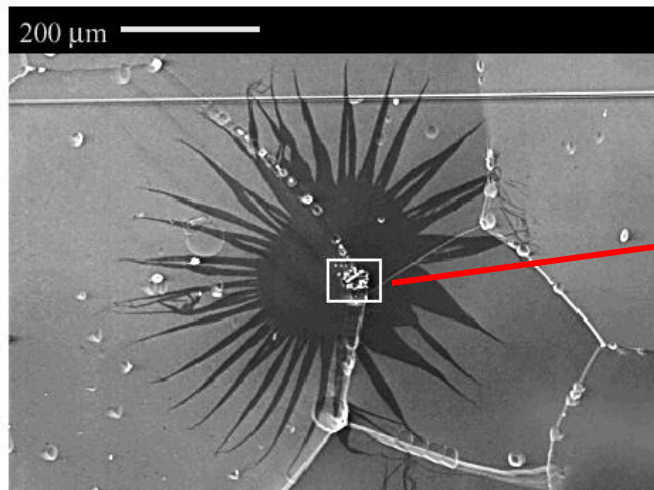
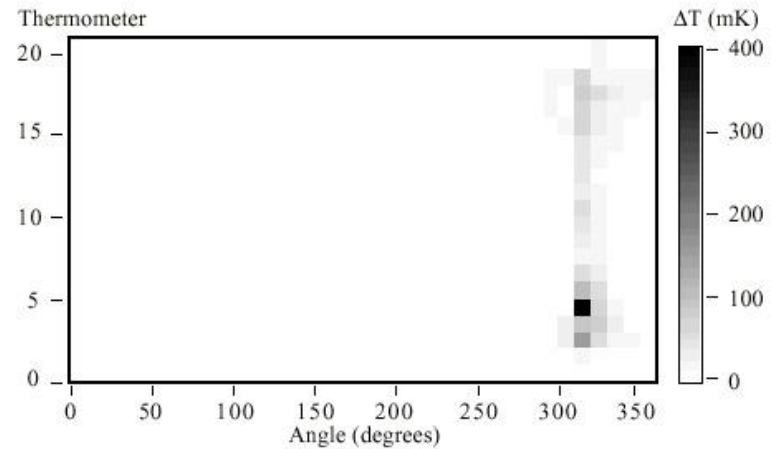
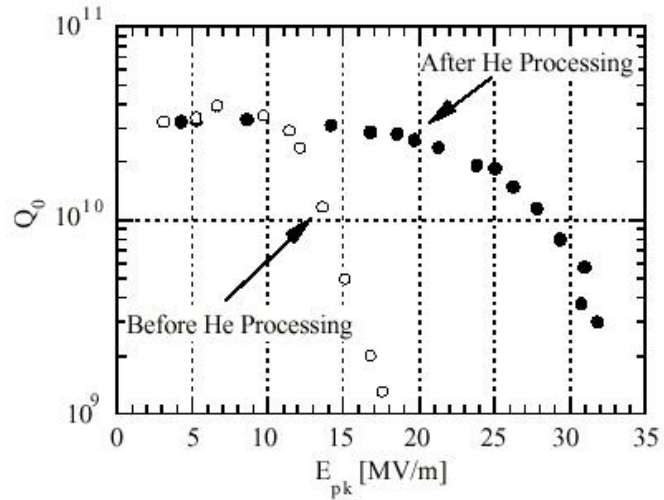
Cures for Field Emission

- **Prevention:**
 - Semiconductor grade acids and solvents
 - High-Pressure Rinsing with ultra-pure water
 - Clean-room assembly
 - Simplified procedures and components for assembly
 - Clean vacuum systems (evacuation and venting without re-contamination)
- **Post-processing:**
 - Helium processing
 - High Peak Power (HPP) processing

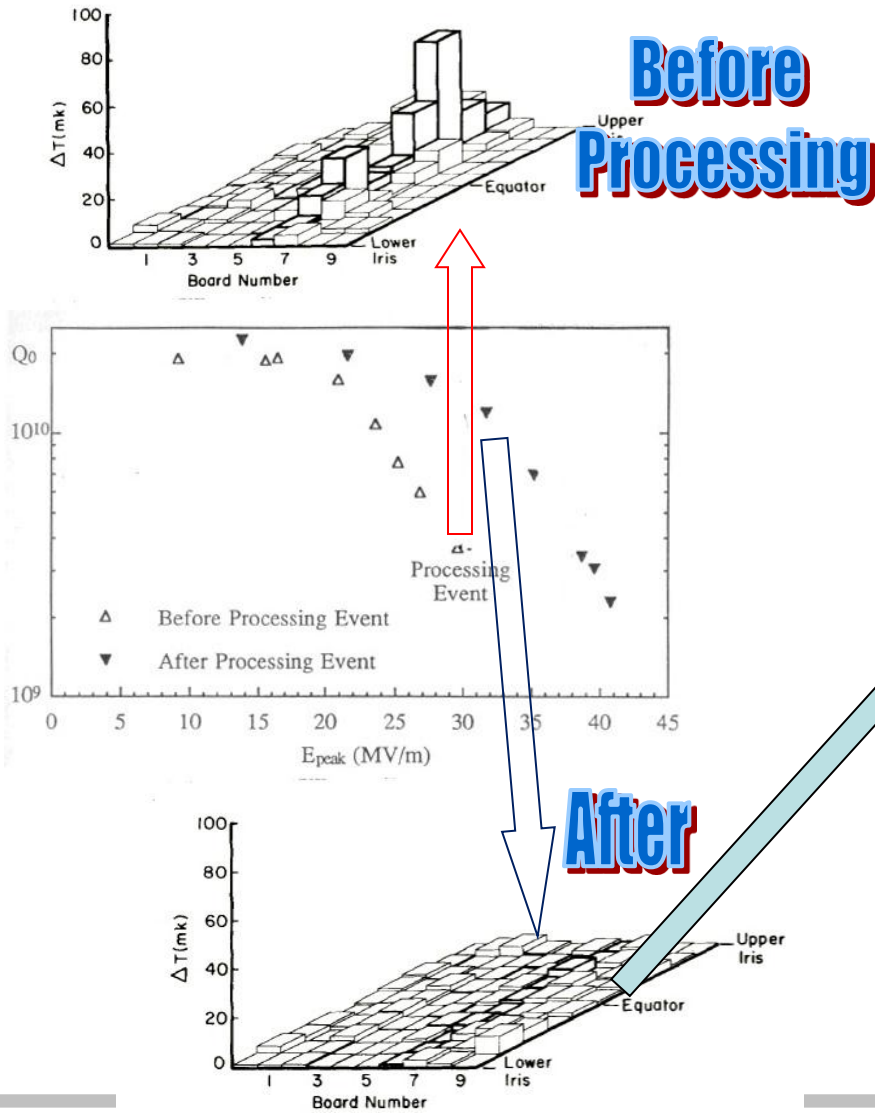
Helium Processing

- Helium gas is introduced in the cavity at a pressure just below breakdown ($\sim 10^{-5}$ torr)
- Cavity is operating at the highest field possible (in heavy field emission regime)
- Duty cycle is adjusted to remain thermally stable
- Field emitted electrons ionized helium gas
- Helium ions stream back to emitting site
 - Cleans surface contamination
 - Sputters sharp protrusions

Helium Processing

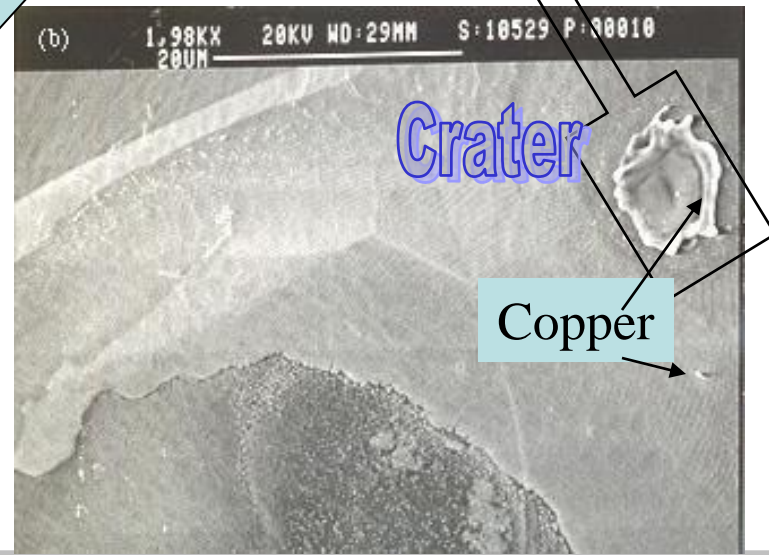


Helium Processing



Starburst
&
Crater

SEM



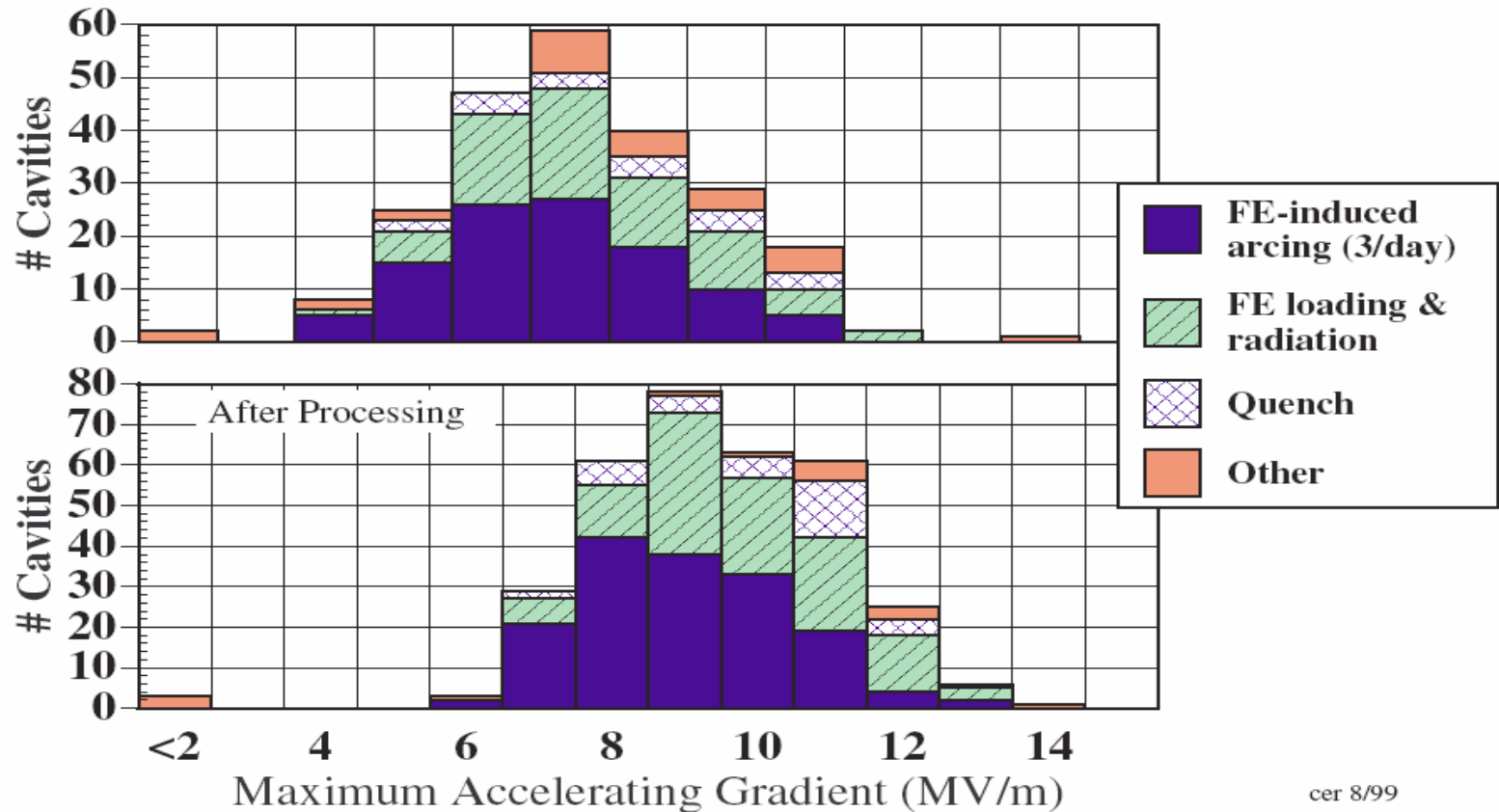
Crater

Copper

Helium Processing in CEBAF

Improvement of Cavity Performance with Helium Processing

Distribution of Maximum Gradients by Type of Limitation



cer 8/99

Helium Processing in CEBAF

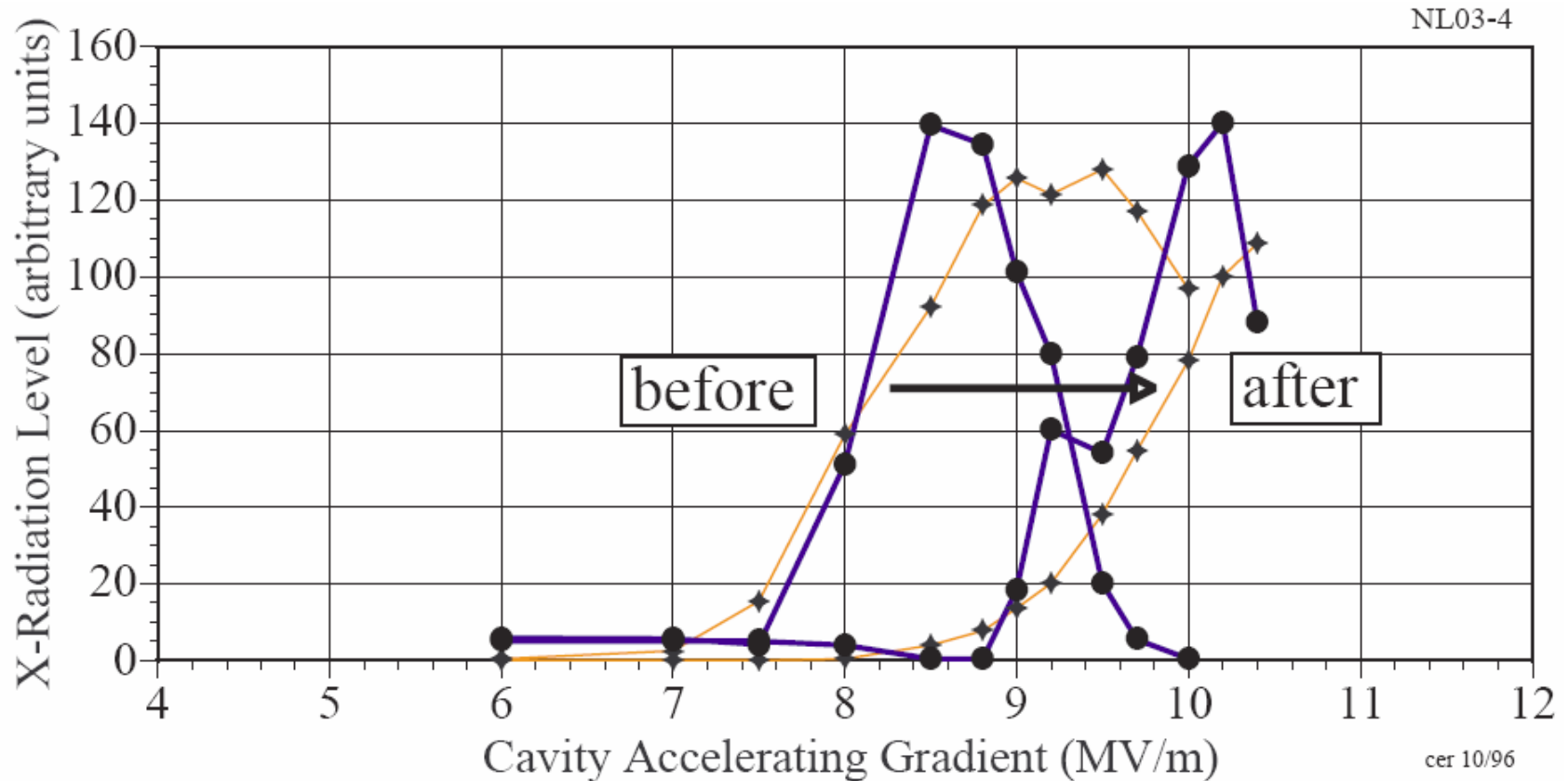
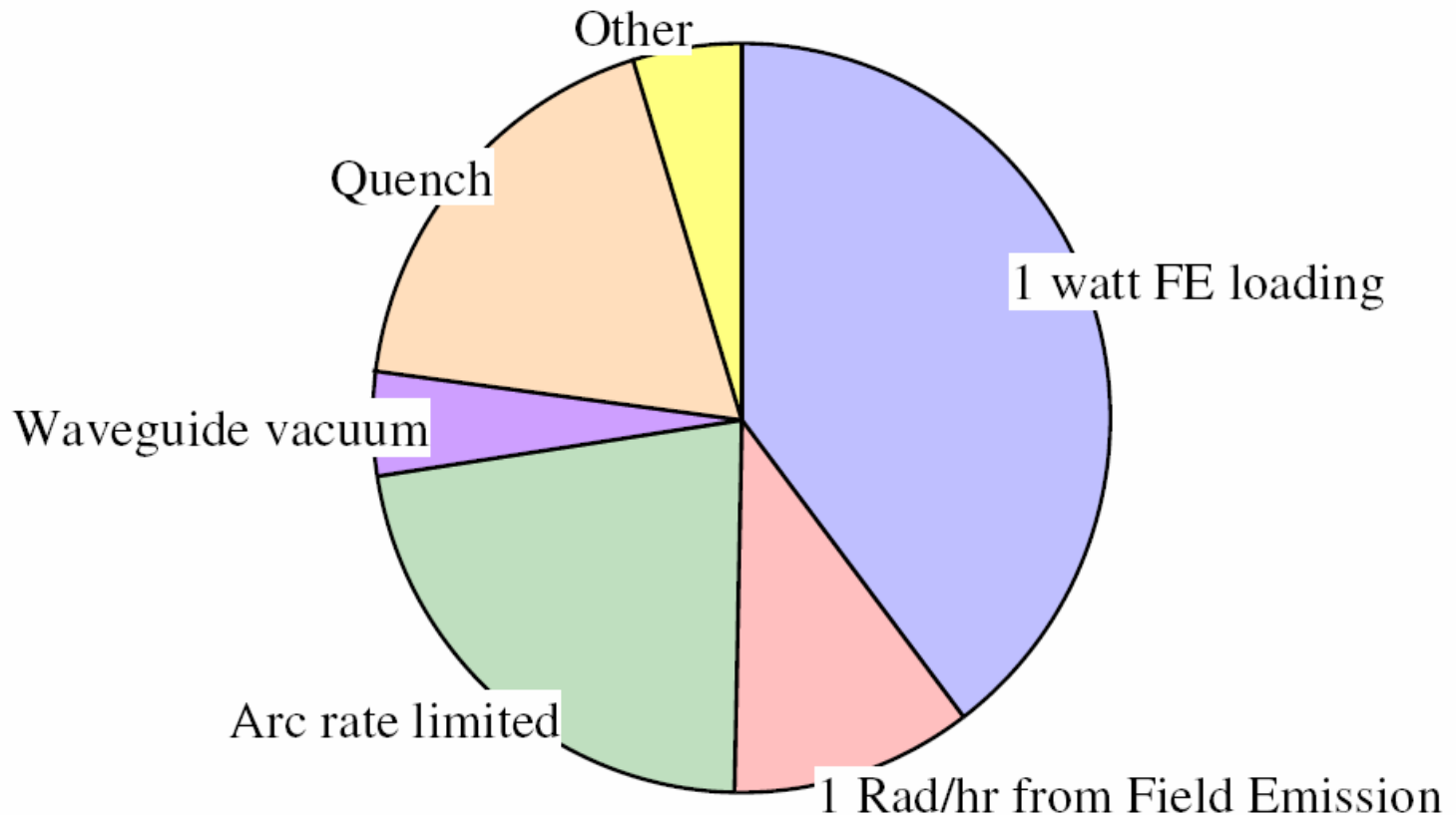
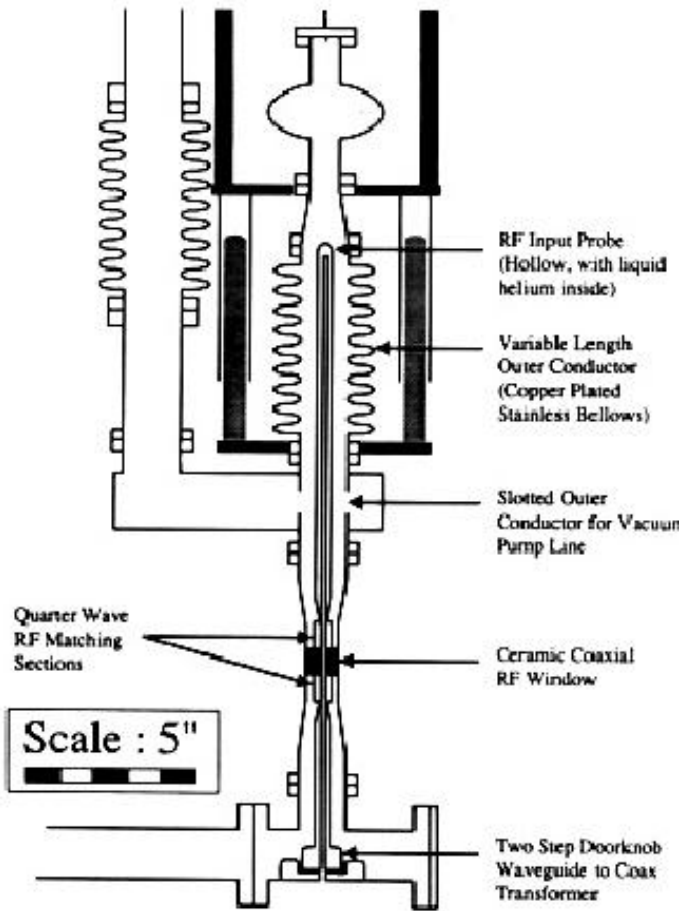


Figure 1. Radiation reduction with He processing.

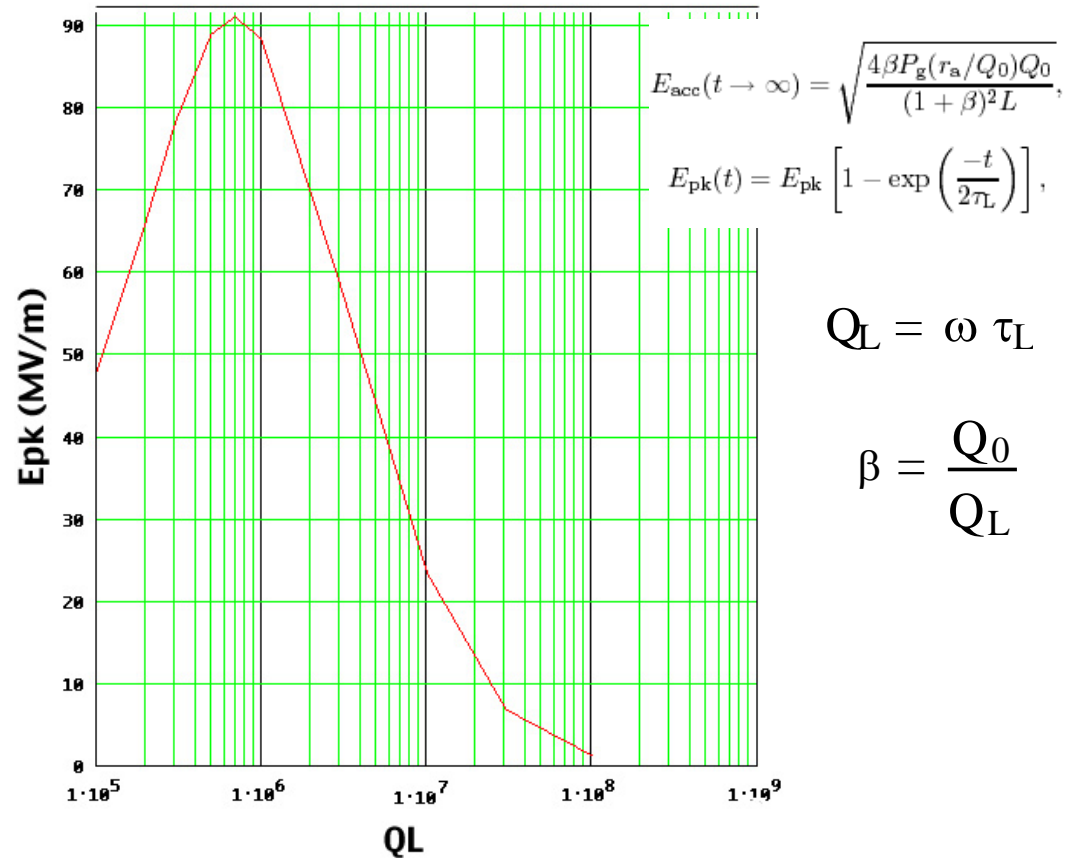
Practical Limitations (CEBAF)



High Peak Power Processing

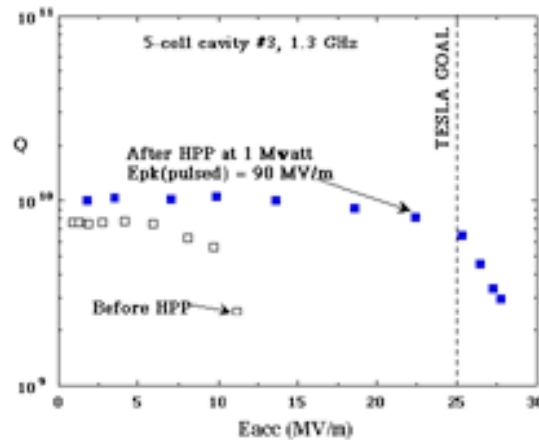
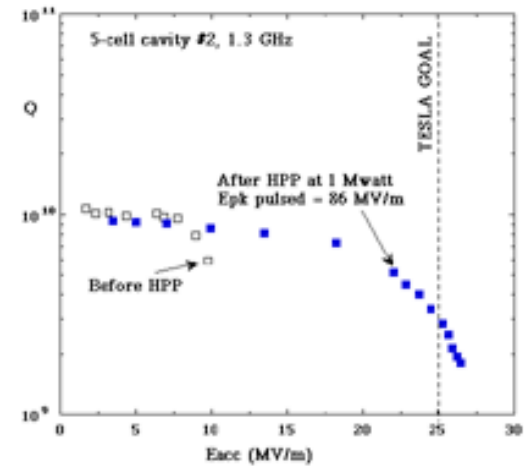
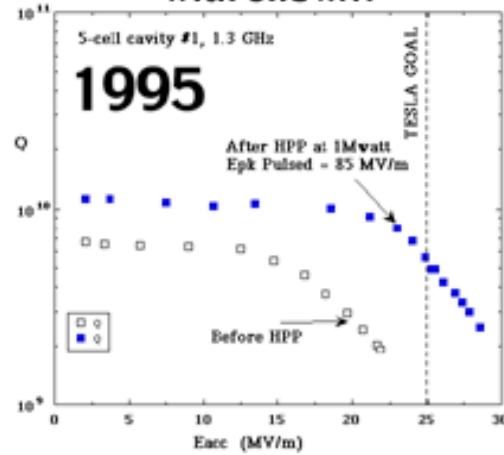
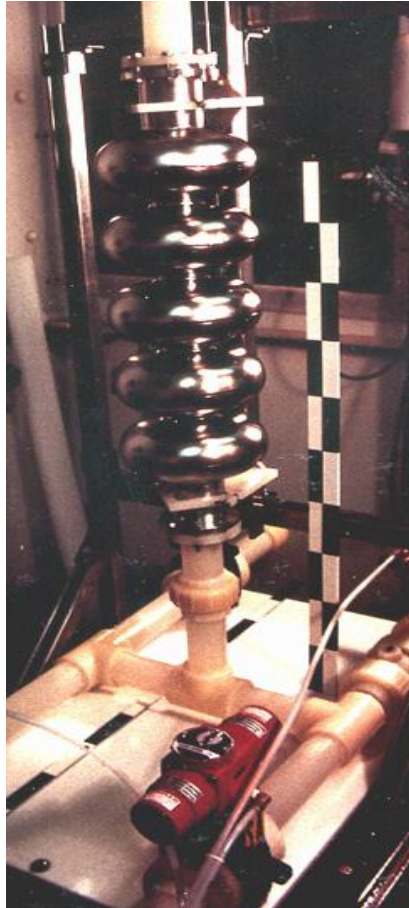


Power = 1.5 MW
Pulse Length = 250 us



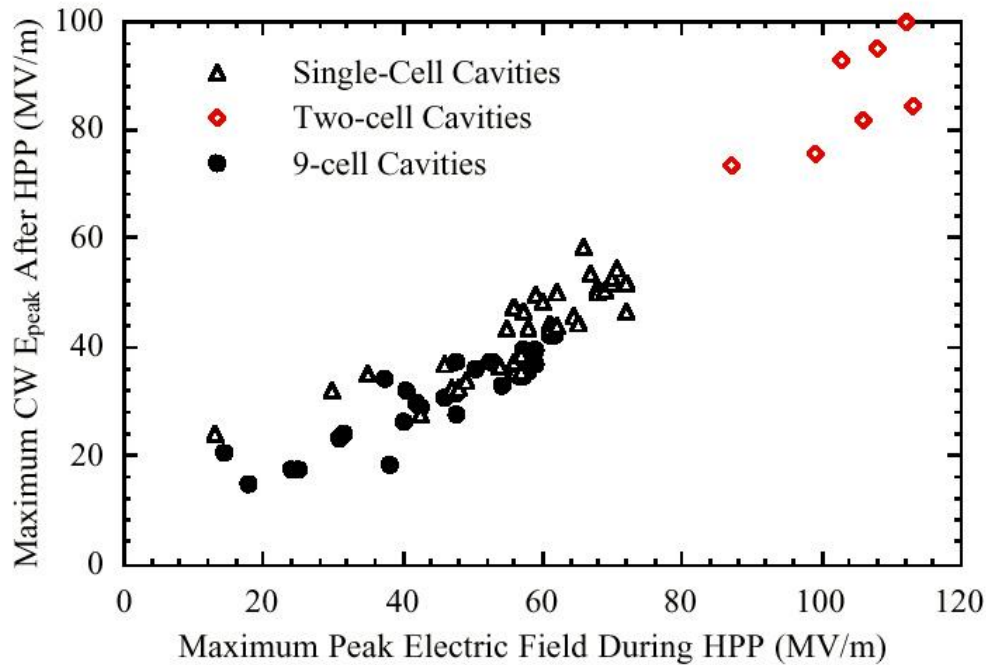
High Peak Power Processing

5-cell 1.3 GHz cavities High Pulse Power Processing with one MW



local melting leads to formation of a plasma
and finally to the explosion of the emitter
→ “star bursts” caused by the plasma

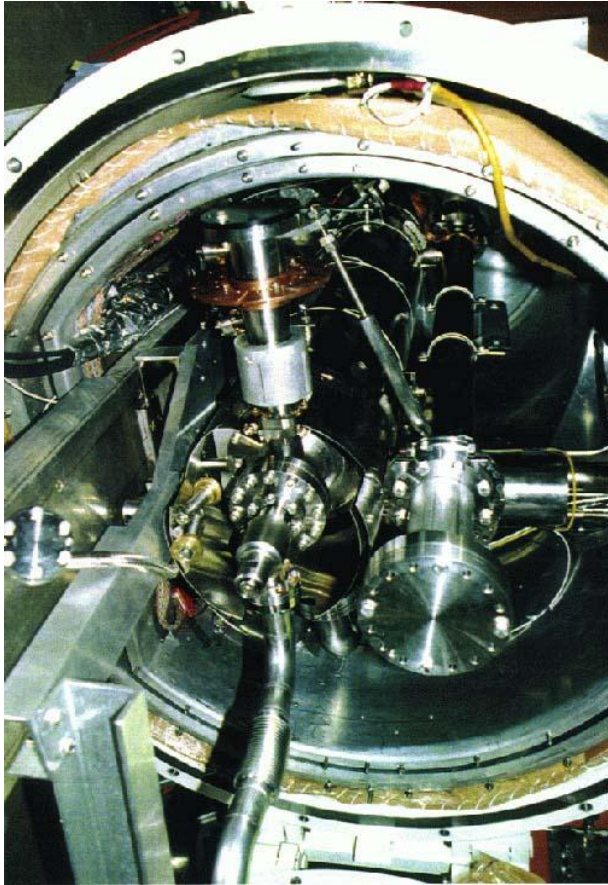
High Peak Power Processing



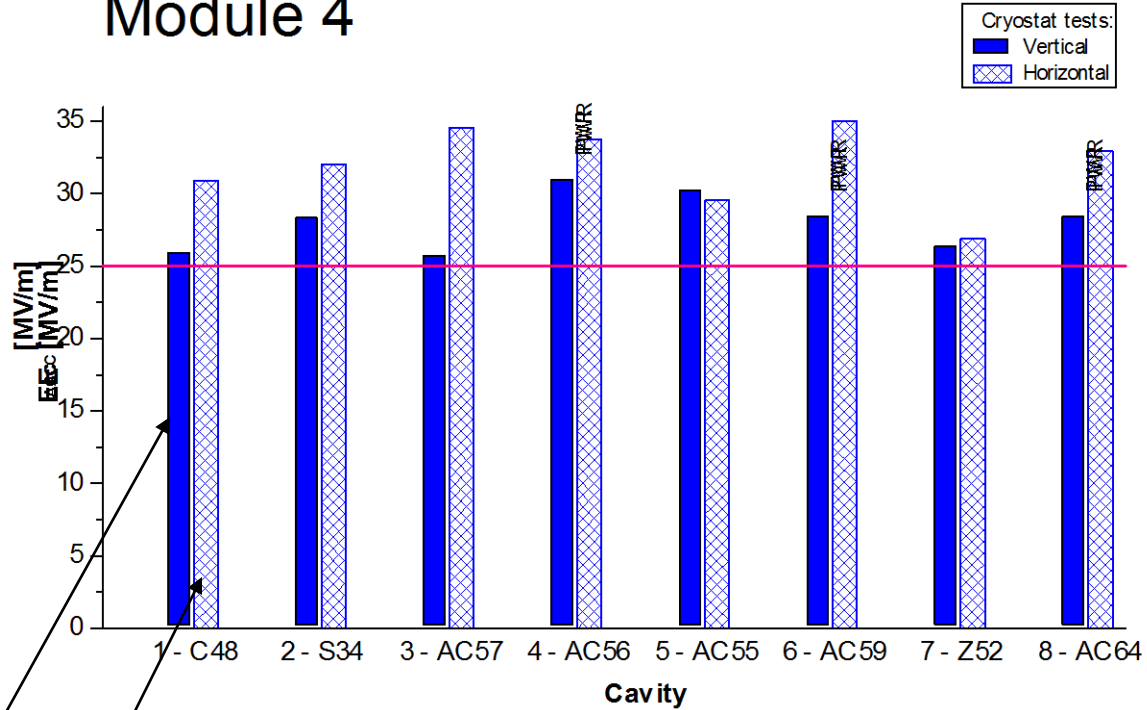
For field emission free

$$E_p (\text{pulsed}) = 2 \times E_p (\text{cw})$$

High Peak Power Processing



Module 4



Bare Vert. Cavity vs.
Equipped Hor. Cavity Test

Issues with HPP

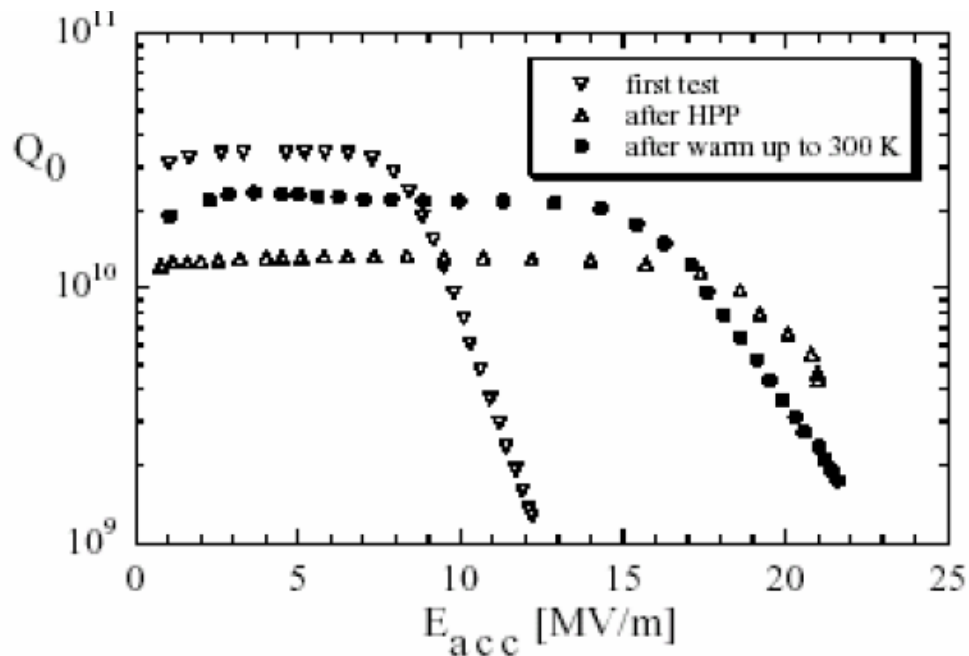


Fig. 2: Cavity C19 before and after HPP. The Q_0 recovered partially after warm up to room temperature.

- Reduced Q_0 after processing
- No experience with HPP above $E_{acc} = 30$ MV/m in 9-cell cavities
- Very high power required

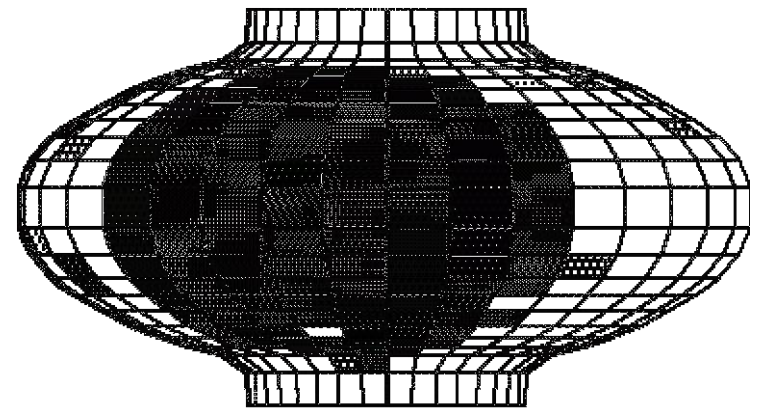
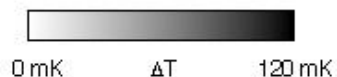
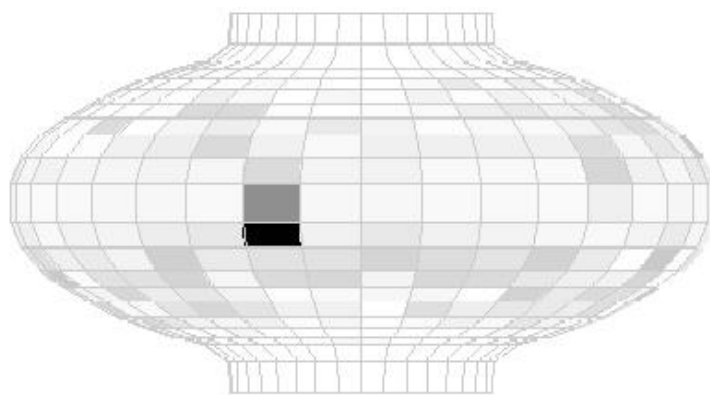
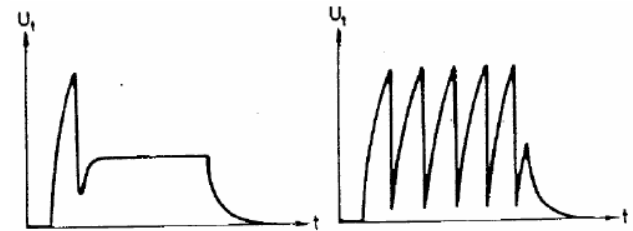
Thermal Breakdown (Quench)

Localized heating

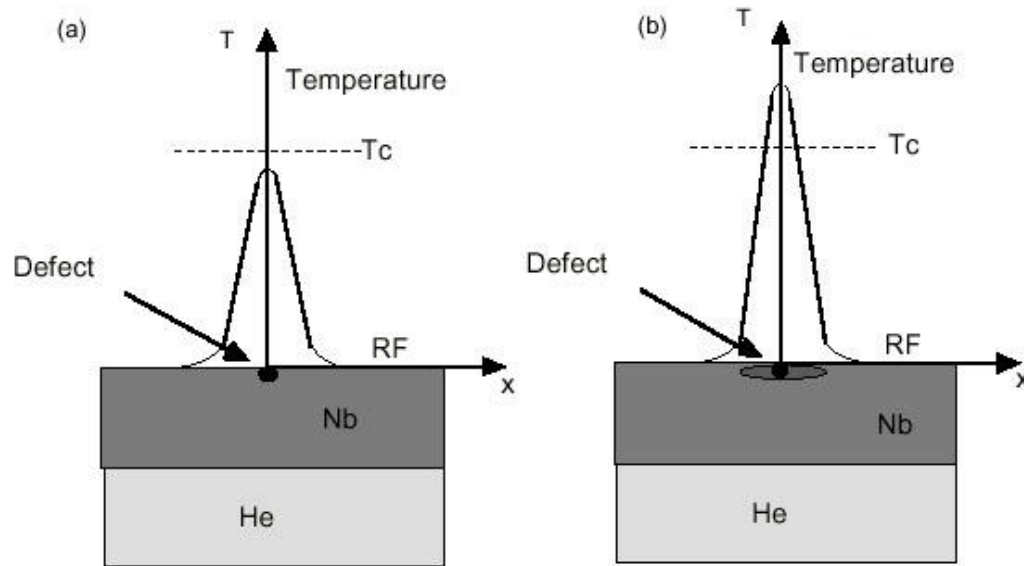
Hot area increases with field

At a certain field there is a thermal runaway, the field collapses

- sometimes displays a oscillator behavior
- sometimes settles at a lower value
- sometimes displays a hysteretic behavior

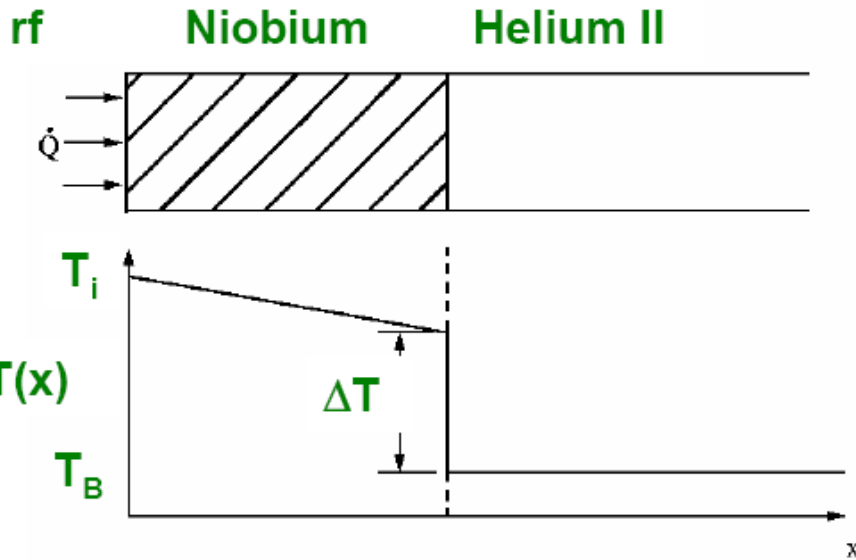


Thermal Breakdown



Thermal breakdown occurs when the heat generated at the hot spot is larger than that can be transferred to the helium bath causing $T > T_c$: “quench” of the superconducting state

Quench Mechanism



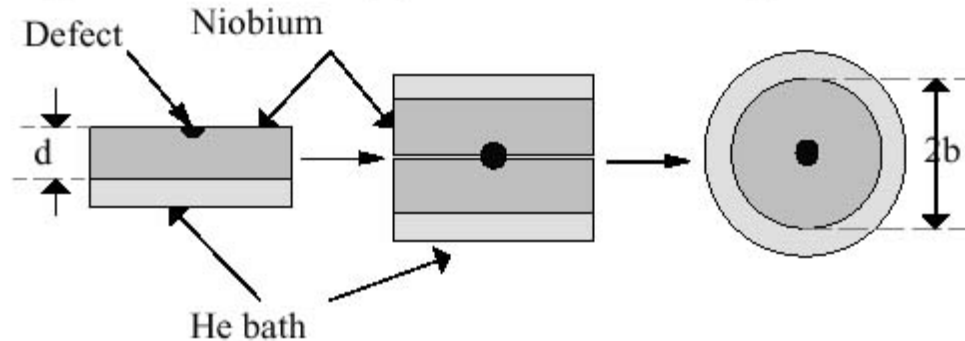
Temperature difference between inner surface and helium bath temperature (two dimensional case):

- The RF current produces heat
- Superconductors are bad thermal conductors:
 - Thermal conductivity
 - Kapitza Nb/He interface resistance
- A small normalconducting defect can produce a very large heating (Factor 10^6 surface resistance!)

$$T_i - T_B = \frac{\dot{Q}}{A} \left(\frac{d}{\lambda} + \frac{1}{h_k} \right)$$

High thermal and Kapitza conductivity required !!

Thermal Breakdown: Simple Model



The power dissipation (in watts) at the defect is

$$\dot{Q}_T = \frac{1}{2} R_n H^2 \pi a^2.$$

Heat flow out through a spherical surface:

$$-4\pi r^2 \kappa \frac{\partial T}{\partial r} = 2\dot{Q}_T$$

When the defect reaches T_c , the field reaches its maximum value

$$H_{\max} = \sqrt{\frac{4\kappa(T_c - T_b)}{aR_n}}.$$

Breakdown field given by (very approximately):

$$H_{tb} = \sqrt{\frac{4\kappa_T (T_c - T_b)}{r_d R_d}}$$

κ_T : Thermal conductivity of Nb

R_d : Defect surface resistance

T_c : Critical temperature of Nb

T_b : Bath temperature

Thermal Conductivity of Nb

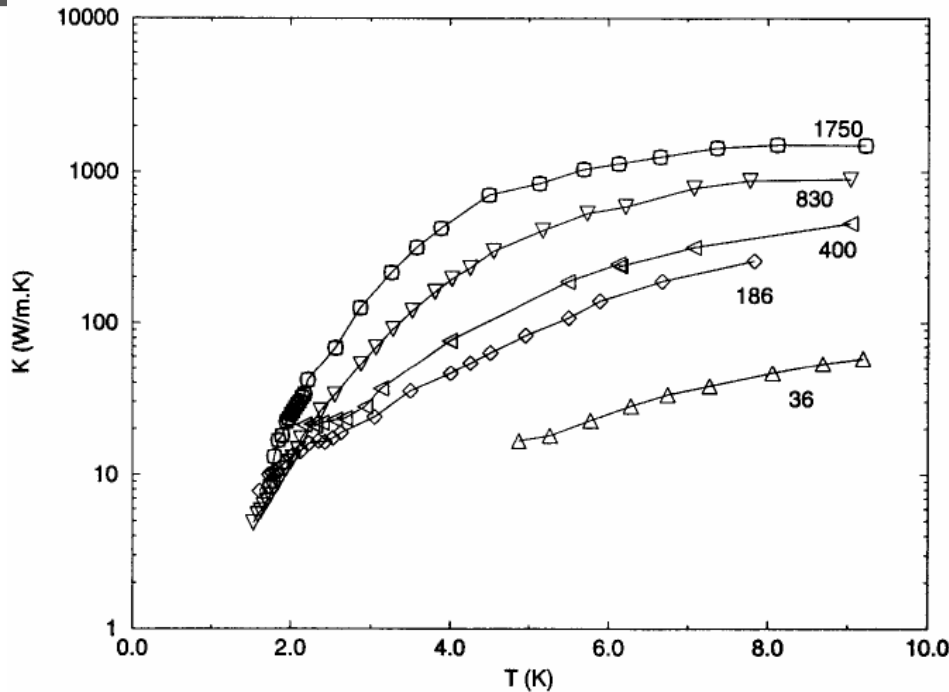


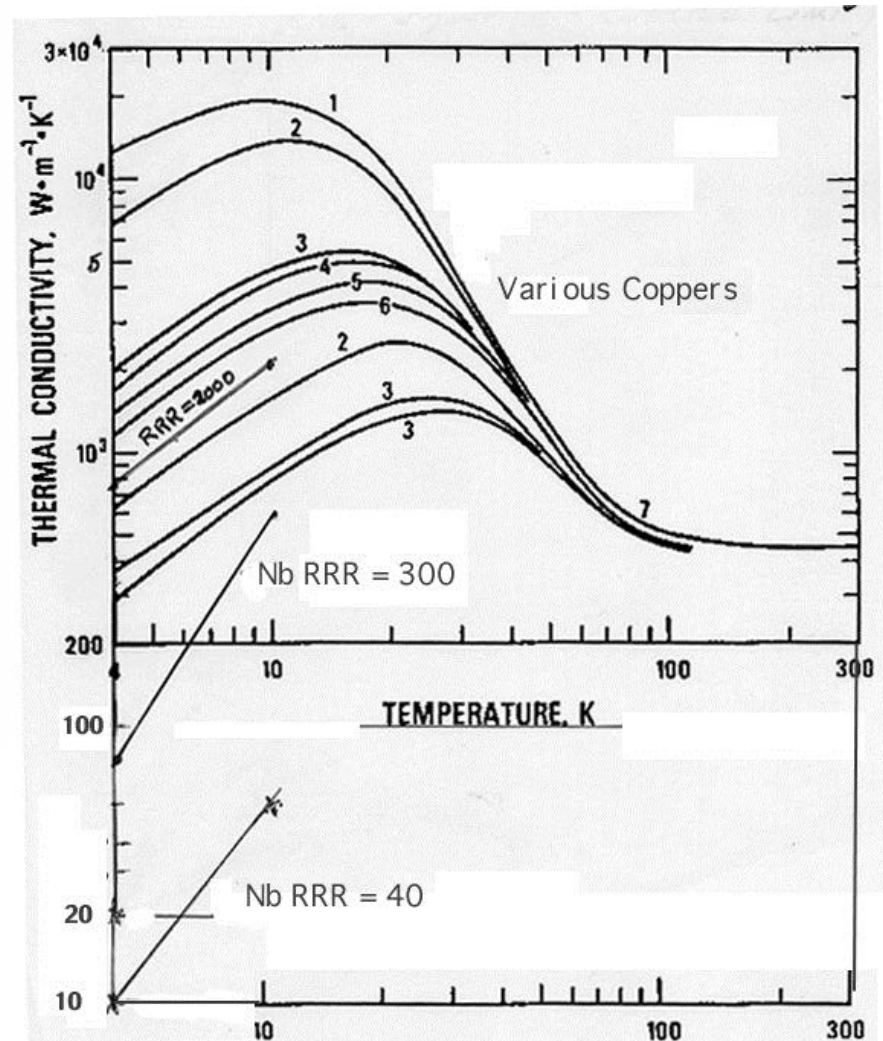
Fig. 3 The thermal conductivity of niobium as a function of temperature, for various RRR values.

RRR is the ratio of the resistivity at 300K and 4.2K

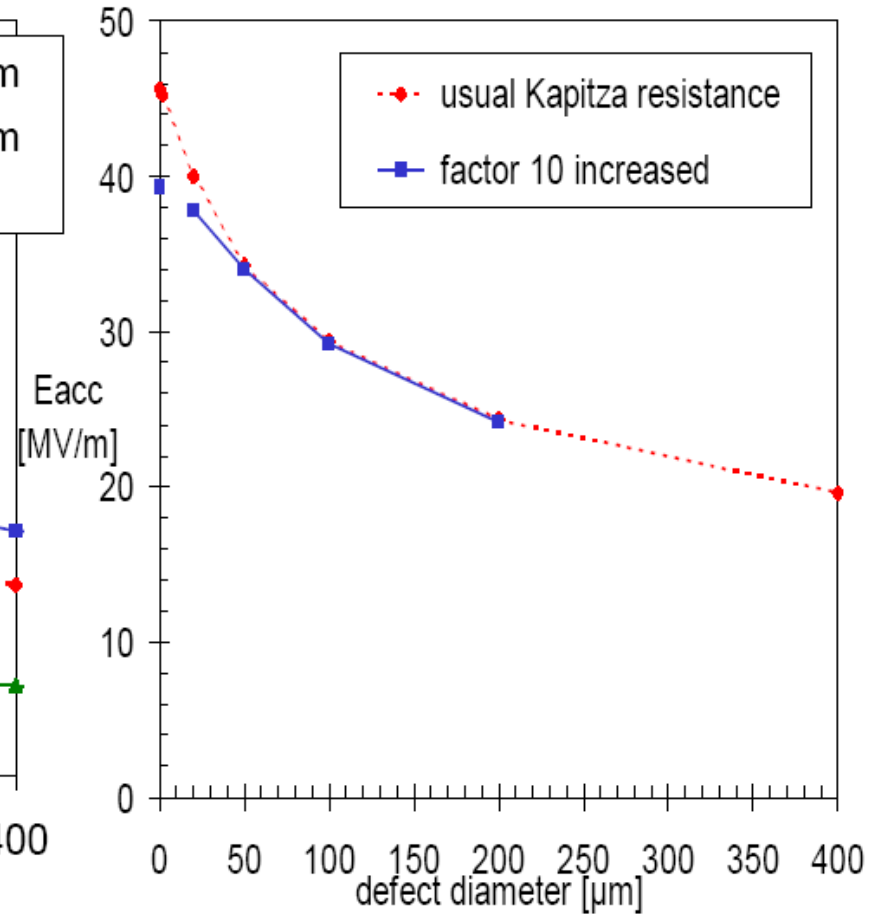
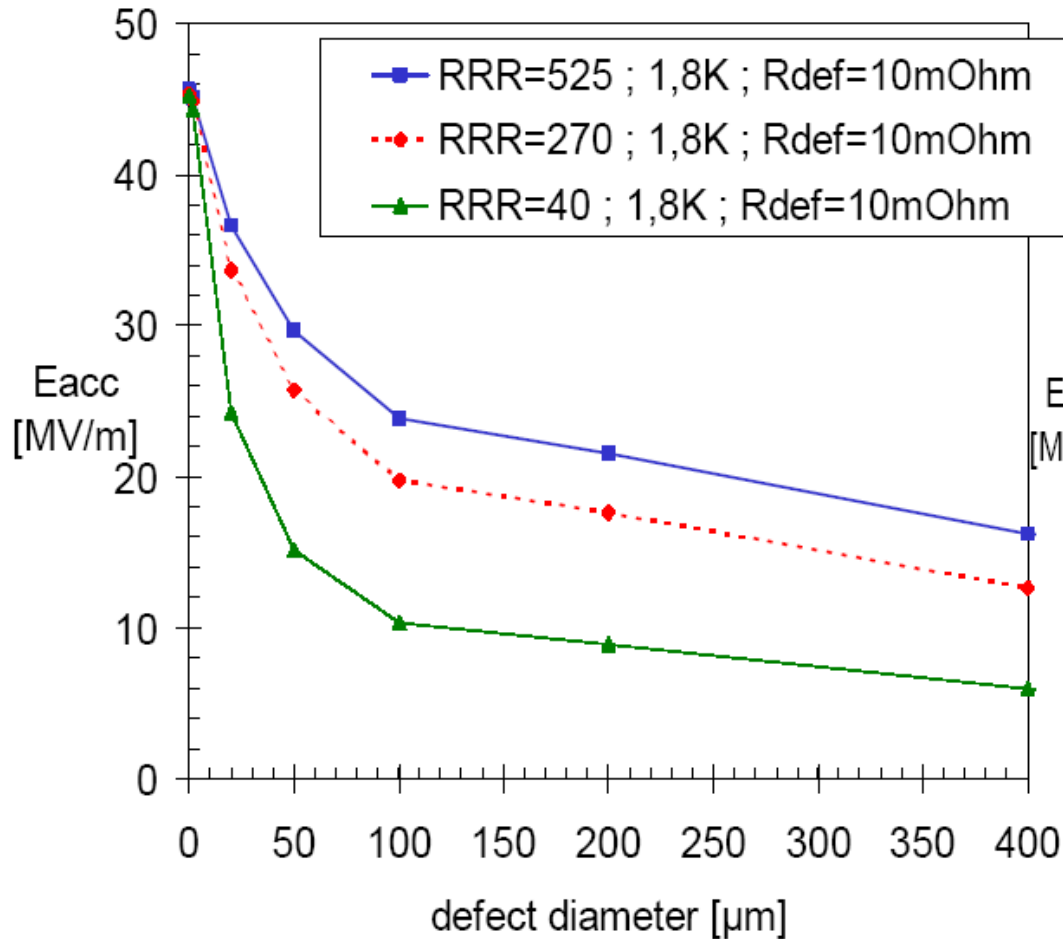
$$RRR = \frac{\rho(300K)}{\rho(4.2K)}$$

RRR is related to the thermal conductivity

For Nb: $\lambda(T = 4.2K) \approx RRR / 4$ (W. m⁻¹. K⁻¹)



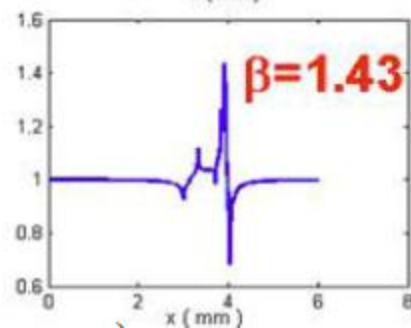
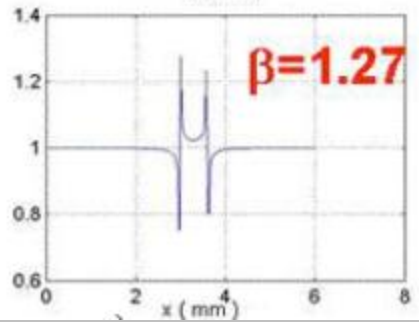
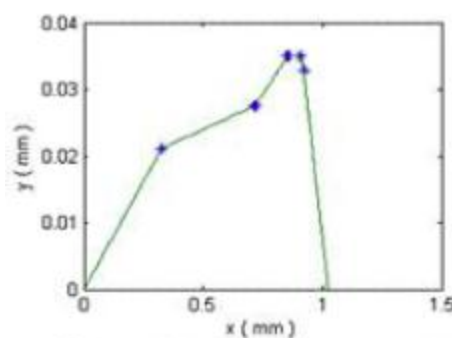
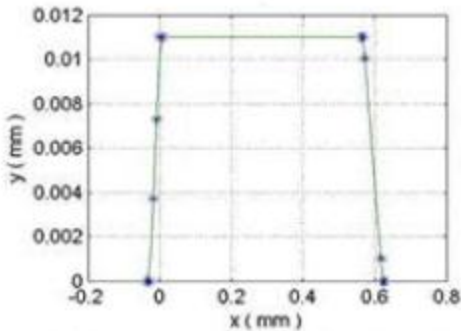
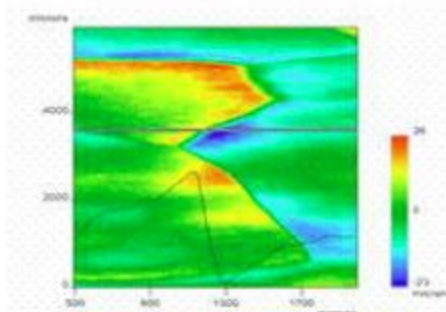
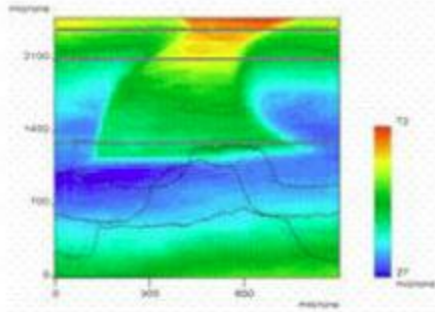
Numerical Thermal Model Calculations



Note: H_{tb} has nearly no dependence on $T_B < 2.1\text{K}$

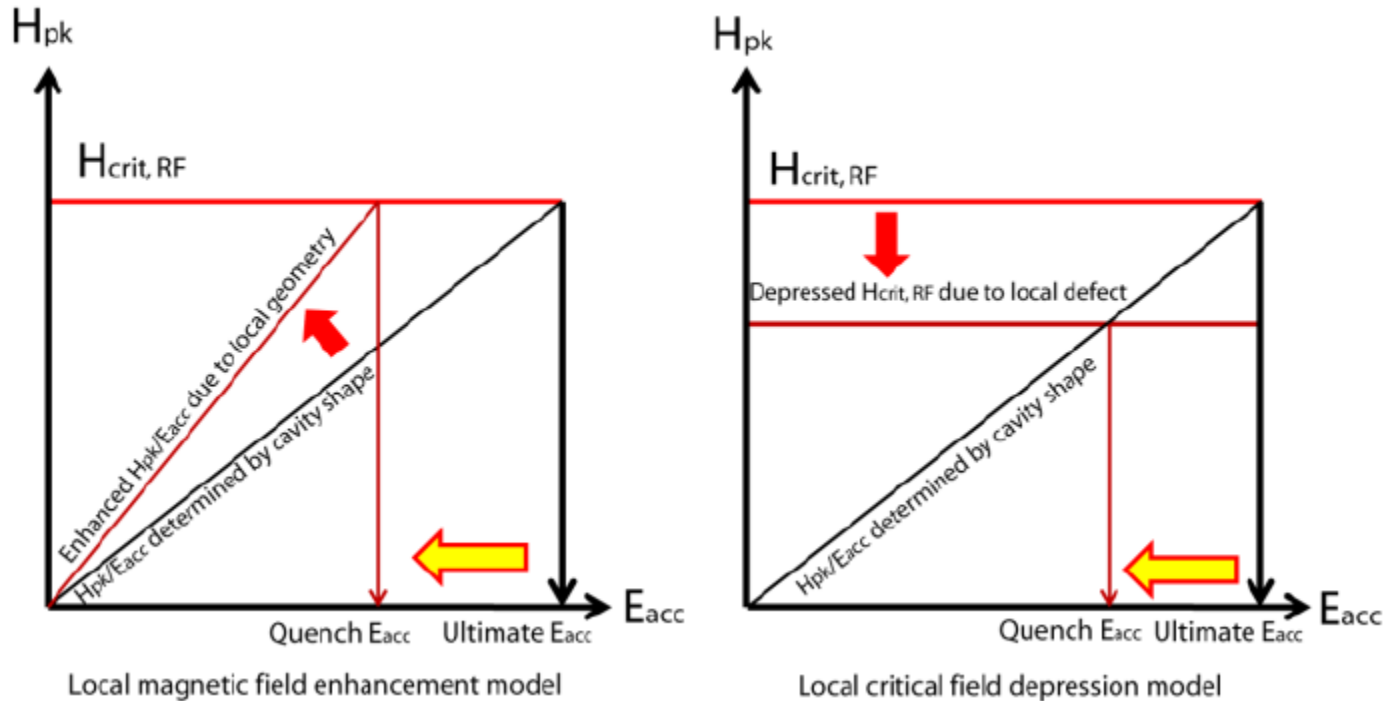
Magneto-thermal Breakdown

- Quench location identified by T-mapping
- Morphology of quench site reproduced by replica technique



Local Magnetic Field Enhancement:
Quench when $\beta H > H_c$

Magneto-thermal Breakdown: Maximum E_{acc}



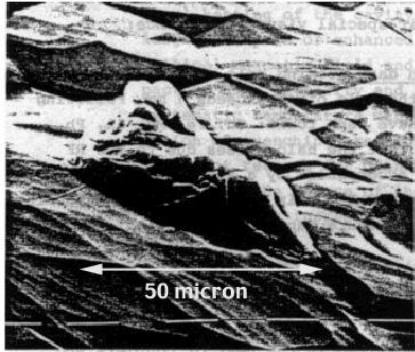
$$E_{acc}^{max} = d \frac{r H_{c,RF}}{\beta_m \left(H_p / E_{acc} \right)}$$

$r \leq 1$, reduction of the local critical field within the penetration depth, due to impurities or lattice imperfection

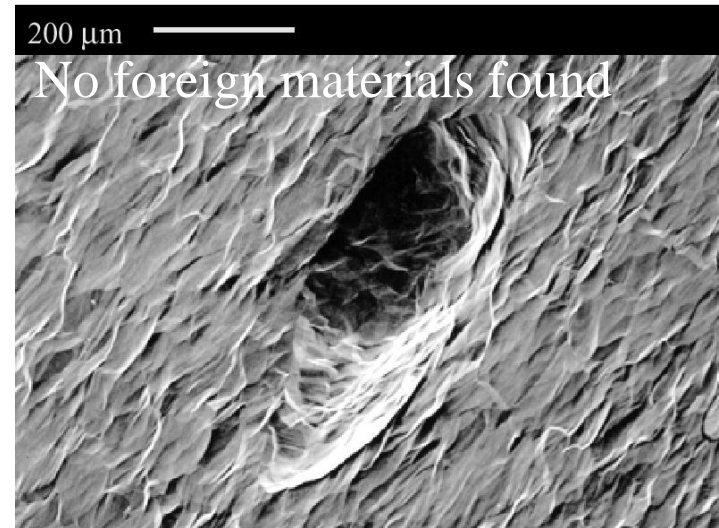
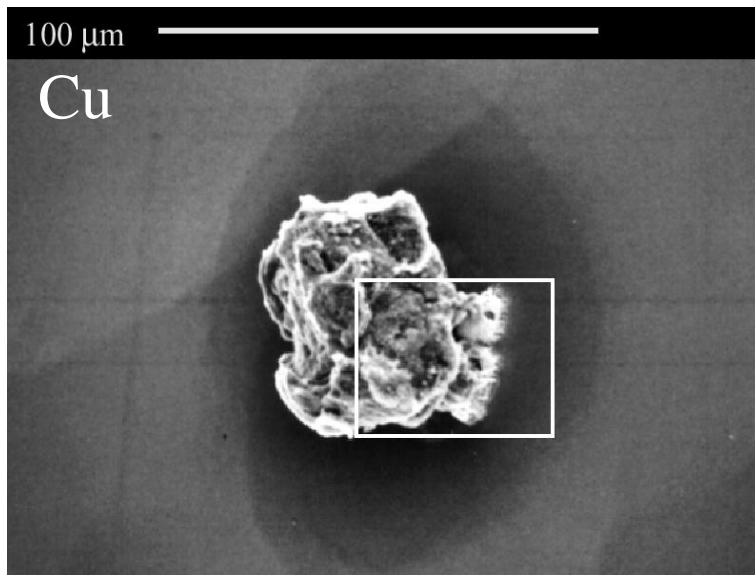
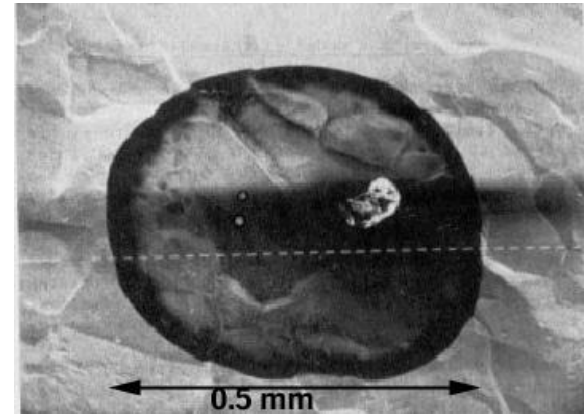
d , thermal stabilization parameter $\propto \sqrt{\kappa}$

$\beta_m > 1$, geometric field enhancement factor

Type of Defects



SEM

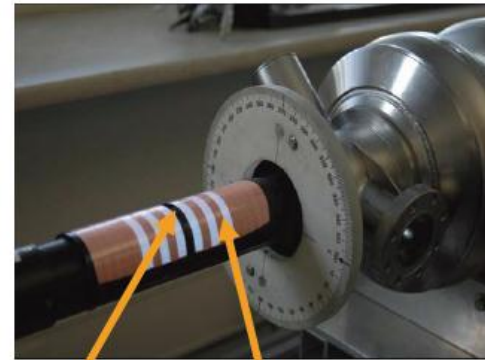


Surface defects, holes can also cause TB

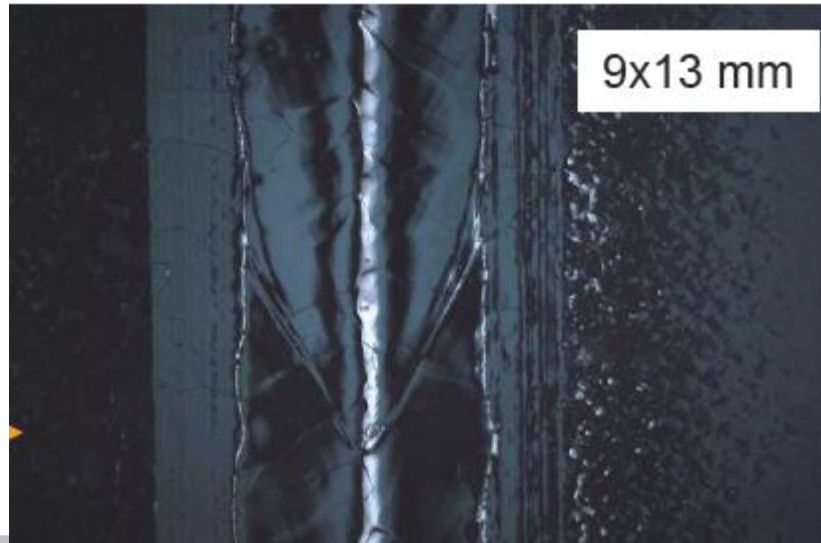
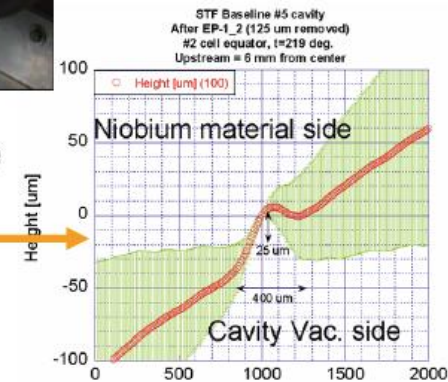
0.1 – 1 mm size defects cause TB

Optical Inspection

- long distance microscope (Cornell)
 - resolution: 12 $\mu\text{m}/\text{pixel}$ (limited by camera)
- University Kyoto and KEK camera system
 - resolution: 7 $\mu\text{m}/\text{pixel}$
 - variable light system for height measurement



camera light source



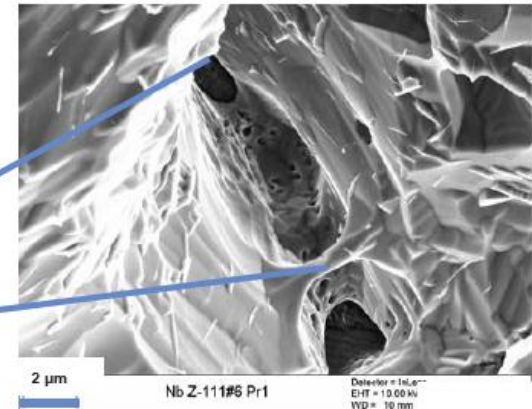
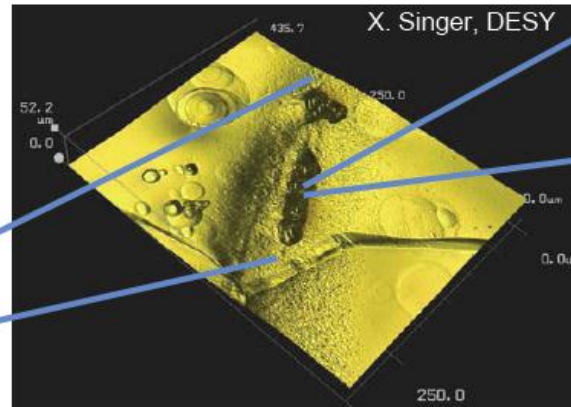
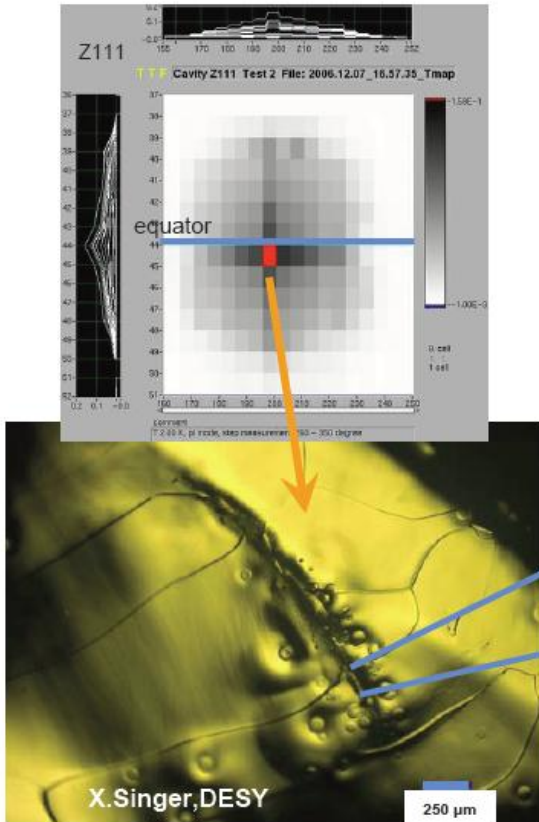
Defects Seen by Optical Inspection

Cell 6, Quench at 16 MV/m on equator

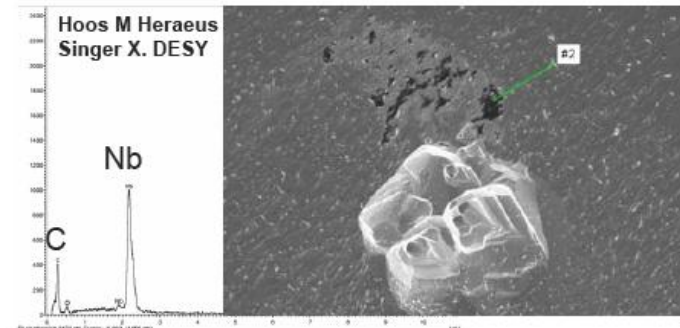
DESY

- Holes with sharp edges along the grain boundaries in the equator weld
- Pits around the holes.

SEM

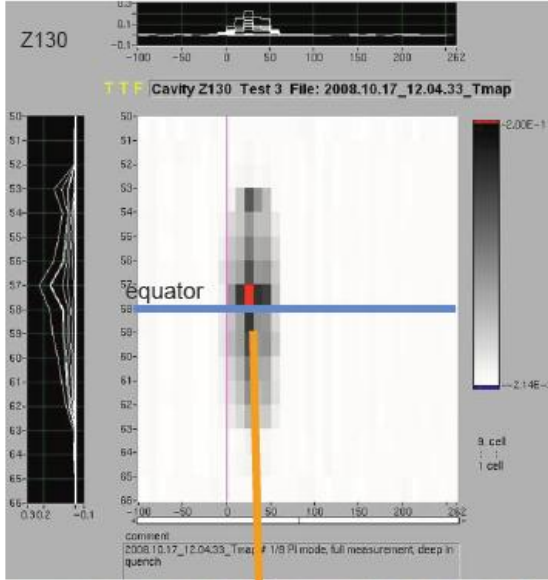


- Auger analysis: no foreign material
- EDX analysis: increased content of carbon in black spots

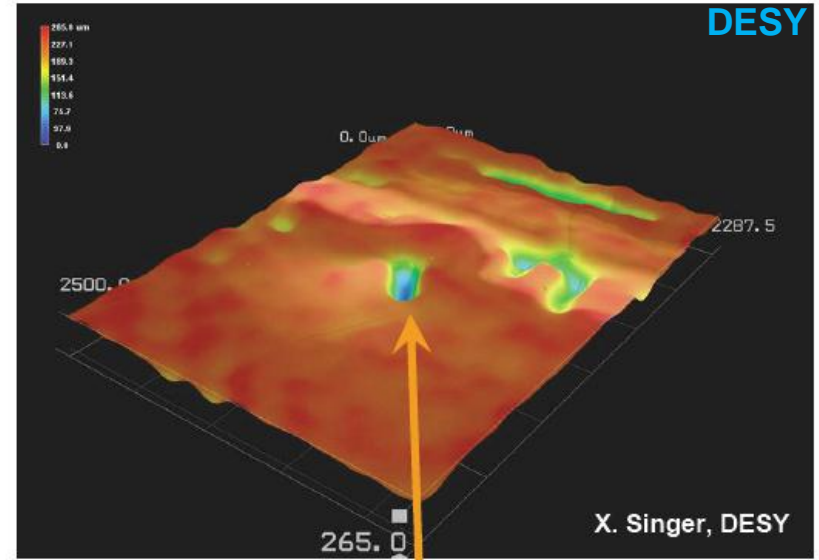


Defects Seen by Optical Inspection

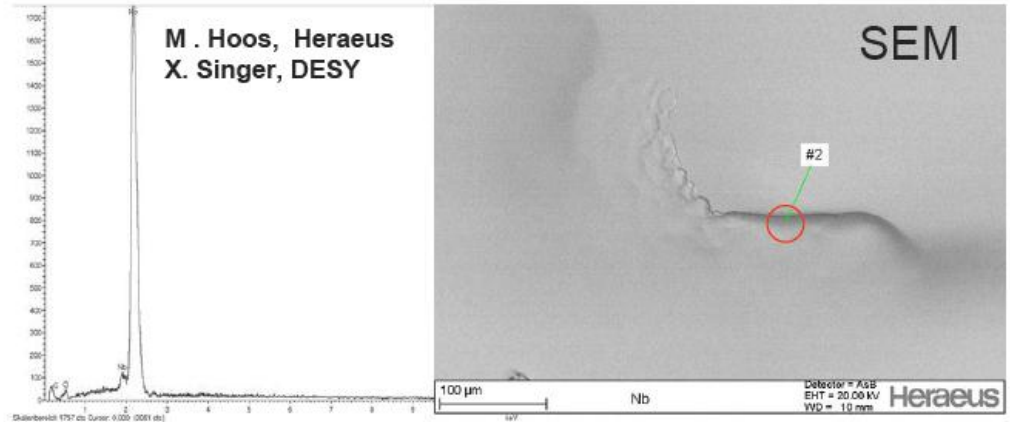
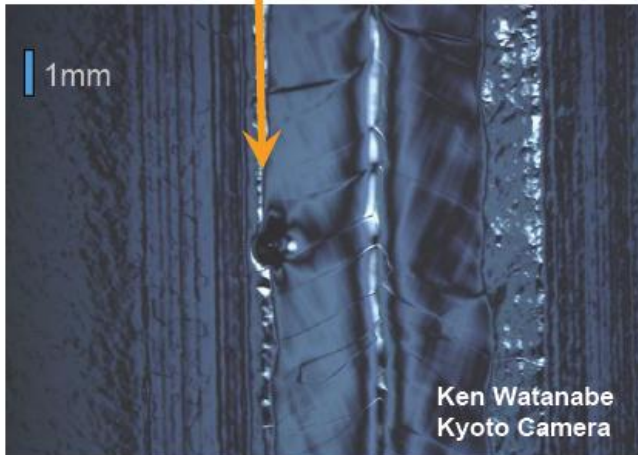
Cell 5, Quench at 23 MV/m on equator



hole in the equator weld



3D image, bump and hole up to 200 μm deep

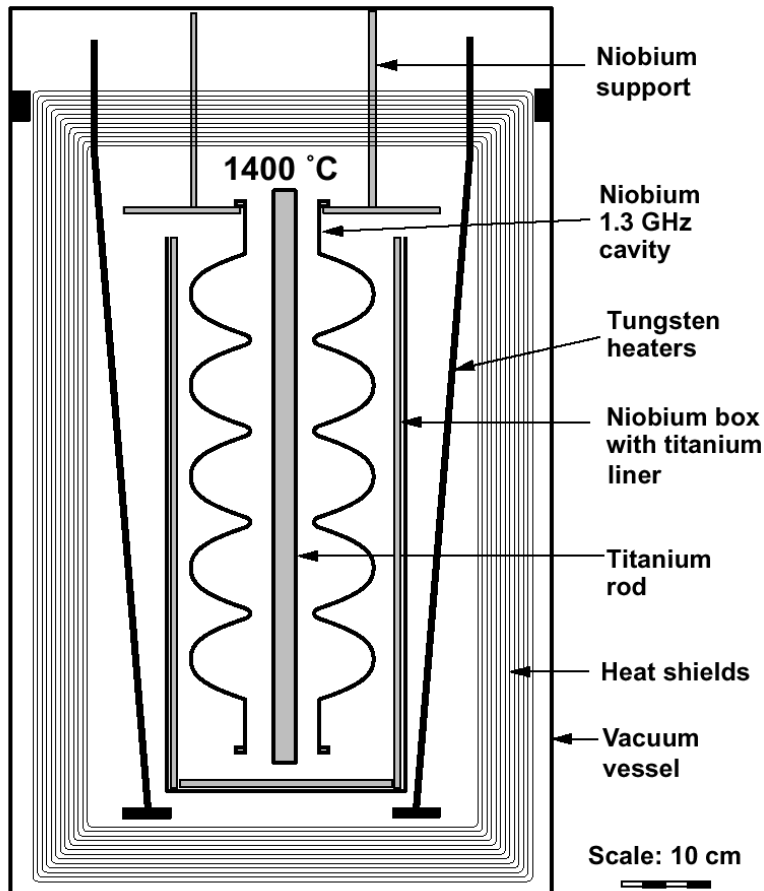


No foreign material inclusions detected by EDX

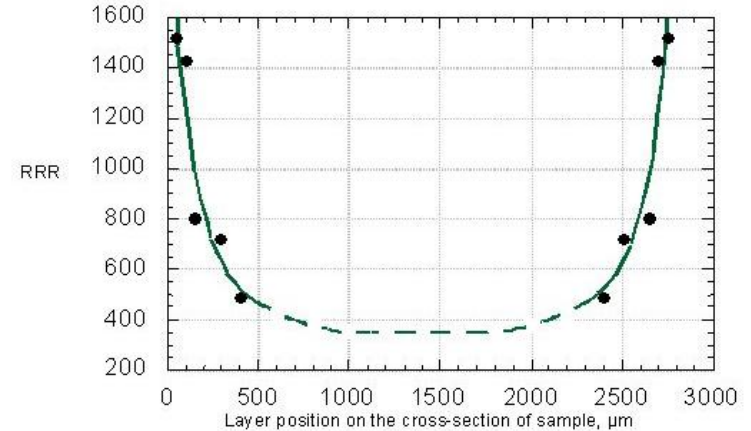
Cures for Quench

- **Prevention: avoid the defects**
 - High-quality Nb sheets
 - Eddy-current scanning of Nb sheets
 - Great care during cavity fabrication steps
- **Post-treatment:**
 - Thermally stabilize defects by increasing the RRR
 - Remove defects: local grinding

Post-purification for Higher RRR



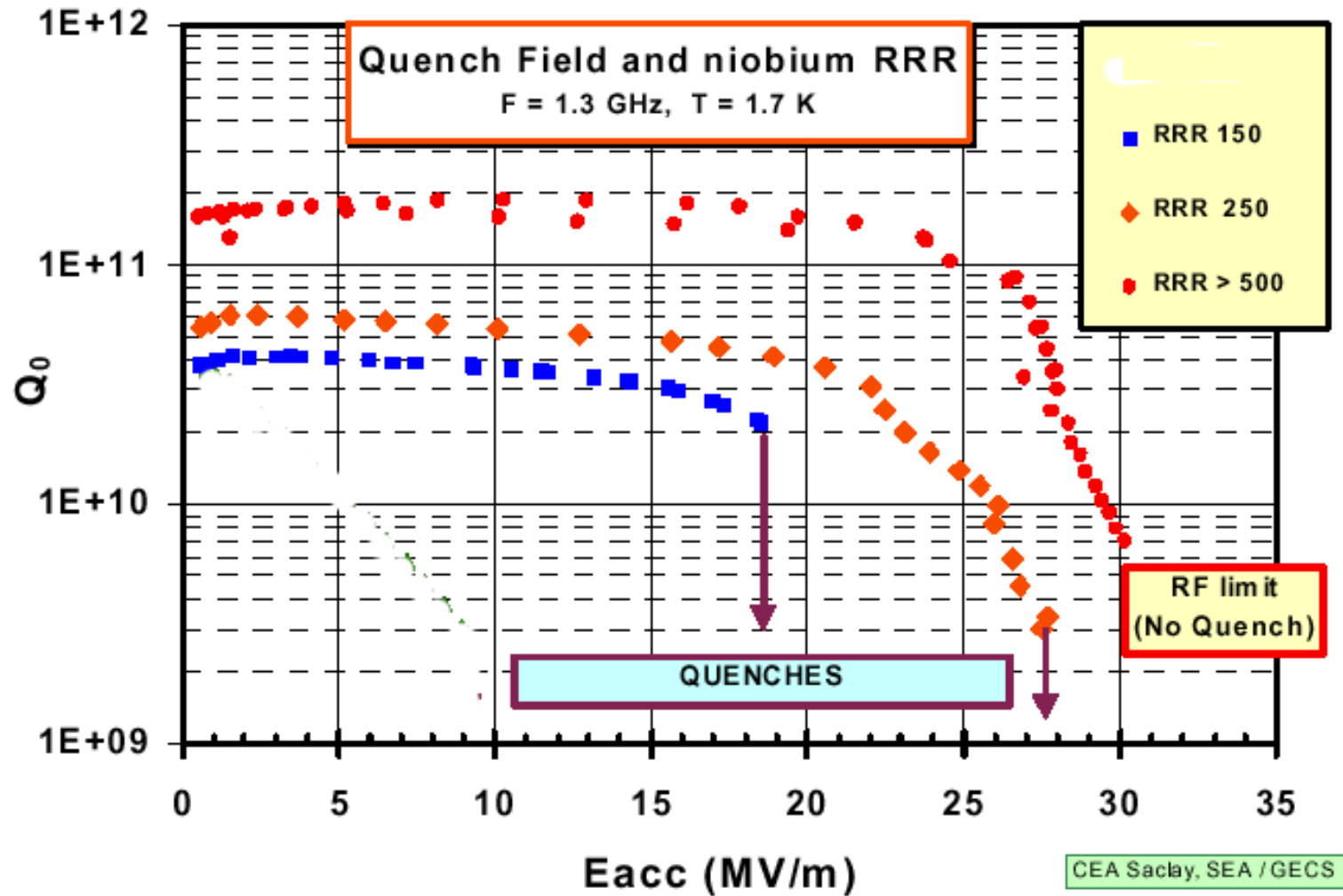
- Post-purification by solid-state gettering
- use Ti (or Y) as getter material => higher affinity for O, (N, C) than Nb
 - coating of cups or cavity with getter material at 1350 C (Ti) under UHV
 - diffusion of O from Nb to Ti until equilibrium
- 1) Increase of RRR = 250-300 to RRR = 500 – 700
- 2) Homogenizing impurities



Disadvantages:

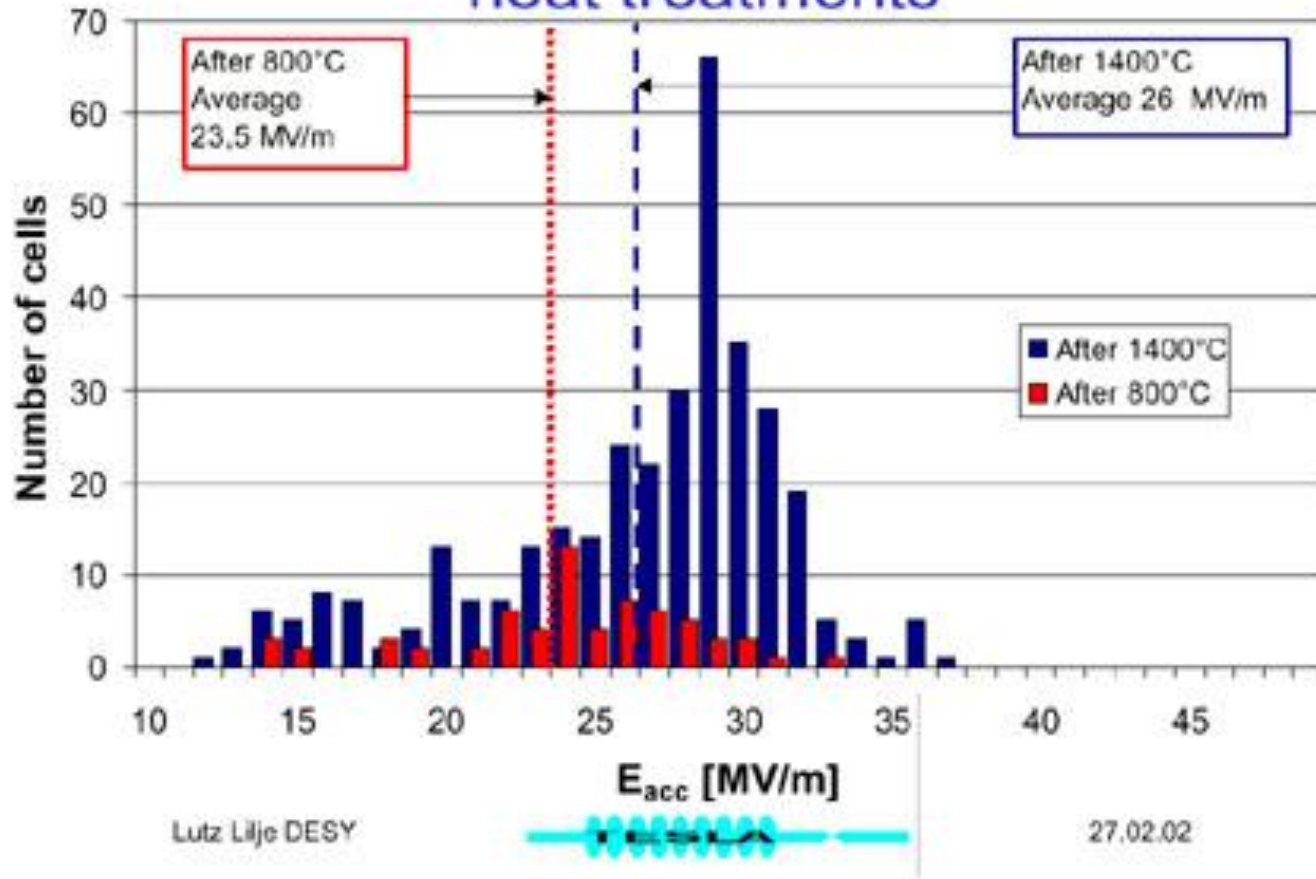
- > 50 μm material removal necessary after heat treatment
- Significant reduction of yield strength of the Nb

Post-purification



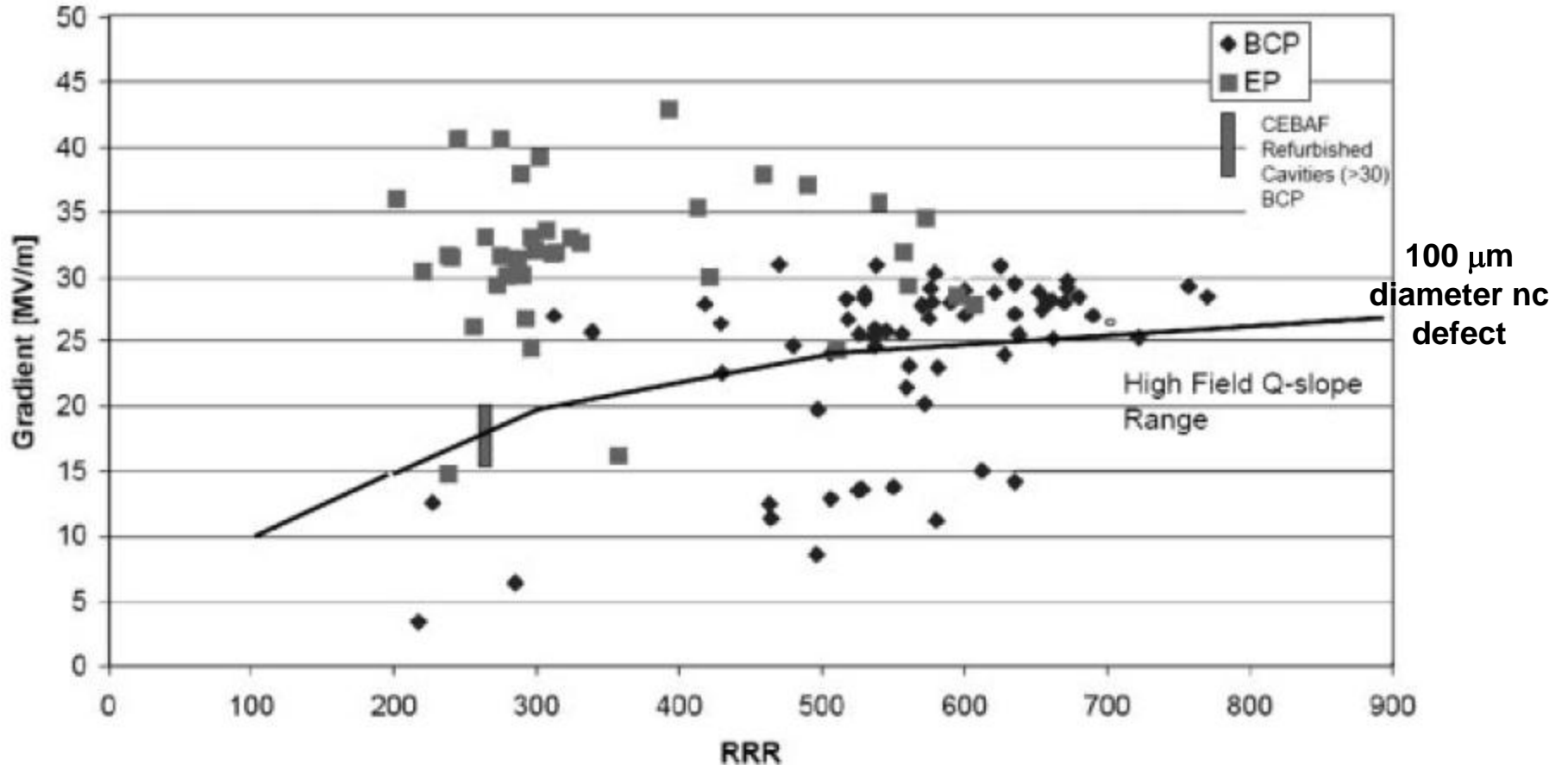
Post-purification

Benefit of the high temperature heat treatments

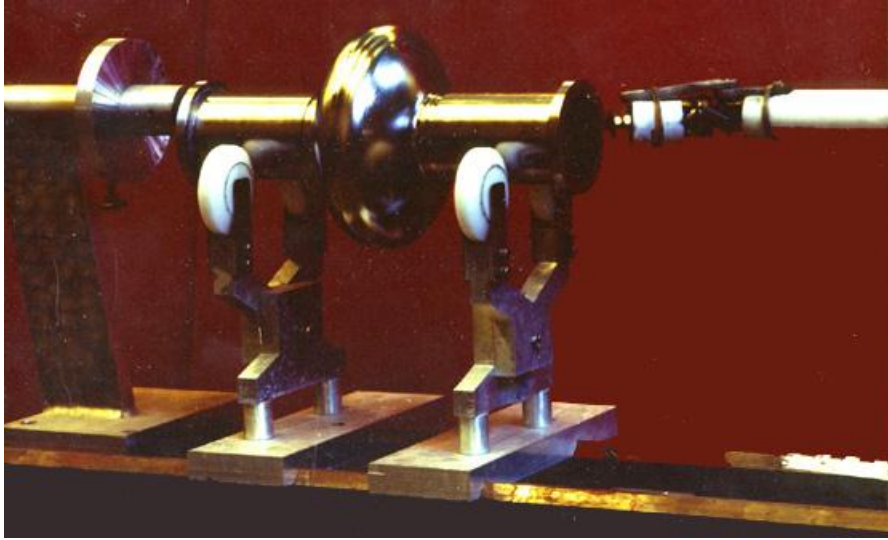


How High of RRR Value is Necessary?

9-cell ILC cavities



Defect Repair: Local Grinding

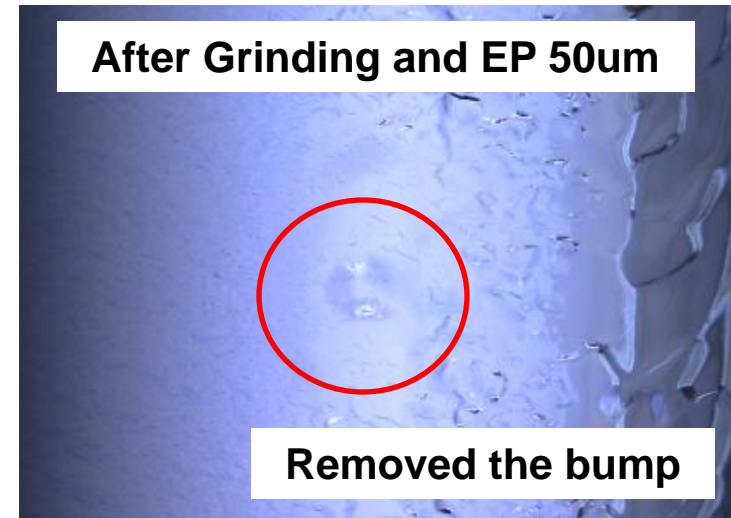
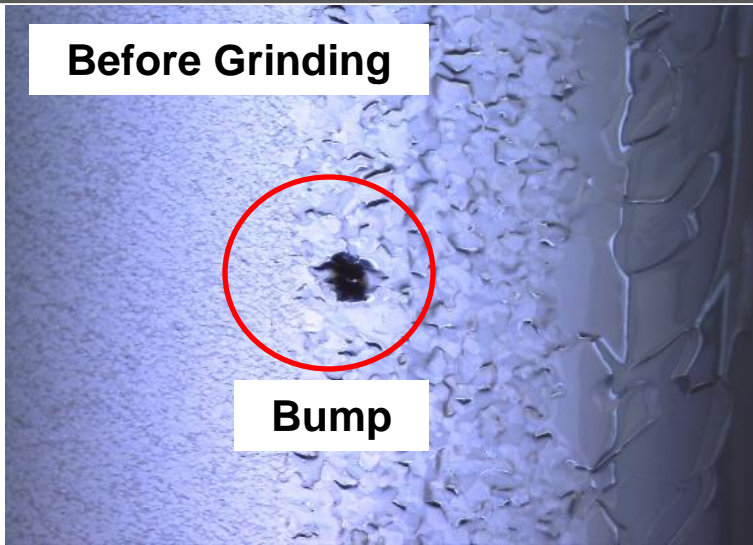


Polymond + water for grinding

**Polymond: diamond particles in a resin
(particle size = 40 ~ 3 μm)**



Defect Repair: Local Grinding



Quench at $E_{acc}=20$ MV/m

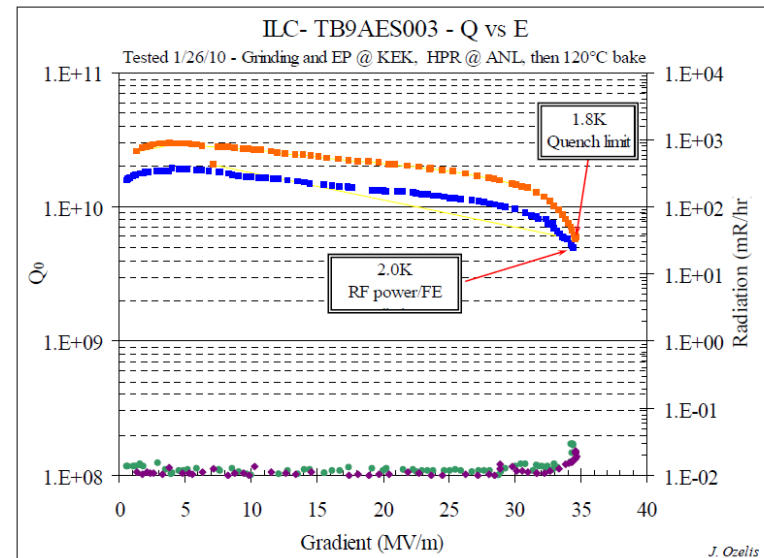
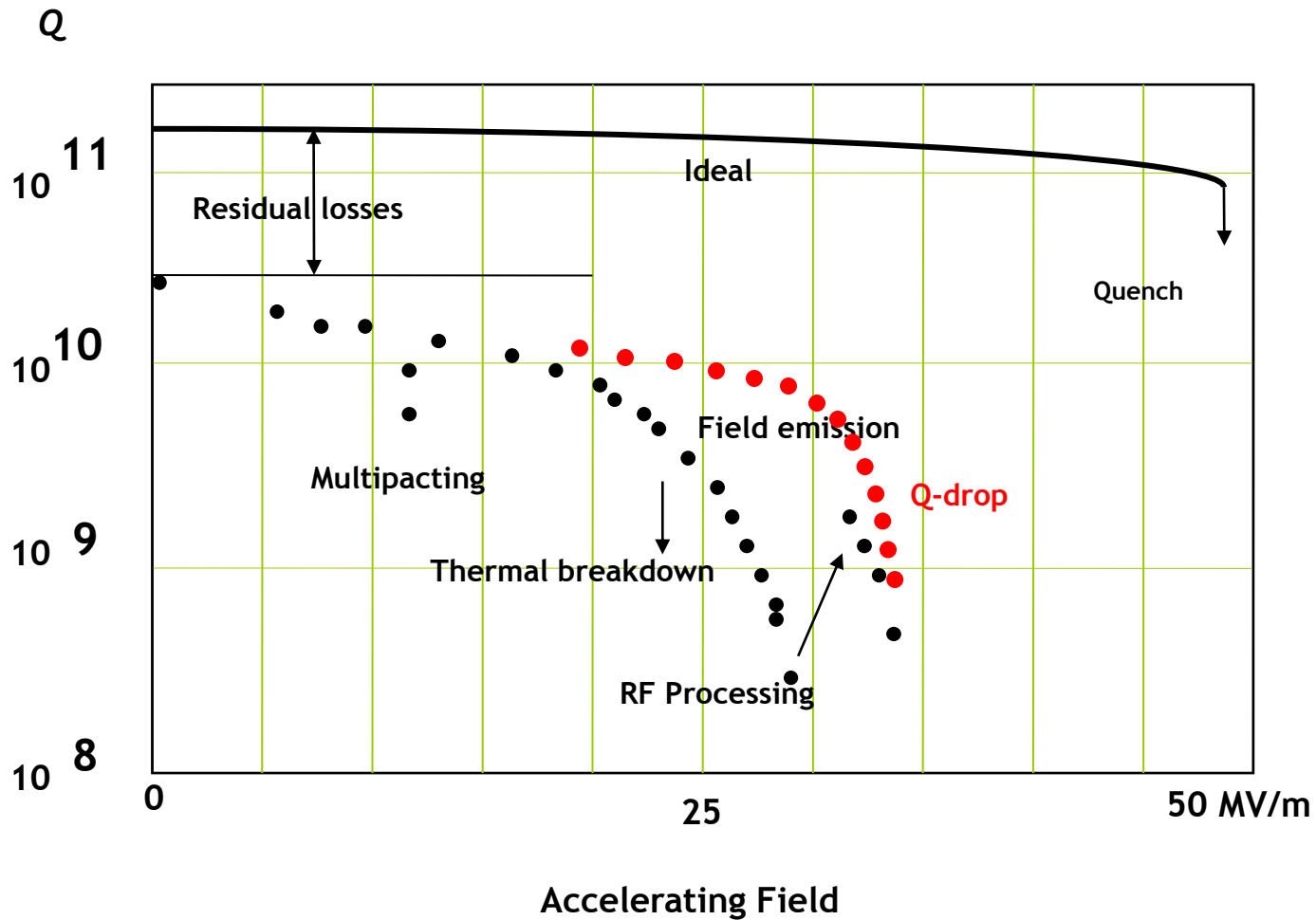


Figure 1.) Q_0 vs E runs at 2.00K and 1.80K.

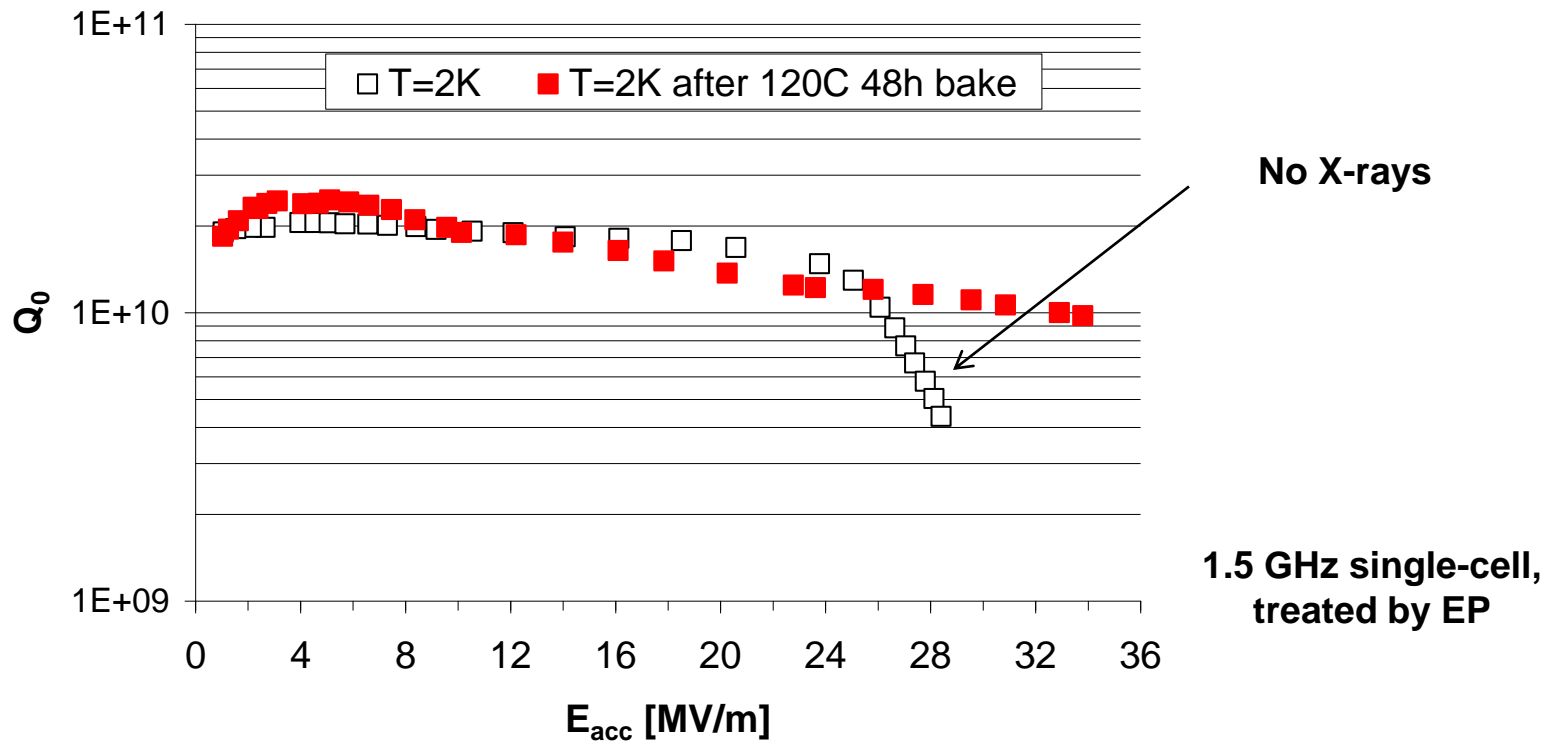
Summary on Quench

- **Big improvement in Cavity fabrication and treatment**
less foreign materials found (at limitations $<20\text{MV/m}$ only)
- **Visual inspection systems are available**
- **Many irregularities in the cavity surface are found with this systems**
during and after fabrication and treatment
 - pits and bumps**
 - weld irregularities**
- **Often one defect limits the whole cavity**
- **Some correlations are found between defects and quench locations**
at higher fields
 - But often no correlation between suspicious pits and bumps**
and quench location
- **At gradient limitations in the range $>30\text{ MV/m}$ defects are often not identified**

High-Field Q-Slope (“Q-drop”)



Q-drop and Baking

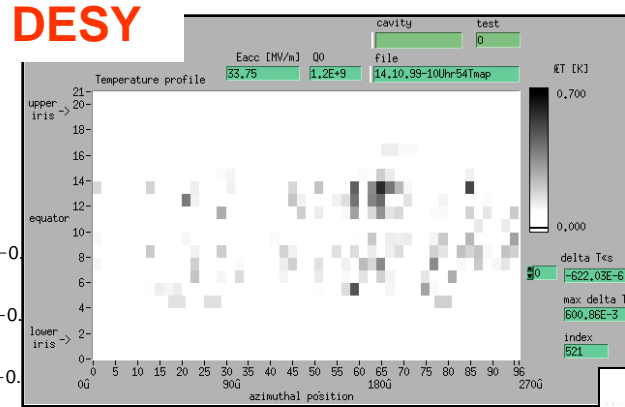


- The origin of the Q-drop is still unclear. Occurs for all Nb material/treatment combinations
- The Q-drop recovers after UHV bake at 120 °C/48h for certain material/treatment combinations

Experimental Results on Q-drop

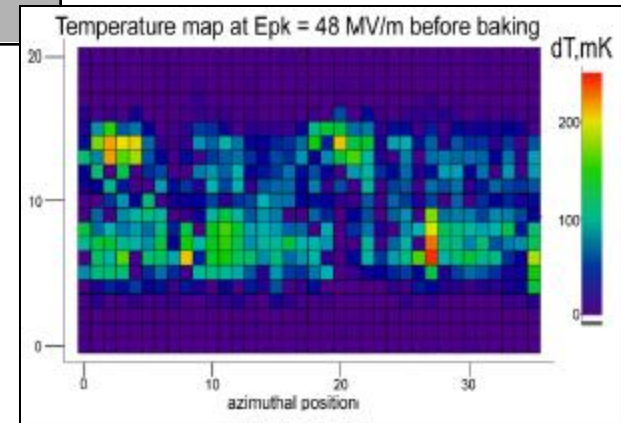
$$Q_0 = 2.8 \cdot 10^9$$

$$B_p = 110 \text{ mT}$$

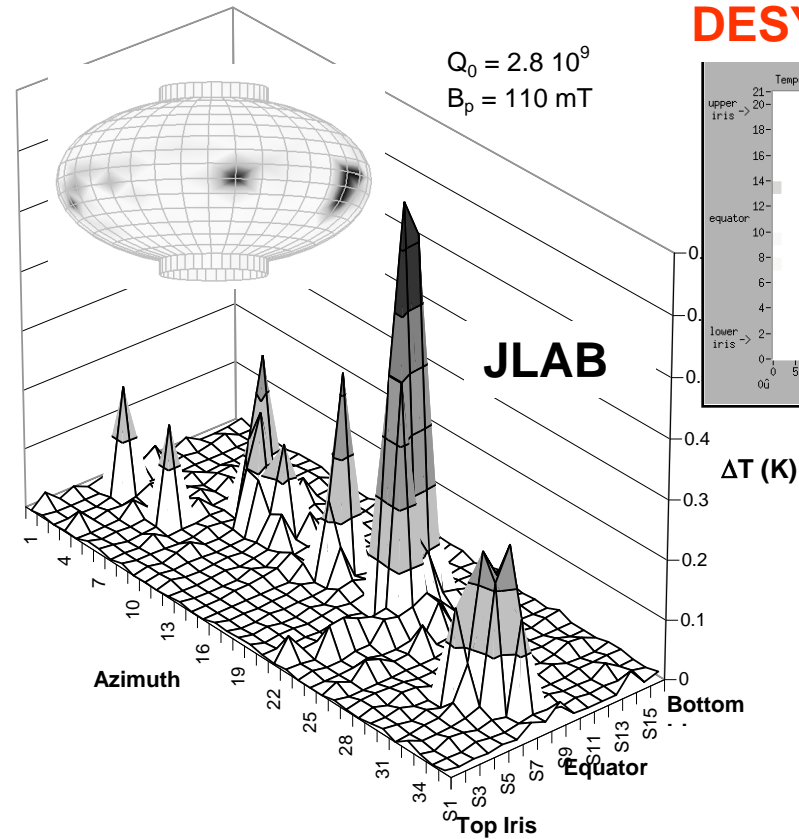


T-Maps

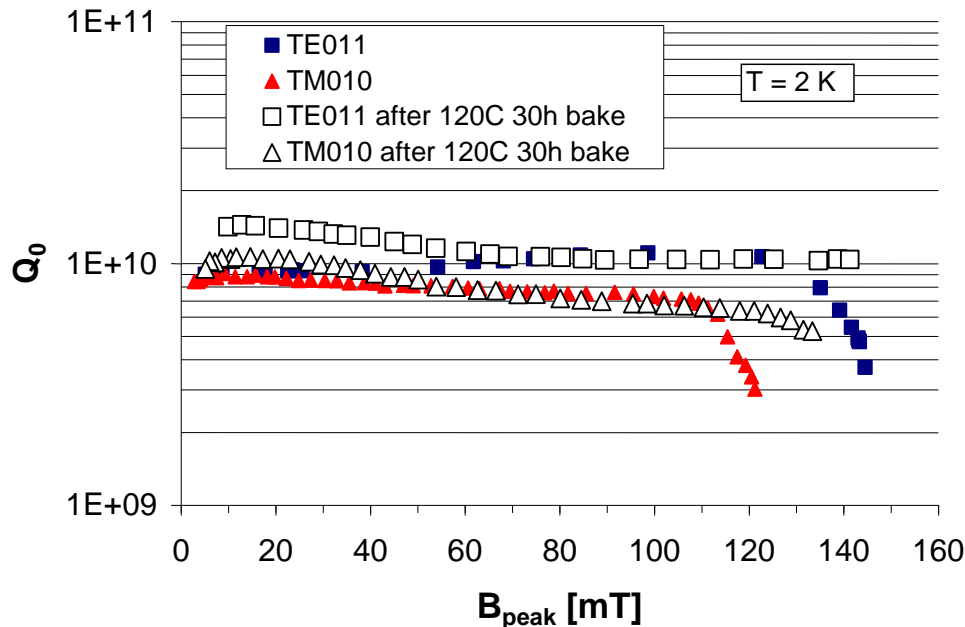
CORNELL



- “Hot-spots” in the equator area (high-magnetic field)



Experimental Results on Q-drop



- Q-drop and baking effect observed in both TM_{010} and TE_{011} modes. TE mode has no surface electric field

Q-drop: high magnetic field phenomenon

Onset of Q-drop is higher for

- smooth surfaces
- reduced number of grain boundaries

Baking: Material and Preparation Dependence

Baking **works** on cavities made of:

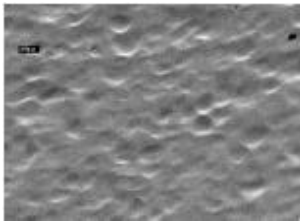
- Large-grain Nb (buffered chemical polished or electropolished)



50 μm

Smooth surface, few grain boundaries

- Fine-grain Nb, electropolished



100 μm

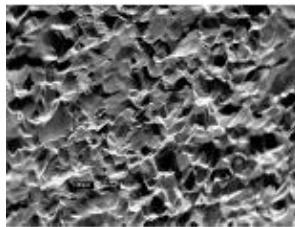
Smooth surface, many grain boundaries

- Fine-grain Nb, post-purified, BCP

Smooth surface, fewer grain boundaries

Baking **does not work** on cavities made of:

- Fine-grain Nb, buffered chemical polished

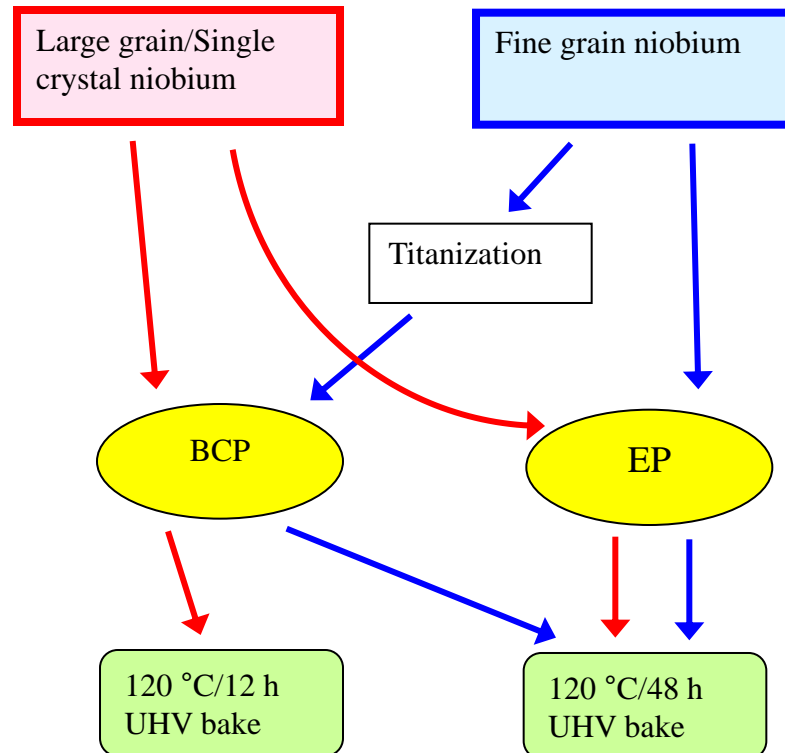


100 μm

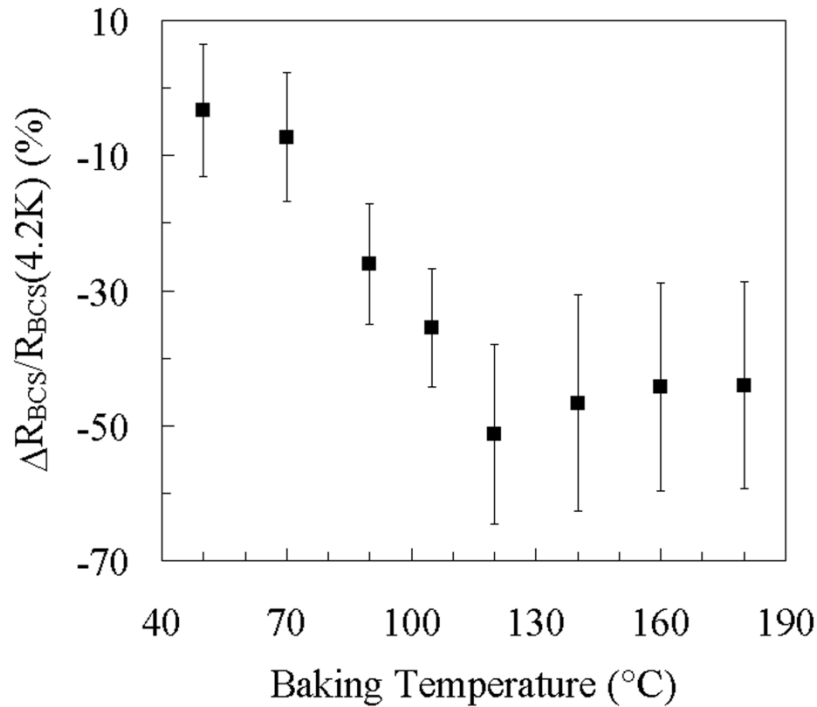
Rough surface, many grain boundaries

Recipe against Q-drop

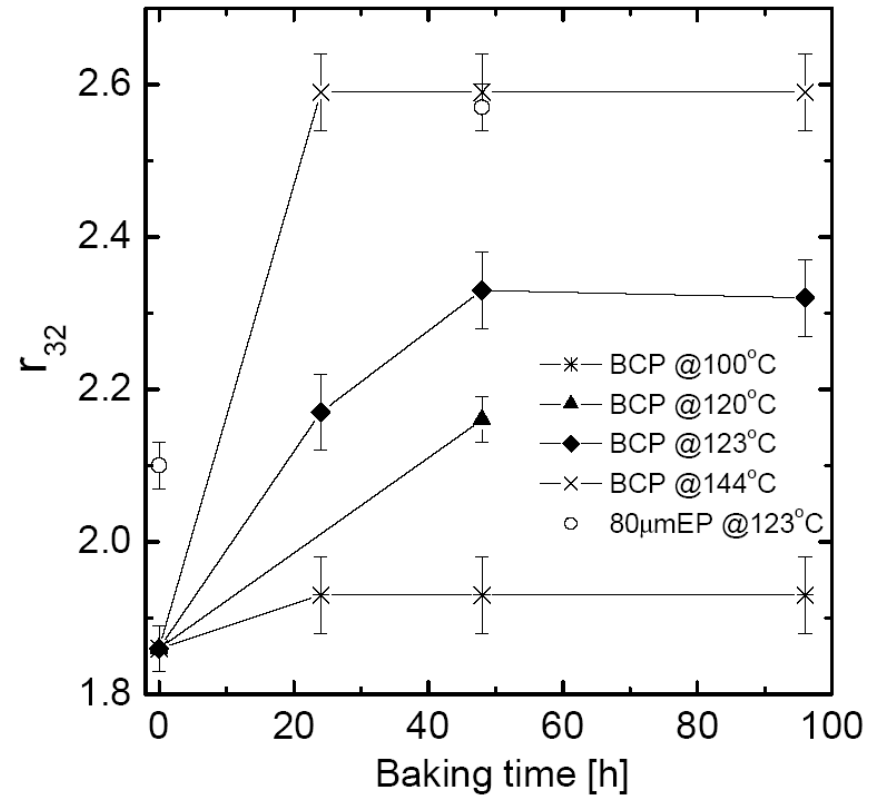
Recipes necessary to overcome the Q-drop, depending on the starting material, based on current data:



Baking Effects on Low-field R_s and H_{c3}



$r_{32} = B_{c3}/B_{c2}$: depends on bake temperature and duration

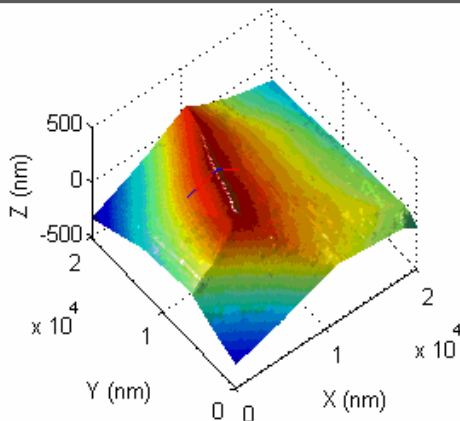


- Decrease of R_{BCS} due to \downarrow of l and \uparrow of energy gap
- The physics of the niobium surface changes from **CLEAN** ($l > 200$ nm) to **DIRTY LIMIT** ($l \approx 25$ nm $\cong \xi_0$)

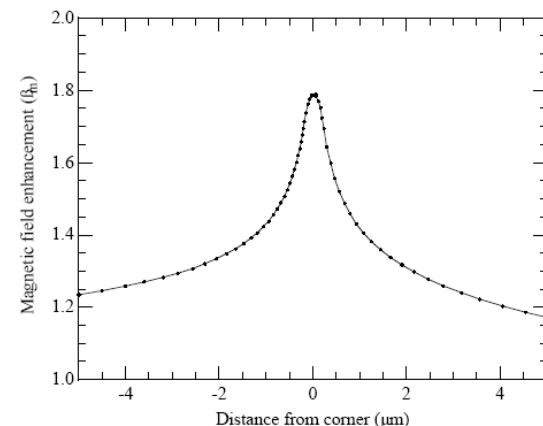
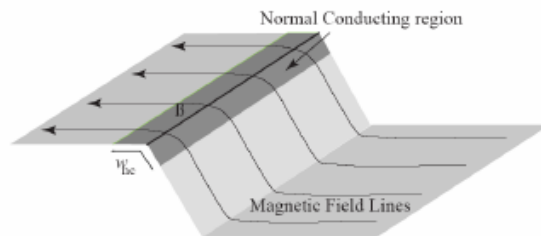
Models of Q-drop & Baking

- Magnetic field enhancement
- Oxide losses
- Oxygen pollution
- Magnetic vortices

Magnetic Field Enhancement Model



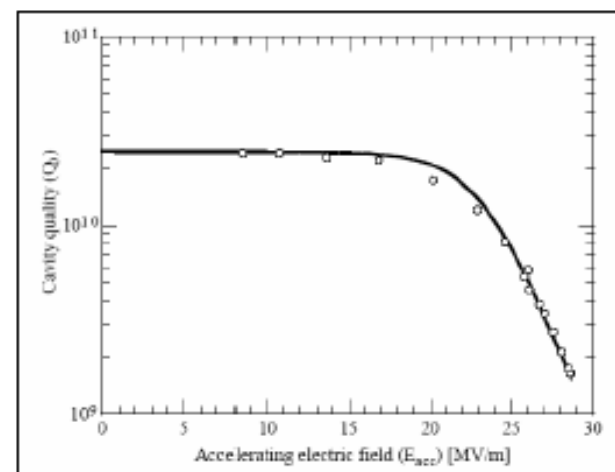
AFM image of a grain boundary edge



Local quenches at sharp steps (grain boundaries) when $\beta_m H > H_c$

β_m : Field enhancement factor

- $Q_0(B_p)$ calculated assuming
 - ✓ Distribution function for β_m values
 - ✓ The additional power dissipated by a quenched grain boundary is estimated to be $\sim 17 \text{ W/m}$



J. Knobloch et al., *Proc. of the 9th SRF Workshop*, (1999), p.

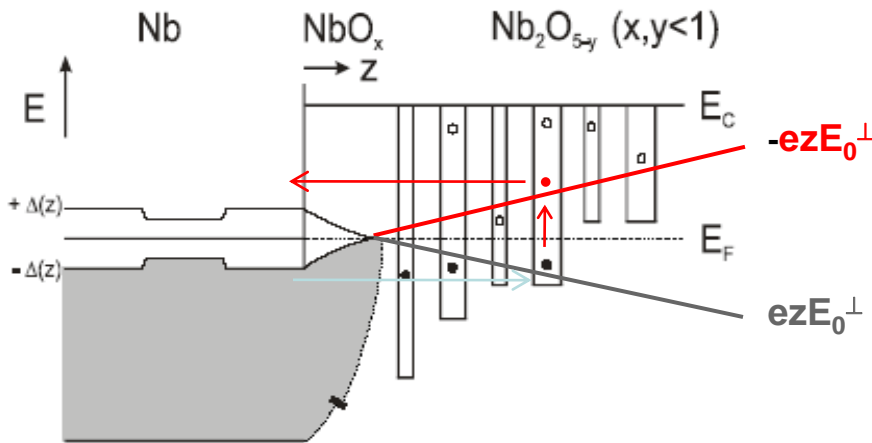
77

MFE Model: Shortcomings

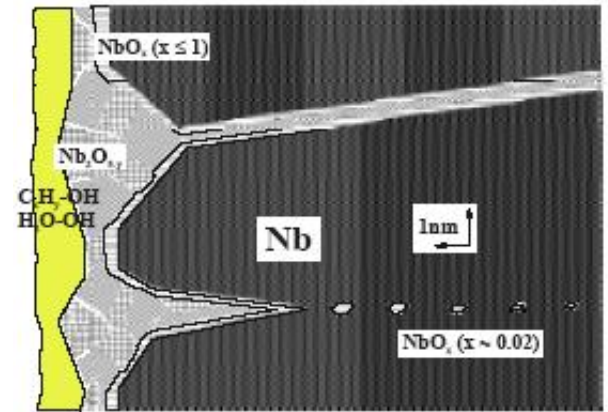
The model cannot explain the following experimental results:

- Single-crystal cavities have Q-drop
- Seamless cavities have Q-drop
- Low-temperature baking does not change the surface roughness
- Electropolished cavities have Q-drop, in spite of smoother surface

Interface Tunnel Exchange Model



Band structure at Nb-NbO_x-Nb₂O_{5-y} interfaces

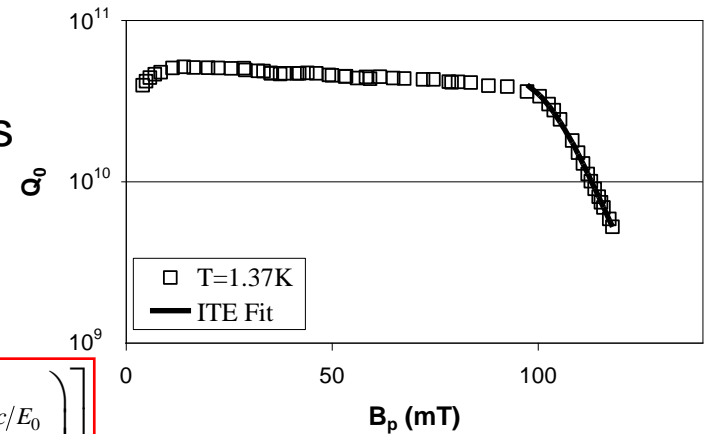


Schematic representation of the Nb surface

- Interface Tunnel Exchange (ITE) model
 - Resonant energy absorption by quasiparticles in localized states in the oxide layer
 - Driven by electric field

$$E_0 > \frac{\epsilon_r \Delta}{e \beta^* z^*}$$

$$R_s^E = b \left[\left(e^{-c/E_p} - e^{-c/E_0} \right) + \left(\frac{c}{E_p} e^{-c/E_p} - \frac{c}{E_0} e^{-c/E_0} \right) + \frac{1}{2} \left(\frac{c^2}{E_p^2} e^{-c/E_p} - \frac{c^2}{E_0^2} e^{-c/E_0} \right) \right]$$



J. Halbritter et al., *IEEE Trans. Appl. Supercond.* 11 (2001) p. 1864

ITE Model: Shortcomings

The model cannot explain the following experimental results:

- The baking effect is stable after re-oxidation
- The Q-drop was observed in the TE_{011} mode (only magnetic field on the surface)
- The Q-drop is re-established in a baked cavity only after growing an oxide ~ 80 nm thick by anodization

Oxygen Pollution Model

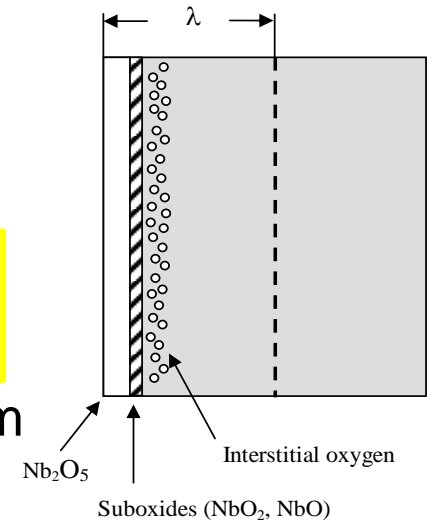
- Surface analysis of Nb samples shows high concentrations of interstitial oxygen (up to ~ 10 at.%) at the Nb/oxide interface
- Interstitial oxygen reduces T_c and the H_{c1}

Magnetic vortices enter the surface at the reduced H_{c1} , their viscous motion dissipating energy

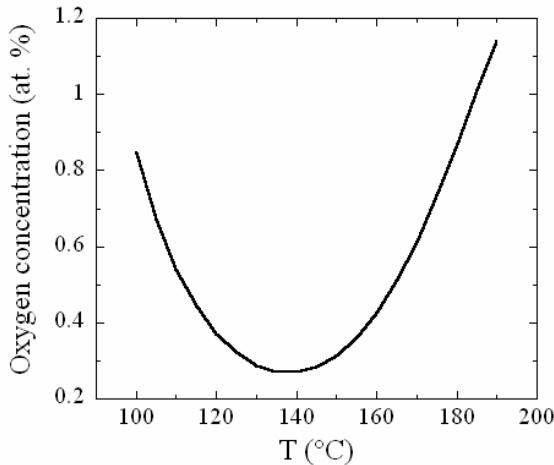
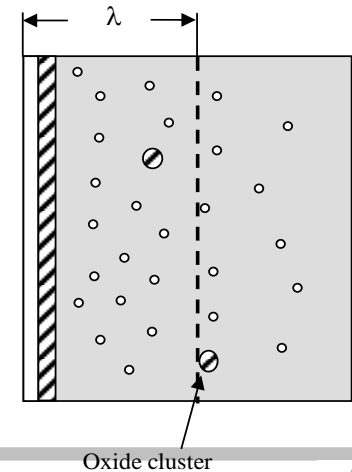
- The calculated O diffusion length at 120°C/48h is ~ 40 nm

Interstitial oxygen is diluted during the 120°C baking, restoring the H_{c1} value for pure Nb

Before baking



After baking



Calculated oxygen concentration at the metal/oxide interface as a function of temperature after 48h baking

G. Giovati, *Appl. Phys. Lett.* 89 (2006) 022507

Oxygen Pollution Model: Shortcomings

The model cannot explain the following experimental results:

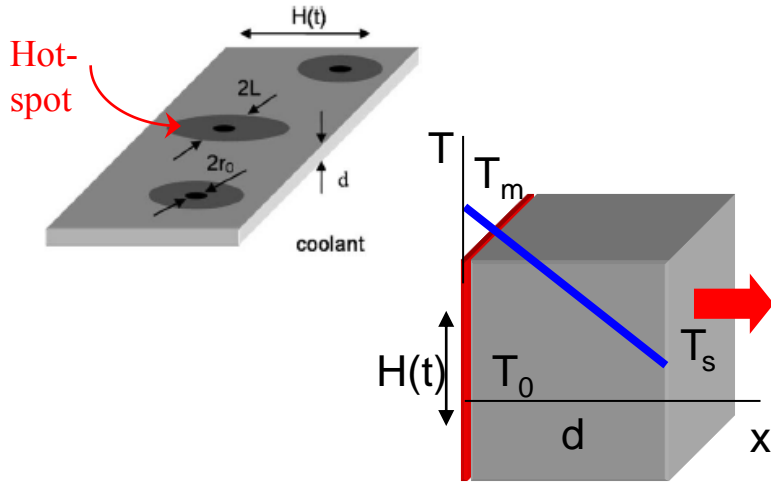
- The Q-drop did not improve after 400°C/2h “in-situ” baking, while O diffuses beyond λ
- The Q-drop was not restored in a baked cavity after additional baking in 1 atm of pure oxygen, while higher O concentration was established at the metal/oxide interface
- Surface analysis of single-crystal Nb samples by X-ray scattering revealed very limited O diffusion after baking at 145°C/5h

Fluxons as Source of Hot-Spots

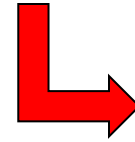
- Motion of magnetic vortices, pinned in Nb during cool-down across T_c , cause localized heating
- Periodic motion of vortices pushed in & out of the Nb surface by strong RF field also cause localized heating

The small, local heating due to vortex motion is amplified by R_{BCS} , causing cm-size hot-spots

Thermal Feedback with Hot-Spots Model

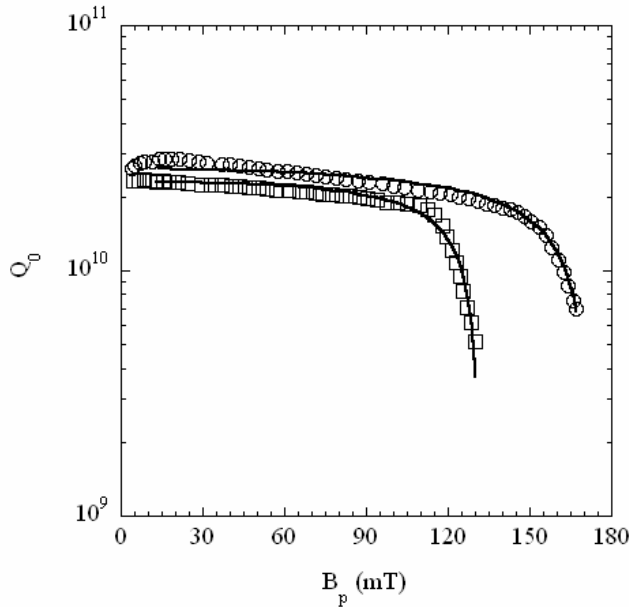


- The effect of “defects” with reduced superconducting parameters is included in the calculation of the cavity R_s



Hot-spots

- This non-linear R_s is used in the heat balance equation



$$u(\theta) = \theta e^{1-\theta}$$

$$\frac{2B_p^2}{B_{b0}^2} = 1 + g + u(\theta) - \sqrt{[1 + g + u(\theta)]^2 - 4u(\theta)}$$

$$Q_0(B_p) = \frac{Q_0(0) e^{-\theta}}{1 + g / [1 - (B_p/B_{b0})^2]}$$

Fit parameters:

- g related to the No. and intensity of hot-spots
- $Q_0(0)$ low-field Q_0
- B_{b0} quench field

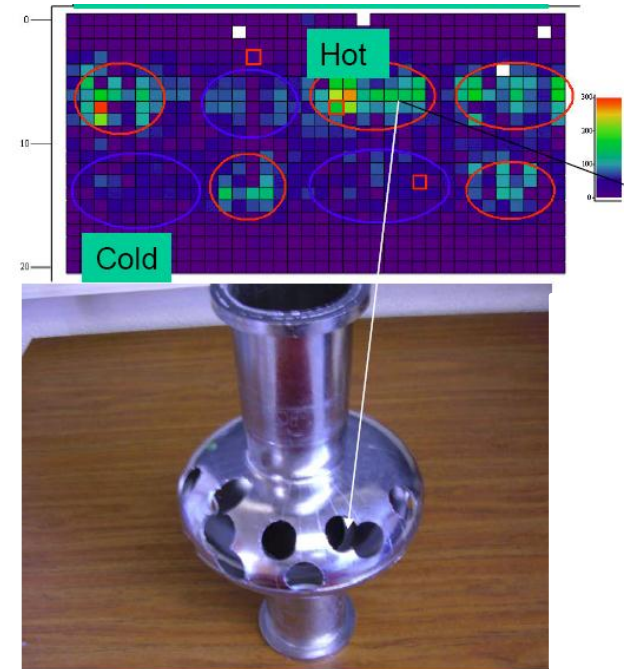
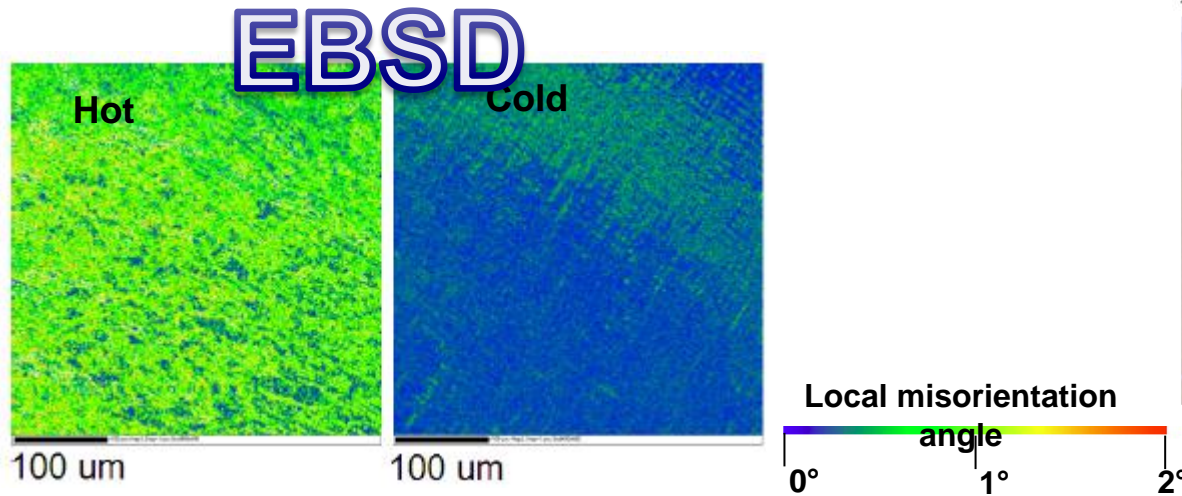
A. Gurevich, *Physica C* 441 (2006) 38

Q-drop: Recent Samples Results

Samples from regions of high and low RF losses were cut from single cell cavities and examined with a variety of surface analytical methods.

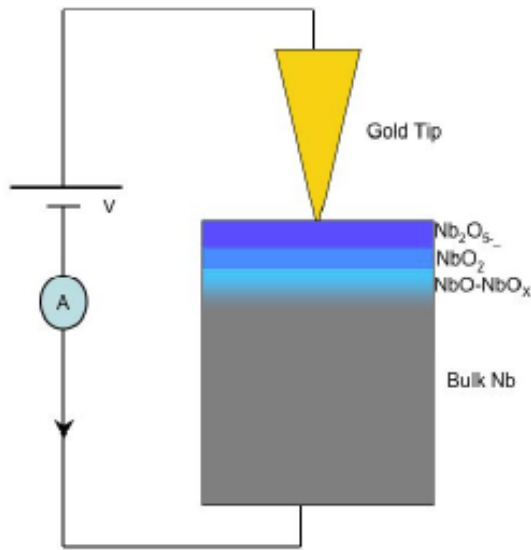
No differences were found in terms of:

- roughness
- oxide structure
- crystalline orientation

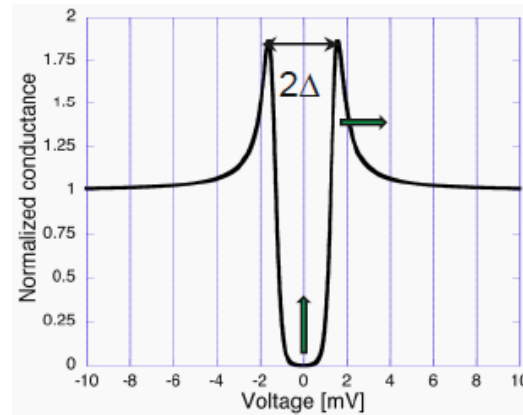


It was found that “hot-spot” samples have a higher density of crystal defects (i.e. vacancies, dislocations) than “cold” samples

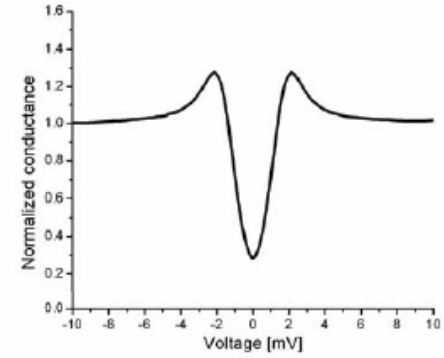
Q-drop: Recent Samples Results



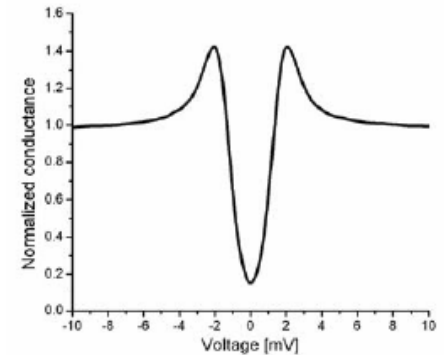
PCT



Ideal BCS, $T \sim 1.7\text{K}$



Unbaked Niobium



Baked Niobium 120C-24h

- Zero-bias conductance peak: presence of dissipative pair-breaking layers on the cavity surface
- Possible source: magnetic impurities ($\text{Nb}_2\text{O}_{5-\delta}$?)